Scale-Up Economics for Cultured Meat

Techno-Economic Analysis and Due Diligence

David Humbird

DWH Process Consulting LLC
Centennial, Colorado USA

Prepared for Open Philanthropy
San Francisco, California USA

December 28 2020

Executive Summary

"Cultured meat" technologies aim to replace conventional meat with analogous or alternative bioproducts from animal cell culture. Developers of these technologies claim their products, also known as "cell-based" or "cultivated" meat, will be safer and more environmentally friendly than conventional meat while offering improved farm-animal welfare. To these ends, Open Philanthropy commissioned this assessment of cultured meat's potential to measurably displace the consumption of conventional meat.

Recognizing that the scalability of any cultured-meat products must in turn depend on the scale and process intensity of animal cell production, this study draws on techno-economic analysis and due-diligence perspectives in industrial fermentation and upstream biopharmaceuticals to assess the extent to which animal cell culture could be scaled like a fermentation process.

The analysis identifies a number of significant barriers to the scale-up of animal cell culture. Bioreactor design principles indicate a variety of issues associated with bulk cell growth in culture: Low growth rate, metabolic inefficiency, catabolite and CO_2 inhibition, and bubble-induced cell damage will all limit practical bioreactor volume and attainable cell density. With existing bioreactor designs and animal cell lines, a significant engineering effort would be required to address even one of these issues.

Economic challenges are further examined. Equipment and facilities with adequate microbial contamination safeguards are expected to have high capital costs. Suitable formulations of amino acids and protein growth factors are not currently produced at scales consistent with food production, and their projected costs at scale are likewise high. The replacement of amino-acid media with plant protein hydrolysates is discussed and requires further study.

Capital- and operating-cost analyses of conceptual cell-mass production facilities indicate production economics that would likely preclude the affordability of their products as food. The analysis concludes that metabolic efficiency enhancements and the development of low-cost media from plant hydrolysates are both necessary but insufficient conditions for the measurable displacement of conventional meat by cultured meat.

Analysis highlights

Bioreactor design and scale-up principles are used to examine practical volumes and attainable cell densities in fed-batch and perfusion suspension cultures.

Equipment costs consistent with appropriate levels of sterility assurance and commoditization are developed with process-industry estimation software and cost-factor techniques.

Price-volume relationships are leveraged for demand-consistent forecasting of amino acid and protein prices in cell-culture media. The costs and suitability of speculative plant hydrolysates as cell-culture media are also considered.

Process designs and production cost estimates are developed for conceptual fed-batch and perfusion facilities producing bulk animal cell mass within a total market of 100 kTA (wet basis). Both are examined in the context of a cellular metabolism significantly enhanced over a wild-type animal cell.

A fed-batch facility of 24×20 m^3 bioreactors is estimated to produce 6.8 kTA of wet cell mass at a production cost of $37/kg. Amino acids contribute 50% of this cost. Clean room costs limit the size of a single facility, while CO_2 accumulation limits the volume of the production bioreactor.

A perfusion facility of 96×2 m^3 bioreactors is estimated to produce 6.9 kTA of wet cell mass at a production cost of $51/kg. The economics of perfusion are disadvantaged by the high installation costs of small bioreactors and the extra capital and consumables costs associated with the perfusion device.

Both estimates exceed a price target of $25/kg wet cell mass asserted for consistency with 100 kTA consumption. Low-cost plant hydrolysate at $2/kg could reduce all production cost estimates by $15–16/kg. A fed-batch process with hydrolysate media would thus fall below $25/kg. Lower-grade materials of construction, elimination of clean rooms, and additional metabolic enhancement offer smaller reductions.

With either technology, reduced metabolic efficiency leads to catabolite-limited cell densities that cause the modeled production cost to increase beyond economically sustainable levels.

Supplemental information

An Excel spreadsheet containing the calculations in this analysis can be downloaded at *https://doi.org/10.17605/OSF.IO/AJSU9*.

Contents

1

Introduction

1.1 Background

"Cultured meat" refers to a nascent field of bioproducts that aim to replace conventional meat produced by farming and slaughter with analogous or alternative products made from edible animal cell culture.[1] In one concept (Figure 1.1), animal cells from a live-animal biopsy are propagated through a series of increasingly large bioreactors, growing in number with each step and ultimately inoculating a 20 m^3 bioreactor [4]. After a total cycle time lasting several months, 2–3 tons of animal cell slurry are harvested from this bioreactor. The cultured cell mass, perhaps blended with vegetable proteins and fats, can be further processed with enzymes[2] and conventional extrusion/texturization operations into edible mincemeat- or nugget-style food products. In Figure 1.1, these are indicated as "unstructured" products. Some developers, probably sensing consumer and investor ambivalence to such products [6, 7], have further proposed that cultured animal cells be deposited onto an edible scaffold material that provides form and possibly hypertrophy, resulting in "structured" products that more closely resemble a cut of meat from an animal.

To its proponents, cultured meat is positioned to address global problems associated with industrial animal farming, such as its contributions to pollution, foodborne illness, and anthropogenic climate change [8–10]. The promises of cultured meat thus include resource-efficient production of human nutrition at a global scale and reduction of livestock populations to

[1] Alternatively, "lab-grown" or "in vitro" meat, along with other terms. During the preparation of this report, the preferred term of art (according to consumer research conducted by The Good Food Institute) shifted from "clean" [1] to "cell-based" [2] to "cultivated" meat [3]. For the present discussion, "cultured" has been retained as a neutral term indicating a product of cell culture.

[2] E.g., transglutaminase AKA "meat glue" [5].

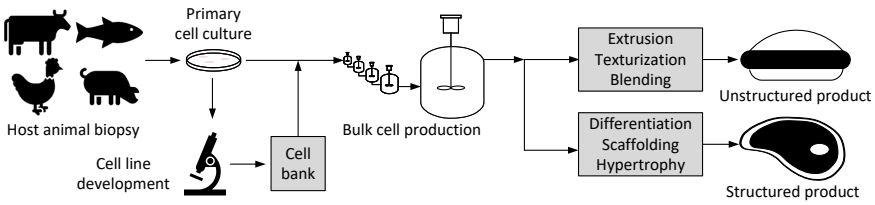

FIGURE 1.1: Conceptual cultured-meat production process.

pre-industrial levels. At the heart of cultured meat's conceptual appeal is the further promise that all of this could be accomplished without requiring existing meat consumers to significantly change their diet [11]. In many cases, however, these promises are contingent upon, e.g, concomitant major advances in renewable energy [12], a wholesale "rethink" of the composition and cost structure of cell-culture media [13], presumptive future feedstock sources such as mass-cultivated algae or cyanobacteria [14], or a correction to the consumer price of conventional meat that brings it up to parity with its toll on the environment [15]. The consumer price of cultured meat, meanwhile, is unknown. The present analysis was therefore commissioned to assess cultured meat's potential to measurably displace the human consumption of conventional meat.

The reader is likely familiar with Mark Post's 2013 media event [16] in which a ~$325,000 (€250,000) lab-grown hamburger was presented to a panel of food critics. This figure was computed by totaling Post's direct costs leading up to the event, including the wages of the scientists and technicians who labored for some months to make the item [17]. In 2015, Post offered a preliminary production-cost estimate for such products of $65/kg [18, 19], which some observers extrapolated to $11 per burger [20].[3] Subsequently, this analyst has encountered bioproducts entrepreneurs and investors who somehow inferred from these events that Post et al. were able to reduce the cost of animal cell culture by five orders of magnitude in two years. The reader may also be familiar with this sentiment regarding cultured meat, which is expressed in the popular media through hopeful invocations of "Moore's law" and awed remarks about the steadily declining price of something that is not available for purchase [21–25]. Ultimately, however, there is no responsible comparison to be made between these two costs. The lower figure was merely a *scale-up projection*—an opaque one at that, as its details were not published for examination.

[3] In a historical aside, the original projection was "eighty dollars" per kg, which resolves to $11 for a 5-oz burger. These words, however, were not uttered by Post, but by an Australian radio reporter [18] and had likely been converted to AUD for the audience. Later that week, it was reported that Post had claimed a production cost of USD 65/kg [19], consistent with the exchange rate at the time.

The art of the scale-up projection is sometimes known as techno-economic analysis (TEA). In the (bio)process industries, TEA leverages conceptual process design, simulation, and equipment costing techniques to develop estimates of the capital, operating, and total production costs[4] of technologies at full scale, based on lab/pilot-scale performance and projected improvements [26]. Referring to the conceptual cultured-meat process in Figure 1.1, it can be concluded that the scalability of either class of products from cell culture (structured or unstructured) depends on the scalability of the bulk cell production step. As further indicated in Figure 1.1, there is an expectation that this step would be carried out in large (≥200 m^3) stainless-steel tanks, such that the production facility would resemble a large-scale fermentation plant or perhaps a brewery [27–30]. A nebulous precedent for this concept comes from the biopharmaceutical industry, where therapeutic proteins are produced from recombinant mammalian cell lines in (much smaller) stainless steel bioreactors[5] of up to 20–25 m^3. Drawing on techno-economic analysis and scale-up techniques from industrial biotechnology (biofuels, baker's yeast,

[4] CAPEX, OPEX, and COP (cost of production).

[5] Terminology note: *fermentor* will be used for microbial culture equipment; *bioreactor* for animal cell-culture equipment.

commercial enzymes) as well as from conventional animal cell culture as carried out in the biopharmaceutical industry, this analysis examines the extent to which an animal cell-culture process could be scaled like a fermentation process. Its ultimate goal is to provide a transparent scale-up projection of a bulk cell-mass process that produces a new, commoditized starting material for downstream processing into an array of meat substitutes. Technical and economic aspects will be explored in detail so that scale-up challenges can be well understood and discussed. To begin, perhaps some management of expectations is in order.

1.2 Industrial scale-up perspectives

The promises of cultured meat may sound very familiar to erstwhile practitioners of another modern biotechnology once seemingly destined to save the planet: biofuels. In the 1990s and 2000s, many biotechnology developers sought to leverage modern advances in metabolic engineering and recombinant DNA technology (together known as synthetic biology [31–33]) to produce fuels and chemicals in workhorse microbes like *E. coli* or *S. cerevisiae*. With a few notable exceptions [34, 35], however, the great promise of synthetic biology for fuels and chemicals was largely waylaid by low-level difficulties in engineering, scale-up, and cost-competitiveness.

For U.S. developers in particular, the biofuels wager was twofold. First, the price of oil would have to remain high—on the order of $100/barrel, as was observed before and after the 2008 financial crisis (Figure 1.2a). A high oil price would ensure the eventual cost-competitiveness of new biofuels with petroleum incumbents and help drive interest and funding in biofuels research in the meantime. Second, these new bioprocesses needed tremendous potential to *scale*, that is, to operate in extremely large fermentors and at a very high intensity. Scale-up presented biofuels process engineers with several challenges. The metabolic pathways to the molecules of interest generally required highly aerobic fermentations. Compared to an anaerobic process (e.g., ethanol production), aerobic fermentations generally have a lower carbon efficiency, significantly higher capital and utility expenses, tighter sterility and contamination constraints, and additional heat and mass transfer complexities.

To illustrate the effects of scale and intensity, Figure 1.3 presents curves of aggregate capital and utility costs required to transfer oxygen to a fermentor [38]. Per kg of O_2 transferred to living microorganisms, the cost to own and operate an aerobic fermentor decreases with increasing size and increasing oxygen uptake rate. Larger fermentors leverage economies of scale in vessel costs, support equipment costs (air compressor, chiller, etc.) as well as in the labor associated with reactor operation and monitoring.[6] The oxygen uptake rate (OUR) is the volumetric consumption rate of dissolved O_2 by cells (mol O_2/m^3-h). Attaining a high OUR requires the development of a robust, metabolically efficient organism, capable of high cell density, high

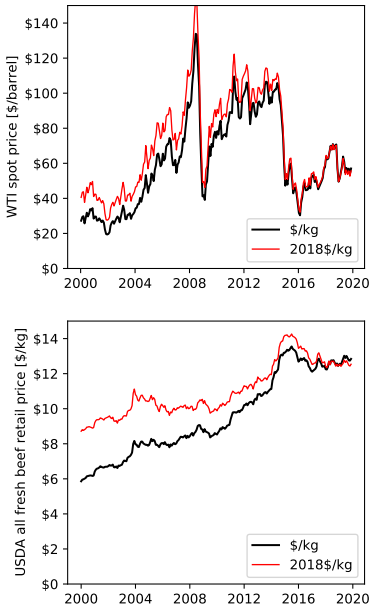

FIGURE 1.2: 2000–2019 prices, unadjusted and adjusted to 2018$, for (a) WTI crude oil [36] and (b) fresh beef [37].

[6] A key difference between Figure 1.3 and the results in [38] is that one full-time employee (FTE) has been added to monitor the bioreactor (five shifts at 0.2 FTE per shift) at a loaded operating expense of $100k/y. In the aggregate cost, this expense is negligible at the 200,000 L scale, but represents ~25% of the total at the 2,000 L scale.

growth rate, and high productivity. Attaining an equally high oxygen *transfer* rate (OTR, volumetric dissolution rate of O_2 from sparged gas), especially in desirably large vessels, requires a significant fermentor design effort to improve mixing and heat/mass transfer. The OUR and OTR thus stand for the less concrete metric of process intensity. The concerted biological and engineering development activities aimed at increasing these quantities are known as process intensification: getting the most yield from every liter of the fermentor [39].

Many biofuels/chemicals developers found that their microbes were either insufficiently robust to scale into economically large fermentors or too inefficient to operate at high OUR. As a result, developers found themselves with unacceptably high capital costs when trying to design large plants [40]. Others discovered new problems at scale: heat and mass transfer deficiencies, uncontrollable contamination, or the inability to keep recombinant organisms from reverting to their wild type. In the U.S., many scale-up commitments made by industry and government in the early 2000s were missed or deferred [41]. Even somewhat successful biofuels developers eventually found their business models obliterated by drastic reductions in the price of oil (Figure 1.2a), resulting in a series of high-profile failures, bankruptcies, and acquisitions in the sector [42–48].

Cultured meat doesn't seem to present an easier problem from either a technical or an economic perspective [49]. To permit process intensification, metabolic efficiency must be as high as possible.[7] To attract investment, capital costs must be as low as possible. Furthermore, the relatively stable price of conventional meat (Figure 1.2b) doesn't present a clear and immediate economic opportunity in the way that rising oil prices once did for biofuels. Considering Figure 1.3, a key question seems to be: can an animal cell-culture process be designed and operated at a scale and intensity where its consumption as food becomes economically sustainable? Unfortunately, though several *microbial* bioprocess technologies have scaled over decades to extremely large production volumes (e.g., fuel ethanol, baker's yeast, lysine for animal feed, wastewater treatment), it is difficult to reconcile even basic concepts of industrial bioprocess design with known characteristics of animal cell culture as practiced today. For instance:

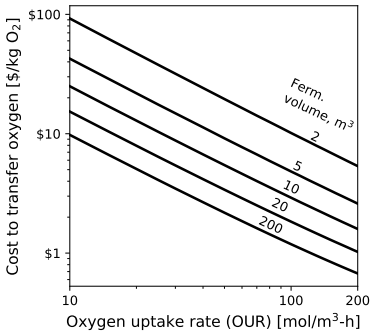

FIGURE 1.3: Specific aggregate capital and operating cost to transfer O_2 to aerobic stirred-tank fermentors of varying size.

[7] In this case, sugars and amino acids to cellular protein.

TABLE 1.1: Hydrated diameter, mass, and doubling time τ_d for common cell types.

	diam.	mass	τ_d
Mycoplasma	0.4 μm	0.03 pg	6–12 h
Bacteria	1 μm	0.5 pg	20 min
Yeast	5 μm	60 pg	1–3 h
Fibroblast	14 μm	1500 pg	24–48 h

► THE GROWTH RATE IS SLOWER.

Animal cells proliferate much more slowly than microbial cells (Table 1.1). Commercial strains of baker's yeast, for instance, are grown with a doubling time of about 3.5 hours.[8] After a week of inoculum preparation, a production batch of yeast thus lasts ~16 hours [50]. Given a doubling time of 24–48 hours, a facility that produces an equivalent mass of animal cells would require 8–16× more bioreactor volume. Production batches would last several days to a week, following months of inoculum preparation. At food scale, the total number and volume of installed bioreactors would be staggering.

[8] Cell growth is usually expressed as a rate μ having units of g cells/g cells-h (or h^{-1}). A growth rate of μ=0.20/h means that 1 g of cells will multiply into 1.20 g of cells in 1 hour. The doubling time τ_D is the time it takes for 1 g of cells to double into 2 g. The two quantities are related by $\tau_D = \ln(2)/\mu$.

- THE BIOREACTOR VOLUMES ARE SMALLER.

  In a conventionally configured fermentor or bioreactor (gas-sparged and/or agitated), maximum practical reactor size is often determined by the cells' ability to withstand spatial heterogeneities in, e.g., temperature, pH, or nutrient concentrations [51]. Individual cells in suspension are mixed throughout the fermentor and are thus subject to varying conditions, which may stress them. In large fermentors, heterogeneity is typically counteracted with increased sparging and/or increased agitation. Either action increases turbulence and bubble-induced shear forces in the fluid, which may damage animal cells due to their relatively large size and lack of a rigid cell wall [52]. Maximum practical bioreactor size is thus in part determined by the efficacy of mixing at the limits of shear tolerance. Today, animal cell culture is not practiced in bioreactors larger than 25 m^3—significantly smaller than the 200–1,000 m^3 vessels employed in industrial aerobic fermentation.

- THE FINAL CELL DENSITY IS LOWER.

  In high-density fermentation, typical design limits are a sparge rate up to ~2 vvm (standard volumes of gas per volume of liquid per minute) and an agitation rate up to ~5,000 W/m^3 (agitator power input per volume of liquid). The equivalent limits for animal cell culture are ~0.01 vvm and ~100 W/m^3. These constraints place animal cell culture in a significantly lower oxygen mass transfer regime than fermentation; upper limits of the O_2 mass transfer coefficient k_La are ~800 h^{-1} in fermentation and ~15 h^{-1} in cell culture [53]. Due to the animal cells' lower growth rate, the OTR achievable with such a low k_La is generally adequate to match OUR as cells multiply to low/medium density [54]. In high-density culture, however, OUR is dominated by the maintenance respiration rate of existing cells. These design limits thus impose constraints on the final cell density.

TABLE 1.2: Market prices of commercial *S. cerevisiae* (2018$, dry matter basis)

$/kg	Strain/Source
$2.82	Baker's, BCC Research [55]
$2.61	Brewer's, BCC [55]
$2.52	Brewer's, SuperPro [56]
$2.34	Baker's, Hacking [57]
$2.20	Baker's, Company 1

TABLE 1.3: Analysis summary for standard and constrained yeast processes. (See Appendix A.)

	Standard	Constrained (equal CAPEX)
Max. growth rate (h^{-1})	0.20	0.03
Max. OTR (mol O_2/m^3-h)	150	25
Production fermentors	6×200 m^3	27×20 m^3
Final seed fermentors	2×85 m^3	9×19 m^3
Cell density (g/L dry)	69	25
Yeast production (kTA)	17.3	1.7
Total CAPEX	$69M	$70M
Total FTE	24	56
Cost of production, $/kg dry matter		
Carbon (molasses)	$0.72	$0.89
Nitrogen (ammonia)	$0.04	$0.04
Water	$0.01	$0.02
Utilities	$0.16	$0.23
Labor	$0.14	$3.34
Overhead	$0.36	$3.63
Annual capital charge	$0.47	$4.74
Total COP, $/kg dry	$1.89	$12.90
Total COP, $/kg wet	$0.57	$3.87

The discussion can be paused here to demonstrate the economic impact of the above constraints on a microbial process where cells are the product: baker's yeast (*Saccharomyces cerevisiae*). While production of mass quantities of animal cells in large-scale, high-density culture is a novel problem, bakeries, breweries, and fuel ethanol plants all receive daily shipments of yeast cells. Commercial yeast is typically produced in large (~200 m^3) bubble-column bioreactors at cell density approaching 4×10^9/mL (70 g/L dry matter) and extremely high OUR of ~150 mol O_2/m^3-h. To avoid ethanol formation, yeast growth is controlled to a doubling time of 3.5 h [58].[9] As shown in Table 1.2, wholesale baker's yeast prices are in the range of \$2.20–\$2.80/kg on a dry basis, so the actual production cost should be just under \$2/kg. This cost can be reproduced with a first-principles TEA model,[10] as summarized in Table 1.3.

If the process described by this model were constrained by the animal cell culture limits anticipated above,[11] the cost of production would be 7× higher. Such a plant would cost the same to build, but make only 10% as much yeast. For animal cell culture, significant economic penalties are thus anticipated due to basic engineering constraints of growth rate, bioreactor size, and oxygen mass transfer. These will tend to push animal cell cultures into the upper-left corner of Figure 1.3. Unfortunately, there are still more constraints to consider:

[9] Much longer than its native doubling time of 90 minutes.

[10] Further details of the techno-economic model for yeast and Table 1.3 are given in Appendix A.

[11] Constraints:

- Doubling time=24 h
- Maximum fermentor size=20 m^3
- Maximum OUR=25 mol O_2/m^3-h

▸ CATABOLITE INHIBITION FURTHER LIMITS THE FINAL CELL DENSITY.
As mentioned above, animal cells lack a rigid cell wall. An individual muscle or fat cell in culture is therefore much less capable of excluding or rejecting unwanted compounds in its environment than a microbial cell.[12] In other words, animal cells have osmolality limits. All dissolved species (sugars, minerals, buffers, waste metabolites, CO_2, etc.) contribute to osmolality and their concentrations must be tightly controlled. Waste catabolites like ammonia and lactate are particularly toxic and inhibit cell growth even at relatively low concentrations. Indeed, in cell culture for biopharmaceuticals, accumulation of toxic catabolites is a more frequently encountered limit than any physical limit of the bioreactor itself. In fed-batch operation, a catabolite-limited cell density of 1×10^6–30×10^6/mL is generally sufficient for protein production, but it would make the accumulation of bulk cell mass very challenging. Perfusion technology continuously removes waste catabolites and other spent media components from the culture to alleviate inhibition. As a rule, perfusion cultures can achieve higher cell densities than fed-batch cultures, but the maximum practical bioreactor size is significantly smaller.

[12] That being the job of a different type of cell in, e.g., the kidneys. Notably, yeast, which evolved in open environment, can regulate internal pH independent of the fermentation broth pH [59].

▸ THE AVAILABILITY OF HIGH-QUALITY MEDIA COMPONENTS IS LIMITED.
In fermentation process design, the limited nutrient slate of industrial microbes is exceptionally handy. Regardless of the organism's metabolism, the starting materials are the same: a single substrate (usually a sugar) for carbon

and energy, a single inorganic nitrogen source (ammonia or nitrate salt), a small amount of phosphate, and very small amounts of sulfur and trace metals. Animal cell-culture media must instead supply a mixture of amino acids to satisfy the cells' nitrogen demand. On an atomic nitrogen basis, these are significantly more expensive than an inorganic nitrogen source, and many are not currently produced at volumes consistent with a significant scale-up of animal cell culture.

Furthermore, if the cells to be cultured are stem cells, then a variety of hormones, cytokines, vitamins, etc. (collectively known as growth factors) must also be provided to keep them from differentiating as they proliferate. At the bench scale, these are typically delivered in complex, animal-derived sera; at food scale, suitable replacements from fermentation or plant-based sources will be required. As expensive as these compounds are likely to be, they may not be a significant contributor to cell mass production cost, as their concentrations in media are extremely small.

- THE CAPITAL COSTS OF ASEPTIC OPERATION ARE SIGNIFICANT.
At neutral pH and elevated temperature (37 °C), an aerated cell-culture bioreactor is quite welcoming to any stray microbe. Given the relative growth rates in Table 1.1, a contamination event will very quickly turn an animal cell culture into a microbial culture, leading to batch loss. The cleanliness of equipment, environment, and media is therefore critical at every stage of the cell-culture process. In comparison to a fermentation process, the additional sterility/asepsis safeguards required by animal cell culture will have a strong effect on the cost of equipment and facility: extra steam piping for point sterilization, extreme automation to avoid contamination by operators, and containment considerations for biosafety. These measures will reduce the economies of scale typically expected as a function of vessel volume, and may limit the ultimate bioreactor size as well, given that current designs of fermentors larger than ~200 m^3 are not practicably sterilized to a level suitable for animal cell culture [60].

- A SIGNIFICANT METABOLIC ENGINEERING IS REQUIRED.
A cell line suitable for an economic bulk-growth process would have several traits that are generally not characteristic of the wild-type cells obtained from a live-animal biopsy (Figure 1.1). Primary cells, which are fully differentiated to their final tissue type (e.g., muscle or fat), can only be propagated for ~50 generations before proliferation ceases—the so-called Hayflick limit. Within this limit, several tons of cell mass could, in principle, be grown from the primary cells in a tiny biopsy. In practice, scaling up mortal cell lines to industrial volumes will be extremely challenging, as phenotypic variations in every new biopsy will demand process re-development and re-qualification.

For repeatability at scale, immortal (or immortalized) cell lines will be required, e.g., adult (partially differentiated) stem cells from tissue, embryonic stem cells (ESCs) from a recently fertilized embryo, or induced pluripotent

stem cells (iPSCs) produced by genetic reprogramming of adult cells [61]. Stem cells, however, are notoriously difficult to culture without differentiating [62]. Furthermore, all normal animal cells are generally anchorage-dependent, meaning that they prefer to adhere to something during growth. In animal tissue, cells adhere both to each other and to a complex extracellular matrix, which is vascularized to ensure that each cell receives nutrients and oxygen via the blood stream. In adherent culture for upstream biopharmaceuticals, cells adhere to the bottom of a T-flask or the inside of a roller bottle.[13] To mimic a suspension culture (albeit one with even stricter shear limitations), some cell lines are adapted for culture on microcarriers[14] Primary cells can also be "transformed" in the lab, a process that in many cases produces an immortalized, anchorage-independent cell line that may be grown in free suspension.

[13] Scale-up law: buy another roller bottle!

[14] Microscopic beads of (e.g.) collagen or polymer.

▸ THE VALUE PROPOSITIONS ARE COMPLETELY DIFFERENT.

Many of the process design challenges and economic disadvantages highlighted above for animal cell culture are only tolerated because the products are extremely valuable. These products include glycosylated protein therapeutics,[15] primarily produced in recombinant Chinese hamster ovary (CHO) cells. Figure 1.4 presents a breakdown of global prescription drug revenue in 2018 [63]. Recombinant glycoproteins belong to a class of drugs called biopharmaceuticals or biologics,[16] and most can also be further classified as monoclonal antibodies, or mAbs. In 2018, biologics accounted for about 25% of global prescription drug revenue, and mAbs made up about half of that share. Of the 80 approved mAb products represented in Figure 1.4, adalimumab (Humira) alone accounted for 20% of revenue: $20B in 2018 [63].

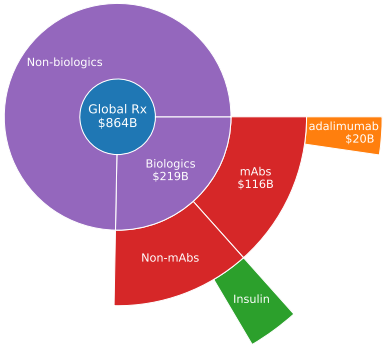

FIGURE 1.4: Global prescription drug revenue, 2018 [63].

In the U.S., Humira (3 months of biweekly doses of 40 mg) was prescribed 4.2M times in 2016 [64, 65]. It can thus be approximated that the U.S. patient base for Humira is about 1M individuals, and its annual U.S. production volume (as a pure ingredient) is 1,100 kg—enough to fill the back of one pickup truck.[17] In 2017, U.S. sales of Humira were $12.4B [66], i.e., the selling price was >$11M/kg.

These figures do not say much about the putative costs of growing animal cells. Petrides [56, 67, 68] presents a techno-economic analysis of a generic mAb facility that produces ~1,500 kg/y of mAb from CHO cell culture in 20 m^3 bioreactors at an estimated unit production cost of $84,000/kg, divided roughly 72% upstream (cell culture) and 28% downstream (recovery and purification of the mAb). In contrast to most fermentation processes [57], the largest upstream cost is not feedstock (i.e., cell-culture media). Rather, it is facility and labor: a $110M clean room and ~130 workers. The largest downstream cost is consumables: resins, filters, etc. used in product purification. Normalizing this analysis for the 42,000 kg/y (wet) of co-produced CHO cell mass would result in $2,200/kg of CHO cells. The comparison is odious; a mAb process of course is not optimized for a high yield of cell mass, which

[15] Protein molecules with a folded structure influenced by attached sugar molecules. Glycosylation of a mammalian protein must be done by a mammalian cell. While a microbial cell could perhaps be engineered to make a protein with the same amino acid sequence, it would not be glycosylated and thus not an effective therapeutic.

[16] This classification includes products from microbial fermentation as well as some made in whole animals and plants.

[17] For comparison, the U.S. ethanol industry produced 16B gallons that year—enough to fill 2M tanker trucks.

is a waste stream in the process and a consumer of carbon and nitrogen that could otherwise be directed to product.[18]

To summarize, the state of the art in large-scale animal cell culture is in addressing very specific problems (production of recombinant glycoprotein therapeutics) by making very small amounts of something (few hundred to ~2,000 kg/y) that improves the lives of a very small number of people (few thousand to ~2M) and sells for a very high price (e.g., $11M/kg) at an arbitrarily high margin [70].[19] It is not, it would seem, a likely platform for making low-value, commodity-scale products like food. Looking to blockbuster[20] mAb processes for scale-up guidance reveals that conventional animal cell-culture processes are carried out on a vastly smaller scale than food production. In addition, they have not necessarily been optimized for the same economic levers as industrial fermentation, e.g., yield of cell mass or even media cost. Instead, they have individually been optimized for something else which is process- and product-specific. The scale-up laws and economics of animal cell mass production thus remain uncertain.

[18] In almost all existing manufacturing processes using animal cells, one would prefer to *minimize* the cell mass. In nascent applications where this is not true, e.g., single-patient cell therapies including CAR-T, the scales are tiny, with bioreactors the size of a deck of cards, or a can of soda [69].

[19] Perhaps also worth noting from Figure 1.4 that 75% of prescription drugs revenues derive from non-biologics: small molecules synthesized without cells. Even in protein therapeutics, the next (albeit controversial) technology on the horizon appears to be cell-free expression [71].

[20] A drug with >$1B in annual sales.

1.3 Analysis approach: powers of ten

At time of writing (Fall 2020), the production volume of edible cultured animal cells is unknown but small—probably on the order of 1–10 kg/y of material generated as demonstration product and in the course of R&D. The current production volume of conventional meat is estimated at 3.2×10^{11} kg/y (320,000 kTA, kilotonne per annum) [72]. Ultimate aspirations for cultured-meat products would thus appear to be on the order of 10^{11} kg/y, or billions of people consuming tens of kg/y [4]. With techno-economic analysis, we gaze into this abyss of ten orders of magnitude. As noted above with the eleven-dollar burger, to conceptualize and mentally process the scales involved, one may be tempted to invoke some form of Moore's law. Indeed, depending on the metric (processing speed/power, consumer price, etc.), it can be argued that certain aspects of computing have progressed by about ten orders of magnitude since the days of Moore [73, 74].[21] Most of this progress can be explained in the context of the original observation—from a nominal transistor size of ~10 μm in 1970 to ~10 nm today, there were at least six orders of magnitude of improvement to be made in the number of 2-D devices crammed into a square centimeter of silicon [76]. The remainder is a result of concomitant advances in chip design, materials, process development, software, etc.

Unfortunately, similar progress cannot be expected of biological systems, whether in vivo or in vitro. The chemical reactions occurring inside a living cell proceed with the usual thermodynamic efficiency of 30–80% [77]. If an organism lives at all, it does not do so orders of magnitude away from its physical limits. Furthermore, in contrast to the semiconductor industry, momentous advances in manufacturing are less expected in the process industries. The basic phenomena of fluid flow, separations, mass transfer, reaction,

[21] And it only took 60 years. To fit this many powers of ten into a time scale that meets contemporary investor expectations, some would suggest that even more accelerationist "laws" are in play for cultured meat [75].

and the process equipment these take place in likewise operate with the usual thermodynamic efficiency of 30–80%. While generally accepted economies of scale in the process industries hold that, e.g., equipment costs scale sub-linearly with capacity [78],[22] or that the unit price of a commodity precursor chemical scales sub-linearly with order quantity [79],[23] these effects do not hold within them multiple orders of magnitude in manufacturing cost reduction. Nor do they necessarily apply in the case of biotechnology, where the process equipment in question is much smaller and more specialized than refinery/chemical equipment, and where the precursor chemicals (e.g., sugars, amino acids, growth factors) are only produced in limited quantities.

Consider, for instance, Figure 1.3: a 10× increase in fermentor volume does not result in a 10× reduction in the cost of O_2 transfer. A 10× increase in OUR *can* result in such a reduction, but this quantity is not infinitely valued. In fermentation, 200 mol O_2/m^3-h is about as high as it gets; in animal cell culture, a practical limit is <50 mol O_2/m^3-h. Thus, unlike the future cost to make a solid-state transistor looking forward from 1965, the absolute minimum cost to make a bioproduct (fuel, chemical, drug, or meat) is not unknowably small. Rather, it can be straightforwardly examined with techno-economic analysis. When performed responsibly, estimates from TEA can claim to be accurate to within 50% [80]. In other words, a projection might be off by a factor of two—not by a factor of ten.

Critically, the above claim is valid only in the context of the TEA's characteristic assumptions. Projections across ten orders of magnitude must carry some uncertainty, however, and care must be taken to avoid unreasonable assumptions and magical thinking. Technical due diligence, a related activity to TEA, is the art of interrogating such projections to distinguish between those that are challenging but achievable and those that are misleading or provably unphysical. For instance, while an "eleven-dollar burger" certainly sounds like a reasonable value for one's money, smart shoppers may note that an $11 hamburger at the factory easily becomes a $30 hamburger at the supermarket and a $100+ hamburger served at a restaurant. Absent other market pressures, one would not expect such an expensive product to measurably displace the consumption of conventional meat. Due diligence of this projection would raise additional questions about its capital equipment and media cost assumptions, facility and overhead costs, the contents of moisture and other fillers in the product, and the degrees to which the laws of biology and physics were upheld in its generation. In this analyst's related experience with biofuels, some commonly observed deficiencies in TEA (public and private) included:

- Yield projections in excess of biological and thermodynamic limits.
- Overestimation of economies of scale in equipment and plant size.
- Unrealistic expectations of supply-chain expansions at scale.
- Arbitrarily high values assigned to hypothetical or unproven co-products.
- A reliance on government intervention to enforce competitiveness.

[22] $$\frac{\text{Cost}_2}{\text{Cost}_1} = \left(\frac{\text{Capacity}_2}{\text{Capacity}_1}\right)^a; \quad a \approx 0.6$$

[23] $$\frac{\text{Unit price}_2}{\text{Unit Price}_1} = \left(\frac{\text{Qty}_1}{\text{Qty}_2}\right)^a; \quad a \approx 0.6$$

All of these are still in play for cultured meat. Others noted during the preparation and review of the present analysis include: media cost projections inconsistent with their required quality and putative demand, media usage projections inconsistent with cellular growth stoichiometry, and a tendency to willfully underestimate or ignore outright the likely capital costs of the ultimate production facility.[24] The present analysis therefore takes a due-diligence approach from the beginning, to provide a transparent techno-economic projection of an animal cell culture process designed for bulk growth of cell mass at commodity scale.

[24] Some of my due-diligence colleagues and I have lately (re-)observed this trend among bioeconomy developers and investors. The reasoning usually follows a line of "CAPEX only matters for the first plant; all subsequent plants will be financed at a low cost of capital." Though not technically incorrect, such treatment from lenders is, more accurately, only enjoyed after the first *successful* plant. This need to reconcile a sense of urgency with a reluctance to be "first" was an exceedingly common source of friction in the days of venture-backed biofuels startups [49].

Section 2 explores technical aspects of cellular growth stoichiometry and metabolism. Basic bioreactor design rules are used to establish maximum cell density as a function of bioreactor size. Sterility issues are also discussed. Section 3 explores economic aspects of capital and operating costs. General cost trends for media components and sterile bioprocessing equipment are developed. Section 4 develops production cost estimates and sensitivities for conceptual fed-batch and perfusion processes. To simplify the problem and the conclusions of the analysis, some characteristics of the model processes are assumed *a priori*. These aspects do not (wittingly) reflect the designs of any existing developer,[25] but will help to identify the general scale-up constraints expected for any cell-culture technology:

[25] In preparing this report, I had limited interactions with cultured-meat developers, and I am not under a confidentiality agreement with any of them.

- A mammalian (warm-blooded) cell line is considered for thermodynamic purposes.
- Conventional stainless-steel construction is assumed for the facility.
- Suspension culture is favored.
- The only inputs to the culture are water, air/O_2, glucose, amino acids, and some key growth factors.[26]
- The only revenue output from the culture is unstructured animal cells, suitable as a starting material for downstream processing to food. Revenue from unspecified co-products (including intellectual property) is not considered.
- Except where noted (mainly Section 2.2), cell mass is reported on a wet-matter basis, assuming 70% moisture.

[26] Buffers and low-cost mineral salt components are not included in the media-cost model.

Certain aspects of the analysis must be examined within the context of an entire industry. In particular, it will be demonstrated that cultured meat scale-up is contingent on concomitant scale-up of other bioproducts (e.g., amino acids and growth factors) and some global scale must be assumed to assess the demand on those industries. For discussion purposes, a threshold for a modest but measurable displacement of conventional meat by cultured meat is taken as 100 kTA of wet animal cell mass, i.e., ten million people consuming 10 kg/y each. In round numbers, 100 kTA is roughly equivalent to the current production volume of ascendant plant-based meat replacements, which have wide recognition and global distribution.[27] Further cost reductions are likely at larger scale, of course, and these will be examined with sensitivity analyses. However, 100 kTA of animal cell mass shall reflect a waypoint in the

[27] Products from, e.g., Beyond Meat and Impossible Foods.

development and adoption of cultured meat, one that should be squarely beyond the "valley of death" associated with new bioproduct development [26]. To assert an affordability threshold at this scale, this analyst submits a target of ~$25/kg of wet animal cell matter produced in a bulk growth step. To reach a market of ten million consumers, it must be assumed that any extravagant price premiums associated with product novelty have expired, and that cultured meat has at least attained the price-acceptance status of a "sometimes" food. After further processing, packaging, distribution, and profit, unstructured products made 100% from bulk cell mass at $25/kg might be expected to reach a minimum of $50/kg ($23/lb) at the supermarket—the price of a premium cut of meat, paid instead for a mincemeat- or nugget-style product. Above this cost, conventional meat displacement may arguably be measurable but increasingly less significant.

2

Technical aspects

2.1 Model cell characteristics

Different animal cell types have been proposed for cultured meat production, including embryonic or pluripotent stem cells (undifferentiated), adult or mesenchymal stem cells (partially differentiated), and primary cells (fully differentiated to their final tissue type) [61]. Each of these would have characteristic growth phases: a proliferation phase in which the cells multiply in number; one or more differentiation phases; and possibly a hypertrophy phase, in which the cells (as muscle tissue) accumulate mass without necessarily increasing in number. Each growth phase might further require a specific media composition, different growth factors, and a different bioreactor design. These details are presently unknown, or at least not scientifically demonstrated in the public sphere.

Much more is known about mammalian cell lines used in biopharmaceuticals manufacturing, most of which derive from CHO (Chinese hamster ovary) cells, as discussed in Section 1.2 [81]. CHO cell lines are immortal, non-cancerous, and morphologically stable [82, 83]. They can be grown in adherent culture or in high-density suspension culture. They can also withstand genetic manipulation with relatively good clonal stability [83], which facilitates batch predictability. CHO cells are not stem cells and require only a limited number of growth factors, making it possible (though still challenging) to design cost-optimized, serum-free media [84]. By degrees, CHO cultures thus overcome some of the process design issues anticipated in Section 1.2. CHO cells are not food, of course, nor is their use as such being proposed. However, this analysis draws on a large body of CHO research to make technical assumptions about mammalian cellular metabolism, growth inhibition, bioreactor design, and other aspects.

To generalize bulk cell culture for modeling purposes, this analysis considers an abstract spherical "cell" with a mammalian metabolism, 70% intracellular water, and a hydrated mass of 3,000 pg—roughly in the middle of the size range for mammalian cells.[28] Noting that suspension culture is likely to be the lowest-cost option for bulk cell growth,[29] it is further assumed

[28] And larger than CHO cells, which are 1,000–2,000 pg wet [85].

[29] To be discussed from a bioreactor design perspective in Section 2.3.

TABLE 2.1: Constituent composition for animal cell mass (dry CHON basis).

	C-formula	ΔH_f kJ/mol	ΔG_f kJ/mol	Wt%	mol/mol
Lipid	$CH_2O_{0.13}$ [Palmitate]	−54.0	−17.8	15%	0.205
Carbohydrate	CH_2O	−205	−147	10%	0.073
RNA/DNA	$CH_{1.13}O_{0.74}N_{0.39}$ [89]	−119	−72.6	5%	0.036
Protein	$CH_{1.57}O_{0.31}N_{0.28}$ [90]	−62.2	−21.7	70%	0.686
Overall (DCM_a)	$CH_{1.68}O_{0.34}N_{0.21}$	−73.0	−31.9		

that the cell line has been adapted for suspension culture, much like CHO cells. If suspended cells are assumed to be spherical and to have a density of 1.03, then this mass resolves to a diameter of 18 μm. Cell growth proceeds in the usual way with a maximum growth rate μ_{max}=0.029/h, equivalent to a doubling time of 24 h.[30] On a bulk-mass basis, if a culture is gaining mass then it must be consuming mass (i.e., nutrients and O_2) at a rate consistent with some growth stoichiometry.[31] If the culture is alive but not gaining mass, then it must still be consuming nutrients for maintenance.

A CHON formula for animal dry cell mass (DCM_a) of $CH_{1.68}O_{0.34}N_{0.21}$ is derived in Table 2.1 from an average composition of a mammalian cell [86] and representative CHON formulas of constituent macromolecules.[32] Enthalpies of formation (ΔH_f) for the constituent macromolecules and cell mass were estimated from the C-formulas and the correlation of Burnham [87]. Entropies of formation (ΔS_f) were estimated with the correlation of Battley [88]. From these values, Gibbs free energies of formation (ΔG_f) were estimated at a reference temperature of 298 K.[33]

Note that choice of cell size does not have a significant effect on process economics, provided that cell- and number-specific quantities are converted to a mass basis. In particular, cell number density (in, e.g., million cells per mL or 10^6/mL) is a commonly reported quantity.[34] Errors in techno-economic assumptions can be introduced if a number density reported for a culture of a given cell size is applied to a cell of a different size. Consider the practical maximum cell density in suspension culture, which occurs at a broth viscosity of ~2 cp. The Krieger-Dougherty model (Equation 2.1) can be used to estimate the viscosity η of a suspension as a function of the volume fraction ϕ occupied by particles.[35]

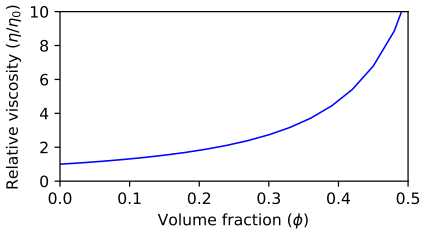

$$\eta/\eta_0 = \left(1 - \frac{\phi}{\phi_{max}}\right)^{-2.5\phi_{max}} \qquad (2.1)$$

Allowing for additional viscosity contributions from growth-factor and extracellular proteins, a limiting volume fraction of cells can be taken as ϕ~0.25. Viscosity increases sharply above this limit, as cell-cell collisions become more frequent. Indeed, microscopy of CHO cells (Figure 2.1) shows that cells are

[30] See Note 8 for a description of "usual" cell growth.

[31] To be discussed in Section 2.2.

[32] For purposes of this analysis, sulfur, phosphorous, and metals are ignored. Additionally, the typically cited 5–10% weight fraction of intracellular small metabolites is assumed to have a composition reflective of the macromolecular composition and is thus normalized out.

[33] $\Delta G_f = \Delta H_f - T\Delta S_f$

[34] As are cell-specific rates of protein production, oxygen uptake, media perfusion, etc.

[35] Here, η_0 is the native liquid viscosity (~0.8 cp for cell-culture media at 37 °C) and ϕ_{max}=0.65, an appropriate packing limit for soft spheres [91].

crowded on the slide at 20% volume fraction. At 30%, the cells are fully stacked on one another.

Table 2.2 tabulates number and mass densities for various cell sizes at the viscosity limit of $\phi = 0.25$. While the attainable number density changes with cell size, the attainable mass density is invariant. Thus, to contextualize some cell-density assumptions in cultured-meat TEA, a "conservative" assumption of 40×10^6/mL for a cell size approaching 4,500 pg [13] is in fact much closer to the viscosity limit than a "challenging" assumption of 128×10^6/mL for a cell size of 1,000 pg [4]. To avoid ambiguity in later calculations, cell density is reported on both a number basis and a wet mass basis.

TABLE 2.2: Attainable number and mass density at volume fraction $\phi = 0.25$ for various cell sizes. Specific O_2 uptake rates predicted by Reaction 2.9 are also shown.

Wet mass	Diam.	Max. density		Specific OUR	
pg/cell	μm	10^6/mL	g/L wet	pmol O_2/cell-h	mg O_2/g-h
1,000	12.3	258	258	0.178	5.68
2,000	15.5	129	258	0.299	4.78
3,000	17.7	86	258	0.405	4.32
4,000	19.5	64	258	0.502	4.02
5,000	21.0	52	258	0.594	3.80

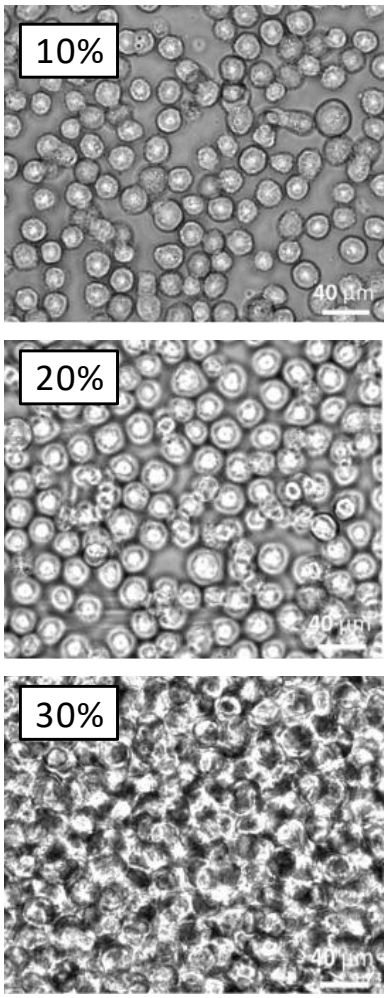

FIGURE 2.1: Phase-contrast microscopy of CHO cell suspensions at 10–30% volume fraction [91].

2.2 Stoichiometry of animal cell growth

The stoichiometry of life is the sum of anabolism, growth-associated catabolism, and maintenance-associated catabolism [92]. Anabolism, or biosynthesis, describes the formation of complex molecules from simple ones. Catabolism provides the energy required to perform anabolism and maintain organismal function. Industrial fermentation processes are typically designed to provide a single carbon source, a single inorganic nitrogen source (ammonia or metal nitrate), a small amount of phosphate, and very small amounts of sulfur and trace metals. In most fermentations, cells also use the carbon source for energy. Animal cells, however, evolved to take energy and structural carbon from carbohydrates and fats, and *organic* nitrogen from digested protein, i.e., amino acids. They also evolved to take chemical signaling cues (including whether to live or die) from outside the cell. In addition to sugar (glucose), animal cell-culture media thus contain up to 20 essential and non-essential amino acids, fatty acids, phosphate, trace minerals, and various vitamins, hormones, and cytokines (collectively known as growth factors).

From this wide array of nutrients, Xie and Zhou [90] provide some characteristics of ideal growth stoichiometry:

- Glucose is utilized solely for energy production and the synthesis of lipids, structural carbohydrates, and nucleotides.
- Glucose catabolism for energy production is completely oxidative: no lactate is produced.
- The amino acid glutamine is utilized solely for protein and nucleotide synthesis.

- Other amino acids are utilized for protein synthesis only.
- No amino acids are catabolized.

The degree to which cells adhere to these idealities depends on the instantaneous culture environment as well as their specific metabolic wiring. These factors give a cell "options" for managing its metabolism. Excess glucose may be catabolized to lactate. Excess amino acids, particularly glutamine, may be catabolized to ammonia. At sufficiently high concentration, either catabolite will inhibit cell growth. In principle, if the concentrations of all media components (along with O_2, CO_2, pH, temperature, etc.) could be controlled dynamically and independently in cell culture, the options could be eliminated and these idealities could be realized. To that end, metabolic engineering is usually employed to predict and/or manipulate a given cell's nutrient uptake rates and thereby gain a level of control over the culture [93]. In practice, this is not so easily achieved—even well-studied, workhorse CHO lines do not have ideal metabolisms, despite decades of incremental progress [90]. Process limitations associated with nonideality need to be considered at scale.

Anabolism

The anabolic reaction for 1 mole of DCM_a (Table 2.1) can be divided into subreactions for the constituent components.[36] The lipid fraction, which comprises cellular membranes, is assumed to be synthesized from glucose (Glc):[37]

$$0.049\ \text{Glc} \rightarrow 0.205\ \text{Lipid} + 0.090\ CO_2 + 0.090\ H_2O$$
$$\Delta H = -11.9\,\text{kJ/mol} \quad \Delta G = -14.6\,\text{kJ/mol} \qquad (2.2)$$

The carbohydrate (polysaccharide) fraction is synthesized by glucose polymerization:

$$0.012\ \text{Glc} \rightarrow 0.073\ \text{Carbohydrate}$$
$$\Delta H = 0.4\,\text{kJ/mol} \quad \Delta G = 0.4\,\text{kJ/mol} \qquad (2.3)$$

In a simplified view [95], nucleotide synthesis is carried out with carbon from glucose and only one of the N atoms on glutamine (Gln), rejecting glutamate (Glu). After balancing N, glucose balances the reaction:[38]

$$0.004\ \text{Glc} + 0.014\ \text{Gln} + 0.014\ CO_2 \rightarrow$$
$$0.036\ \text{RNA/DNA} + 0.014\ \text{Glu} + 0.009\ H_2O$$
$$\Delta H = 1.0\,\text{kJ/mol} \quad \Delta G = 1.5\,\text{kJ/mol} \qquad (2.4)$$

[36] Abbreviations, CHON formulas, and formation energies for the components appearing in the following reactions can be found in Appendix B.

[37] Cellular lipids can also be partially synthesized from exogenous fatty acids (e.g., palmitate) [94], but these can be expensive to isolate and refine from plant sources. Further, choline and inositol are required vitamins for lipid synthesis, but are consumed at rates too low to appear in an overall stoichiometry [90].

[38] Note that the apparent CO_2 requirement in Reaction 2.4 is more than satisfied by the CO_2 generated in Reaction 2.2.

Finally, the formula for protein in Table 2.1 was derived from an average amino acid profile of 207 cellular proteins [90]. The anabolic reaction for forming this protein is the sum of the individual amino acids in the correct ratios:

$$\begin{aligned}&0.007\ \text{Arg} + 0.004\ \text{Cys} + 0.006\ \text{Gln} + 0.003\ \text{His} + 0.007\ \text{Ile} + 0.010\ \text{Lys}\\&+0.002\ \text{Met} + 0.005\ \text{Phe} + 0.009\ \text{Thr} + 0.002\ \text{Trp} + 0.005\ \text{Tyr} + 0.010\ \text{Val}\\&+0.013\ \text{Ala} + 0.006\ \text{Asn} + 0.008\ \text{Asp} + 0.009\ \text{Glu} + 0.011\ \text{Gly} + 0.011\ \text{Leu}\\&+0.007\ \text{Pro} + 0.010\ \text{Ser} \rightarrow 0.686\ \text{Protein}\ (\text{CH}_{1.57}\text{O}_{0.31}\text{N}_{0.28}) + 0.142\ \text{H}_2\text{O}\\&\Delta H = 2.9\,\text{kJ/mol} \quad \Delta G = 9.9\,\text{kJ/mol} \quad (2.5)\end{aligned}$$

For cell mass growth from individual amino acids, the following anabolic reaction (the superposition of Reactions 2.2–2.5) is used throughout the analysis:

$$\begin{aligned}&0.065\ \text{Glc} + 0.007\ \text{Arg} + 0.004\ \text{Cys} + 0.020\ \text{Gln} + 0.003\ \text{His} + 0.007\ \text{Ile}\\&+0.010\ \text{Lys} + 0.002\ \text{Met} + 0.005\ \text{Phe} + 0.009\ \text{Thr} + 0.002\ \text{Trp} + 0.005\ \text{Tyr}\\&+0.010\ \text{Val} + 0.013\ \text{Ala} + 0.006\ \text{Asn} + 0.008\ \text{Asp} + 0.011\ \text{Gly} + 0.011\ \text{Leu}\\&+0.007\ \text{Pro} + 0.010\ \text{Ser} \rightarrow \text{DCM}_\text{a} + 0.005\ \text{Glu} + 0.076\ \text{CO}_2 + 0.240\ \text{H}_2\text{O}\\&\Delta H = -7.5\,\text{kJ/mol} \quad \Delta G = -2.8\,\text{kJ/mol} \quad (2.6)\end{aligned}$$

Wild-type catabolism

As is evident in the subreactions, anabolism uses no oxygen and has a small to negligible reaction energy. Cell growth is an irreversible process, however, and Gibbs free energy must be dissipated during growth. This ΔG is captured by the catabolic reaction. Experimentally, the sensible heat (enthalpy, ΔH) dissipated during cell growth can be measured with calorimetry, then converted to a ΔG dissipation by correcting for the entropy change.[39] Guan and Kemp measured the enthalpy dissipation in a batch CHO culture producing interferon (IFN-γ) along with lactate (Lac), CO_2, and NH_3 [101]. At different times in the batch, the authors deduced anabolic and catabolic reactions that matched the formation rates of products and cells as well as the observed heat dissipation. Reaction 2.7 was deduced at the end of the batch, when the culture was in decline and no further anabolism was taking place:

[39] Decades of such experiments for industrial microbes have generated an array of engineering correlations describing fermentation energetics for first-principles process design [88, 96–98]. Only limited examples exist in the literature of similar calorimetric experiments on animal cell cultures [99, 100]. This line of investigation seems to have lost steam ~20 years ago, probably in favor of metabolic flux analysis and omics techniques.

$$\begin{aligned}&1.0\ \text{Glc} + 0.13\ \text{Gln} + 1.28\ \text{O}_2 \rightarrow\\&\qquad 0.26\ \text{NH}_3 + 1.77\ \text{Lac} + 1.34\ \text{CO}_2 + 0.95\ \text{H}_2\text{O}\\&\qquad \Delta H = -681\,\text{kJ/mol} \quad \Delta G = -700\,\text{kJ/mol} \quad (2.7)\end{aligned}$$

Reaction 2.7 has a few notable aspects. First, its ΔH_r and ΔG_r are reasonably similar, i.e., the Gibbs energy of cell growth is mostly dissipated as heat rather than as entropy. This means that calorimetry measurements (of enthalpy) do not need significant correction for entropy. Second, for sufficiently

slow growth, it can be assumed that maintenance-associated catabolism is much larger than growth-associated catabolism; therefore this reaction primarily represents the former. Finally, this reaction appears to be a superposition of respiration, glycolysis, and some form of glutamine catabolism, e.g., glutaminolysis [102]. On a basis of one mole glucose, Reaction 2.7 can thus be specified with two degrees of freedom.[40] For example, as written, it has a lactate/glucose ratio (Lac/Glc) of 1.77 and glutamine/glucose ratio (Gln/Glc) of 0.13.

[40] These can be thought of as the metabolic "options" discussed above.

With the ΔH_r of anabolism being nearly zero, it can be assumed that the catabolic reaction proceeds at a rate that meets an observed sensible heat dissipation. Guan and Kemp [101] reported an enthalpy dissipation (metabolic power) in CHO culture of 22–25 pW/cell. In similar experiments on mouse hybridoma, they reported a metabolic power of ~34 pW/cell. West et al. [103] noted that this result is general: across all mammalian species, cells of similar size (e.g., CHO cells and hybridomas) have similar metabolic powers in vitro. West et al. further showed that in vitro metabolic power P_M can be scaled to hydrated cell mass with a 3/4 exponent:[41]

$$P_M = 0.148 M_c^{0.75} \quad (P_M \text{ in pW},\ M_c \text{ in pg}) \tag{2.8}$$

[41] P_M can also be thought of as the basal metabolic rate of the cell. For CHO cells of 1,167 pg (350 pg dry mass [85] and 70% intracellular water), the correlation of West et al. indeed predicts 30 pW/cell.

In West's relation, cells with wet mass 3,000 pg have a P_M of 60 pW, requiring that Reaction 2.7 proceed at 0.0077 mol/mol DCM_a-h.

An overall reaction that describes a wild-type metabolism can be obtained by assuming μ=0.029/h and combining the anabolic and catabolic contributions into a single reaction in mol/mol DCM_a-h:[42]

$$\begin{aligned} &0.333\ \text{Glc} + 0.342\ \text{O}_2 + 0.007\ \text{Arg} + 0.004\ \text{Cys} + 0.055\ \text{Gln} + 0.003\ \text{His} \\ &+0.007\ \text{Ile} + 0.010\ \text{Lys} + 0.002\ \text{Met} + 0.005\ \text{Phe} + 0.009\ \text{Thr} + 0.002\ \text{Trp} \\ &+0.005\ \text{Tyr} + 0.010\ \text{Val} + 0.013\ \text{Ala} + 0.006\ \text{Asn} + 0.008\ \text{Asp} + 0.011\ \text{Gly} \\ &+0.011\ \text{Leu} + 0.007\ \text{Pro} + 0.010\ \text{Ser} \rightarrow \\ &\quad \text{DCM}_a + 0.005\ \text{Glu} + 0.070\ \text{NH}_3 + 0.474\ \text{Lac} + 0.435\ \text{CO}_2 + 0.495\ \text{H}_2\text{O} \\ &\qquad \Delta H = -190\,\text{kJ/mol} \quad \Delta G = -190\,\text{kJ/mol} \end{aligned} \tag{2.9}$$

[42] Note that glutamate is produced by Reaction 2.4 in excess of what is required in Reaction 2.5.

The amino acids in Reaction 2.9 can be divided into essential amino acids (EAA) that must be supplied in culture media and a non-essential remainder (NAA) that can be synthesized from other available amino acids if not provided in media. At the bench scale, pre-formulated, defined medium DMEM/F12 is a good starting point for serum-free animal cell culture. DMEM/F12 has a general-use amino acid profile that must be supplemented with glutamine (which is not shelf-stable in solution) and any other deficient amino acids [104].

To validate the stoichiometry of Reaction 2.9 against that supplied in DMEM/F12,[43] Figure 2.2 compares their relative macronutrient profiles. With respect to glucose and the essential amino acids, the profiles compare quite favorably, requiring only minor supplementation of cysteine and tryptophan.

[43] High glucose, with glutamine and standard supplementation [105]. Note that amino acid hydrates/hydrochlorides, etc. were normalized to the pure formula.

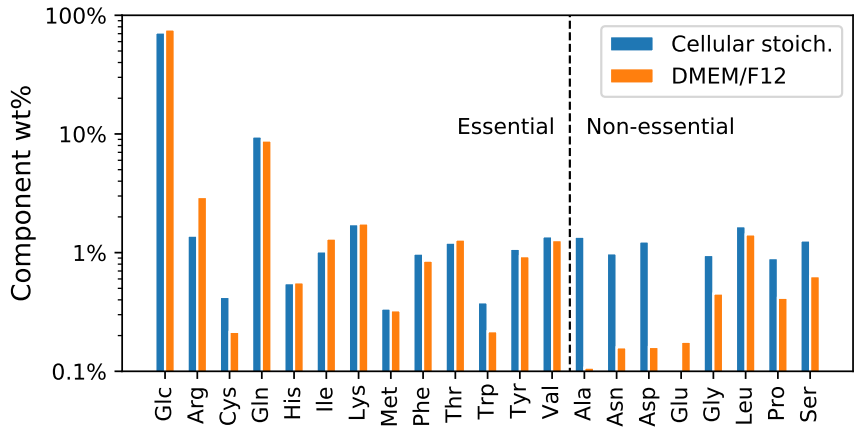

FIGURE 2.2: Macronutrient profile of Reaction 2.9 compared to that supplied by DMEM/F12.

DMEM/F12 would be deficient in several non-essential amino acids, but these could be supplemented with some level of art, based on cost and efficiency of uptake and synthesis.

The cell-specific oxygen uptake rate (SOUR), given in Table 2.2 for various cell sizes, provides a further validation of the growth stoichiometry of Reaction 2.9. For CHO cells (~1,000–2,000 pg), the reported SOUR is 0.25–0.30 pmol O_2/cell-h [106]. At a growth rate of μ=0.029/h, the SOUR predicted by Reaction 2.9 is in good agreement with this value (0.30 pmol O_2/cell-h for a 2,000 pg cell). Also note from Table 2.2 that the choice of cell mass affects both the cell-specific and the mass-specific rate of catabolism through Equation 2.8. The baseline mass of 3,000 pg was thus chosen to fall in the middle of the likely metabolic range.

ENHANCED CATABOLISM

Reactions 2.7 and 2.9 were given a "wild-type" designation and stand in for an unoptimized, inefficient cell line. The high lactate/glucose ratio and overactive glutamine metabolism in Reaction 2.7 are manifestations of a larger metabolic phenomenon known as the Warburg effect [102]. This phenomenon is a hallmark of rapidly proliferating animal cells, including CHO cells in culture and cancer cells in general. The cells choose to route glucose through glycolysis even when ample O_2 for respiration is provided, and to catabolize amino acids for energy even when ample glucose is provided. The Warburg effect is poorly understood; a prevailing hypothesis holds that it allows glycolysis and TCA-cycle intermediates from glucose and glutamine to be used in anabolism for rapid accumulation of biomass. Carbon-labeling experiments have shown that high availability of such intermediates is indeed important for fast growth, but the intermediates do not themselves end up as biomass carbon [94]. Either way, it seems likely[44] that an assumption of high metabolic efficiency is inconsistent with an assumption of high growth rate.

[44] And perhaps thermodynamically intuitive.

In Section 2.3, however, it will be demonstrated that the lactate and ammonia generation rates of Reaction 2.9 preclude this stoichiometry from reaching an economically high cell density. In biopharmaceutical cell culture, there are several strategies for optimizing growth stoichiometry through cell-line characterization and engineering. These include: selection for phenotypes with lactate reuptake capability;[45] genetic modification to express a glutamine synthetase enzyme;[46] and feedback control of glucose concentration and pH [107, 108]. The end result of such metabolic enhancements is difficult to forecast at this stage of analysis, but Reaction 2.10 stands for an enhanced catabolism, with Lac/Glc=0.50 and Gln/Glc=0.025:[47]

[45] Aerobic catabolism of Lac.

[46] Intracellular synthesis of Gln from Glu and NH_3.

[47] The reasoning for these parameters will become clear in Section 2.3.

$$1.0\ \text{Glc} + 0.025\ \text{Gln} + 4.61\ \text{O}_2 \rightarrow$$
$$0.050\ \text{NH}_3 + 0.50\ \text{Lac} + 4.63\ \text{CO}_2 + 4.55\ \text{H}_2\text{O}$$
$$\Delta H = -2,225\ \text{kJ/mol} \quad \Delta G = -2,271\ \text{kJ/mol} \qquad (2.10)$$

For 60 pW/cell, this catabolism proceeds at 0.0024 mol/mol DCM_a-h. The enhanced overall reaction is thus:

$$0.147\ \text{Glc} + 0.378\ \text{O}_2 + 0.007\ \text{Arg} + 0.004\ \text{Cys} + 0.022\ \text{Gln} + 0.003\ \text{His}$$
$$+0.007\ \text{Ile} + 0.010\ \text{Lys} + 0.002\ \text{Met} + 0.005\ \text{Phe} + 0.009\ \text{Thr} + 0.002\ \text{Trp}$$
$$+0.005\ \text{Tyr} + 0.010\ \text{Val} + 0.013\ \text{Ala} + 0.006\ \text{Asn} + 0.008\ \text{Asp} + 0.011\ \text{Gly}$$
$$+0.011\ \text{Leu} + 0.007\ \text{Pro} + 0.010\ \text{Ser} \rightarrow$$
$$\text{DCM}_a + 0.005\ \text{Glu} + 0.004\ \text{NH}_3 + 0.041\ \text{Lac} + 0.455\ \text{CO}_2 + 0.613\ \text{H}_2\text{O}$$
$$\Delta H = -190\ \text{kJ/mol} \quad \Delta G = -189\ \text{kJ/mol} \qquad (2.11)$$

In the context of nutrient utilization, it is worth noting that Reaction 2.11 only reduces the amount of glucose and glutamine consumed in the growth of 1 mol DCM_a by about 60% each over Reaction 2.9 (see Table 2.3). Even if full respiration were assumed, eliminating Lac and NH_3 entirely, the additional improvement is marginal. In either case, the relative O_2 uptake and CO_2 generation rates are *higher* with the more efficient metabolism. These have implications for bioreactor design, to be discussed in Section 2.3.

Table 2.3: Stoichiometric uptake (negative) or generation (positive) per mole of DCM_a for Reactions 2.9, 2.11, and full respiration (hypothetical).

	2.9	2.11	Full resp.
Glc	-0.33	-0.15	-0.13
Gln	-0.05	-0.02	-0.02
O_2	-0.34	-0.38	-0.38
CO_2	0.44	0.46	0.46

Complex amino acid sources

At the hypothetical scale of cultured meat, plant protein hydrolysates may be more cost-effective and sustainable than amino acids produced individually by fermentation. Figure 2.3 presents conceptualized material and energy flows in a cultured-meat future, beginning from sunlight, CO_2, and fossil fuel.[48] These fundamental sources, and the plants produced from them, are already available at scales ranging from huge to practically infinite. Similarly, as a byproduct of soybean oil extraction, soybean meal is already produced at extremely large volumes and is currently used as animal feed. Assuming a reduced-animal future where soybeans are still grown for oil, new outlets will have to be found for this material.

[48] Former sunlight and CO_2.

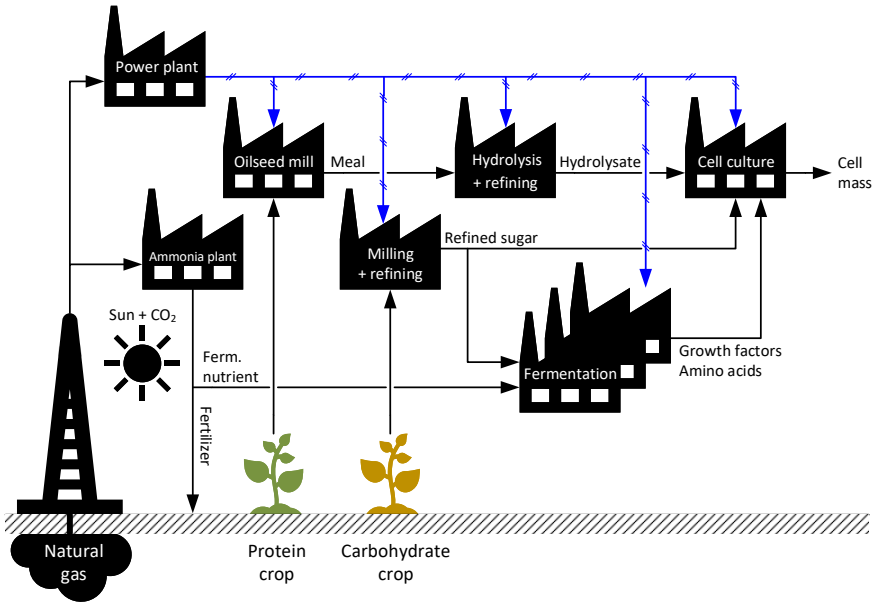

FIGURE 2.3: Material flows upstream of the cell-culture facility, starting from sunlight, CO_2, and natural gas.

Figure 2.4 compares the amino-acid profile of the protein synthesis reaction (2.5) to that of U.S. soybean meal [109]. The EAA profiles are similar enough that if a quantitative hydrolysate of soybean meal were fed at 1.36 mol per mol protein,[49] all EAA requirements could be met except for glutamine (which must be fed separately in any case) and about 75% of tyrosine.[50] With aggregate compounds standing for the soy hydrolysate and the unused amino-acid fraction (including Glu formed in Reaction 2.4), the following alternate reactions can be derived. With the wild-type catabolism of Reaction 2.7:

$$\begin{aligned} &0.333\ \text{Glc} + 0.342\ \text{O}_2 + 0.055\ \text{Gln} + 0.004\ \text{Tyr} \\ &+0.192\ \text{Soy Hydr.}\ (\text{C}_{4.81}\text{H}_{9.49}\text{O}_{2.68}\text{N}_{1.28}) \rightarrow \\ &\qquad \text{DCM}_\text{a} + 0.070\ \text{NH}_3 + 0.474\ \text{Lac} + 0.435\ \text{CO}_2 + 0.495\ \text{H}_2\text{O} \\ &\qquad\qquad +0.142\ \text{Unused AA}\ (\text{C}_{2.63}\text{H}_{4.86}\text{O}_{1.75}\text{N}_{0.60}) \\ &\qquad\qquad \Delta H = -197\,\text{kJ/mol} \quad \Delta G = -205\,\text{kJ/mol} \end{aligned} \tag{2.12}$$

And with the enhanced catabolism of Reaction 2.10:

$$\begin{aligned} &0.147\ \text{Glc} + 0.378\ \text{O}_2 + 0.022\ \text{Gln} + 0.004\ \text{Tyr} \\ &+0.192\ \text{Soy Hydr.}\ (\text{C}_{4.81}\text{H}_{9.49}\text{O}_{2.68}\text{N}_{1.28}) \rightarrow \\ &\qquad \text{DCM}_\text{a} + 0.004\ \text{NH}_3 + 0.041\ \text{Lac} + 0.455\ \text{CO}_2 + 0.613\ \text{H}_2\text{O} \\ &\qquad\qquad +0.142\ \text{Unused AA}\ (\text{C}_{2.63}\text{H}_{4.86}\text{O}_{1.75}\text{N}_{0.60}) \\ &\qquad\qquad \Delta H = -197\,\text{kJ/mol} \quad \Delta G = -204\,\text{kJ/mol} \end{aligned} \tag{2.13}$$

[49] To match on threonine.

[50] Soybeans are not the only nitrogen-rich crop; peas and other legumes could also be used, as could extracts of yeast or indeed algae [14]. Conceivably, a blend of hydrolysates could be designed to fully replace all exogenous amino acids (with the probable exception of Gln) in cell-culture media without supplementation.

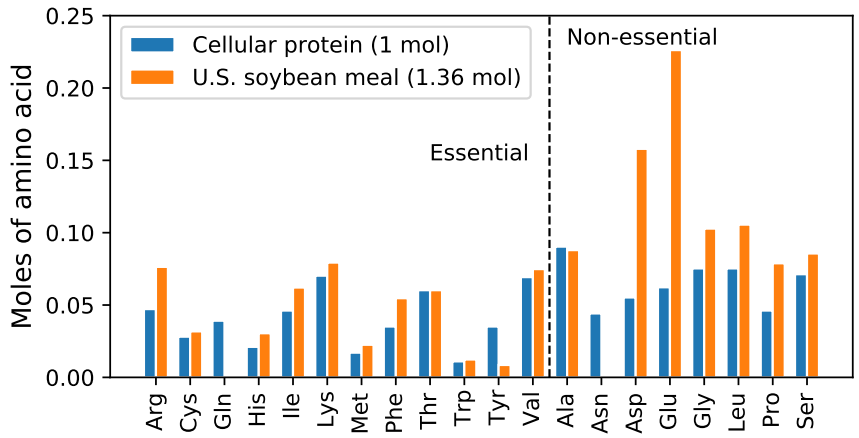

FIGURE 2.4: Amino-acid profiles of cellular protein (Reaction 2.5) and U.S. soybean meal.

2.3 Bioreactor design principles and limitations

Section 2.1 established practical upper limits for attainable cell density as dictated by a maximum suspension viscosity. Whether or not a given bioreactor can support this viscosity-limited cell density depends on its capacity for oxygen transfer, its characteristic mixing efficiency, the rate of inhibitor accumulation, and other factors. For example, the conceptual process of van der Weele and Tramper [4] considered a 20 m^3 stirred-tank bioreactor (STR) as the final production vessel, operating in fed-batch mode with a final cell density of 128×10^6/mL.[51] Individually, this bioreactor volume and cell density are at or near world-record levels (at least for CHO culture), though a combination of the two extremes has not been reported. In suspended CHO culture, typical fed-batch cell densities are rather closer to 10×10^6–30×10^6/mL at any volume, which is sufficient for protein production at modern titers [110]. Cell densities on the order of 100×10^6/mL are more consistent with high-density perfusion cultures.

Figure 2.5 presents a sketch of an STR with construction aspect ratio H/T of 3, two rotating impellers of diameter $D=T/3$, and a final working volume of 80%. In a bubble-column or airlift bioreactor, the aspect ratio is generally higher (H/T=6–10) and no impeller is present. Gas bubbles are used to transfer O_2 into solution and strip CO_2 out in all large bioreactor designs (>∼1 m^3). If the bioreactor is equipped with an impeller, the stirring action can be used to enhance this gas-liquid mass transfer. Stirring and sparging are thus the main operational degrees of freedom in a bioreactor. The gas sparge rate is usually quantified in terms of vvm (standard volumes of sparge gas per volume of liquid per minute) or superficial velocity u_s (m/s, the actual volumetric flow rate of gas divided by the bioreactor cross-sectional area). The stirring or agitation rate is usually quantified as power input per unit of liquid volume (P/V, in W/m^3) or per unit of liquid mass ($\bar{\varepsilon}=P/\rho V$, in W/kg.)

[51] At their assumed cell size of 1,000 pg, this is equivalent to a mass density of 128 g/L, or about halfway to the viscosity limit.

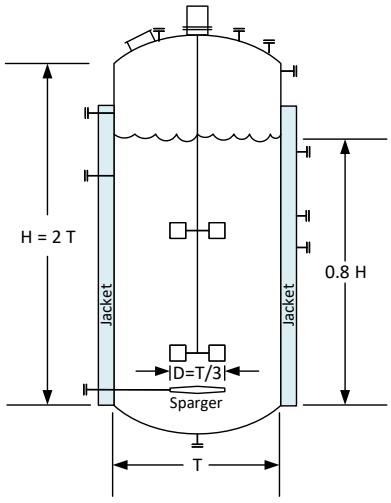

FIGURE 2.5: Schematic of a stirred-tank bioreactor (STR) with external cooling jacket. The bioreactor diameter is denoted T (for "tank") and impeller diameter D.

In sparged bioreactors, cells in suspension tend to attach to a rising bubble's exterior or get dragged in its wake. If cells are too close to the bubble when it ultimately bursts at the top of the bioreactor, they will incur high shear forces. Due to their larger size and lack of a rigid cell wall, animal cells are particularly susceptible to these forces, which can cause physiological changes including death [52]. Under practical cell-culture conditions, bubble-induced shear forces are orders of magnitude higher than shear forces from a rotating impeller. Consensus in the literature therefore holds that the threat of shear from agitation is probably overstated,[52] while that from bursting and collapsing bubbles is real [111]. Gas sparging in animal cell culture is thus used judiciously.[53]

Judicious sparging rules out the bubble-column bioreactor, which has not been successfully used for animal cell culture beyond the bench scale. The airlift reactor with a liquid downcomer has been used for low-density cell culture up to 10 m^3, though much smaller reactors of 1–2 m^3 are more common. At larger scale, O_2 depletion in the ungassed downcomer can become prohibitive [114].[54] Gently sparged STRs are thus preferred. Physical constraints of the STR that limit the ultimate cell density will be discussed below, using bioreactor design concepts.

[52] For suspension culture but not necessarily for microcarrier culture.

[53] A common feature of record-high-density animal cell cultures is that they are not sparged at all, with O_2 instead supplied via the bioreactor headspace [112, 113].

[54] Li et al. [115] offered a CFD model of a hypothetical 300 m^3 airlift reactor for CHO cell culture. Their simulations indicated 46% (3.2 mg/L) dissolved O_2 at the top of the sparged column, about half of which was consumed by cells during a 20-second trip through the downcomer. Upon review, however, I find that the SOUR assumed in the simulation was only half of what was actually observed in the authors' own reference [116], and 20% of that predicted by Reaction 2.9 and other references [106]. With this correction, the simulations would instead have concluded that available O_2 was depleted and that the cells were stressed at the downcomer exit.

O_2 mass transfer

Industrial fermentor scale-up is often approached as a constant O_2 mass transfer problem [38, 117]. Here, the volumetric OTR is modeled as the product of a mass transfer coefficient $k_L a$ and a concentration driving force, which is the deviation of the dissolved oxygen concentration C_{O_2} (also known as DO) from its saturated concentration $C^*_{O_2}$. The saturated concentration is given by Henry's law:

$$C^*_{O_2} = y_{O_2} P \times H_{O_2} \tag{2.14}$$

If the fermentor (or bioreactor) is sparged with air, y_{O_2} at the bottom is 21%. At the top, y_{O_2} is determined with an O_2 mass balance. In a very tall vessel, the local pressure P may be significantly higher at the bottom than at the top. The average driving force is thus usually expressed as a log-mean difference over top and bottom:

$$\text{OTR} = k_L a \frac{\left(C^*_{O_2} - C_{O_2}\right)_{\text{btm}} - \left(C^*_{O_2} - C_{O_2}\right)_{\text{top}}}{\ln\left[\frac{\left(C^*_{O_2} - C_{O_2}\right)_{\text{btm}}}{\left(C^*_{O_2} - C_{O_2}\right)_{\text{top}}}\right]} \tag{2.15}$$

To determine $k_L a$, the correlation of Xing et al. [106] was developed for CHO cell-culture media at 37 °C:

$$k_L a\ [\text{s}^{-1}] = 0.075 (P/V)^{0.47} (u_s)^{0.8} \tag{2.16}$$

As mentioned in Section 1.2, typical limits on sparging and agitation are much lower for animal cell culture than they are for high-density fermentation. STR

design rules for cell culture recommend scale-up at a constant but low vvm, to ensure constant CO_2 stripping when the respiratory quotient is close to 1 [111]. Guidance on maximum sparge rate is usually <0.1 vvm [54, 118], though the O_2 demand of most low- to medium-density cell cultures can usually be satisfied with much less.[55] For agitation, historical guidance has been to limit the impeller rotation to a tip speed of <2 m/s. The theory behind this guidance holds that a low tip speed avoids bubble dispersion (i.e., slicing), which could potentially create bubbles small enough to collapse in the liquid phase, creating locally high shear [120].

However, neither tip speed nor vvm has a constant hydrodynamic effect across reactor sizes. For the present analysis, these design limits are recast into a more constant frame that directly impacts O_2 mass transfer as determined by Equation 2.16. Sparging is limited to a superficial velocity of 0.006 m/s at the top of the vessel.[56] For the agitation limit, more modern analyses prefer the explanation that any cell damage caused by the impeller is more likely a result of turbulent eddies on the length scale of a single cell (~20 μm) [121]. In Kolmogorov's theory, the turbulent eddy length λ_K is a function of turbulent energy dissipation ε_T, with the smallest eddies occurring very close to the impeller at $\varepsilon_{T,max}$:

$$\lambda_K = \left(\nu^3/\varepsilon_{T,max}\right)^{1/4} \tag{2.17}$$

where $\nu=\eta/\rho$ is the kinematic viscosity of the medium fluid.[57] For impellers with relative diameter $D=T/3$, Nienow recommends $\varepsilon_{T,max}=50\bar{\varepsilon}_T$ [123].[58]

With sparging and agitation both at their maximum recommended level, a maximum attainable mass transfer coefficient can be estimated from Equation 2.16, and a maximum OTR from Equation 2.15. At the top of the bioreactor, the DO is taken to be 1.4 mg/L (20% atmospheric saturation) for animal cells. The DO at the bottom is taken to be this value times the bottom-top pressure ratio (P_{top}=5 psig and P_{btm} is a function of liquid height).[59] The cell density is thus limited to the point where the culture's OUR (based on catabolic O_2 demand) is equal to the bioreactor's maximum OTR.

CO_2 MASS TRANSFER

Respiring cells release CO_2, which lowers the broth pH. High CO_2 levels require counteraction with high concentrations of buffering agents, which may in turn cause osmolality constraints [111]. CO_2 mass transfer from the liquid phase to passing bubbles follows a relation much like Equation 2.15, and the CO_2 transfer rate (CTR) is approximately equal to the OTR. Since the respiratory quotient of growth is approximately 1, it follows that CO_2 is stripped from the liquid phase at a rate equal to its generation, and its liquid concentration is a function of OTR, which is in turn a function of the bioreactor sparge rate.

This liquid concentration is typically measured in terms of pCO_2, or the CO_2 partial pressure in equilibrium with the liquid phase.[60] In CHO culture, it has been shown that productivity is maximized when pCO_2 is maintained in

[55] 0.01 vvm is common [53]. Additionally, copious surfactants for foaming and shear control are typically recommended to minimize cell damage in vigorously sparged cultures, e.g., Pluronic F-68 at >0.5 g/L [111]. Though not especially toxic [119], F-68 is probably not very tasty, and vigorous sparging should be avoided.

[56] This sparge rate is equivalent to 0.1 vvm in a 20 m^3 bioreactor with the geometry in Figure 2.5, sparged with air and having 5 psig back pressure.

[57] Not the bulk suspension viscosity [122].

[58] Power input P can also be expressed as a function of the impeller power number N_p and its rotational speed N (rpm) [124]:

$$P = 2N_p N^3 \rho_L D_s^5$$

With this relation, it can be shown that an eddy length of 20 μm is indeed reached at a tip speed of ~2 m/s in a 20 m^3 bioreactor.

[59] In a well-mixed STR, the DO gradient is probably less severe than this. For the vessel sizes considered here, however, any errors introduced by this assumption are small (<0.5%).

[60] $pCO_2 = y_{CO_2} P_{back}$, i.e., the bioreactor back pressure times the mole fraction of CO_2 in the outlet gas, which is computed from a mass balance.

the range of 40–100 mbar; above 130 mbar, growth inhibition is noted [125]. If the bioreactor is well mixed, it can be assumed that gradients in CO_2 liquid concentration are small. With sparging fixed at u_s=0.006 m/s, the cell density must thus be limited such that the CO_2 generation rate does not cause pCO_2>100 mbar.

A corollary to the above discussion: Growth inhibition or cell density limits caused by high pCO_2 cannot easily be mitigated with metabolic efficiency improvements. Consider the earlier catabolic parameters of Lac/Glc and Gln/Glc. No matter how these are specified, the respiratory quotient (CO_2/O_2) of the overall growth reaction will remain ~1 and the CO_2 stripping rate will remain roughly equal to the O_2 transfer rate. The only way to circumvent a pCO_2 limit in a sparged bioreactor is to sparge harder, possibly to the point of cell death. This limitation may preclude the scale-up of animal cell culture into extremely large bioreactors.

- HEAT TRANSFER

As observed in Reactions 2.9 and 2.11, animal cell growth is only slightly exothermic. At low cell density and/or in a small bioreactor having a high surface area/volume ratio, it is common for heat to be lost to the surroundings faster than it is generated in the culture, such that the culture requires heating rather than cooling to maintain a constant 37 °C. This requirement stands in rather stark contrast to high-OUR microbial fermentation, which can have tremendous heat removal loads that may limit the ultimate fermentor size on scale-up when, e.g., a cooling jacket no longer provides enough heat transfer area and aseptic requirements preclude the use of internal coils or external circulation through a heat exchanger [126]. For animal cells in low-OUR suspension culture, heat transfer is not anticipated to pose a significant problem in ≤200 m^3 bioreactors.

- MIXING

In the STR, a mixing time can be estimated with Equation 2.18, which is based on agitator power dissipation and does not require many details of the bioreactor or of the fluid being stirred [121]:

$$t_m \approx 6T^{2/3}(P/V\rho_L)^{-1/3}(D/T)^{-1/3}(H_L/T)^{2.5} \tag{2.18}$$

Here, H_L is the instantaneous liquid height. A good rule of thumb is that the mixing time should be less than $1/k_La$ [127]. At longer mixing times, $t_m > 1/k_La$ would indicate either that dissolved O_2 is not being quickly transported away from the bubble (which reduces the effective concentration driving force), or that concentration gradients created by respiring cells may arise faster than they can be canceled out by stirring.

- WASTE CATABOLITE INHIBITION

In fed-batch operation, which is common in large-scale cell culture, a bioreactor is inoculated into fresh medium at less than full volume (Figure 2.6a). As

the culture grows and the initial medium is depleted, concentrated nutrients are added to replenish. The liquid volume in the bioreactor increases until it reaches a maximum working volume and the batch is harvested. At the start of a fed batch, cell growth may proceed at the maximum rate μ_{max}. As the increasing cell density drives the bioreactor to one or more limits, growth may slow. In fed-batch processes for upstream biopharmaceuticals production, the accumulation of toxic and growth-inhibiting waste metabolites like ammonia and lactate is a more frequently encountered limit than the physical limits discussed so far [128]. In many such processes, growth inhibition late in the batch is not necessarily a concern if the limiting cell density is sufficient for protein accumulation[61] and this limit and corresponding low growth rate can be maintained without cell stress or death. However, for bulk cell production at typical animal-cell growth rates, it would be economically unfavorable to run a fed batch very long after μ drops significantly below μ_{max}. The fed-batch start/end conditions must therefore be set carefully such that μ_{max} is maintained throughout.[62]

The inhibiting concentrations of ammonia and lactate vary with cell line, as do the rates at which cells produce these. A range of 2–10 mmol/L NH_3 has been reported for mammalian cells [90], while lactate inhibition levels are generally an order of magnitude higher. For analysis purposes, consider the limits of 5 mmol/L NH_3 and 50 mmol/L lactate. Figure 2.7a presents a simulation of a fed batch in a 20 m^3 STR where the batch end conditions have been set to a final liquid volume of 16 m^3 (80% working volume) after 6 doublings of the initial cell mass (as suggested in [4]) and a limiting concentration of either NH_3 or lactate (whichever is reached first). The culture in Figure 2.7a follows Reaction 2.9.[63] To meet these end conditions, the batch must be started very close to full (76% WV) and at a very low density of 0.03×10^6/mL (0.09 g/L). This is well below the general recommendation for starting cell density, which is $\sim0.1\times10^6$/mL [129]. Below this density, cultures of many animal cell lines will go into a lag phase (i.e., the initial growth rate will be very low) or die entirely. After 6 doublings, the final cell density at 16 m^3 is only 1.8×10^6/mL (5.4 g/L).

To avoid lag, the recommended split in animal-cell propagation is a multiple of 5–10× (2–3 doublings) per stage [129]. Figure 2.7a (solid lines) shows a shorter simulation limited to 2 doublings. Here, the batch can be started at a more reasonable cell density of 0.6×10^6/mL but the final density is still 2.3×10^6/mL (7.0 g/L). Neither simulation yields more than 100 kg of wet cell mass for the effort. In fact, there is no practical way to reach an economically high cell density in fed-batch operation with a metabolism as inefficient as Reaction 2.9. At any appreciable starting density, the ammonia inhibition limit would be reached in a matter of hours.

As discussed in Section 2.2, the wild-type Reaction 2.9 (Lac/Glc=1.77 and Gln/Glc=0.13) has relatively high rates of lactate and ammonia generation, which is common for rapidly proliferating animal cells. To model a more efficient stoichiometry, consider a (significant) improvement to Lac/Glc=0.94 and

[61] 1×10^6–30×10^6 cell/mL, depending on titer [110]

[62] An example of this is given in Appendix A, in the discussion surrounding Figure A.3.

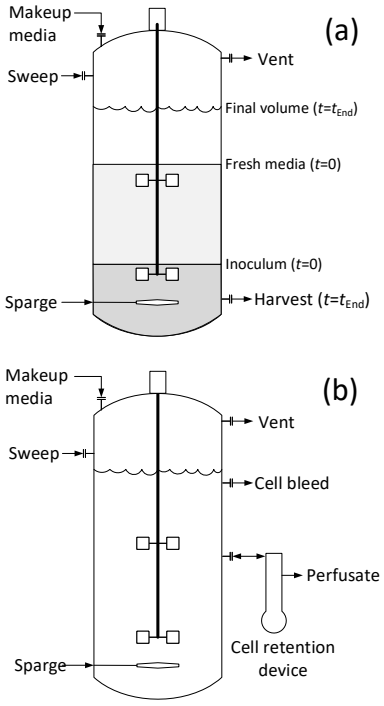

FIGURE 2.6: Bioreactor operating modes. (a) Fed batch. (b) Perfusion.

[63] Additional details of the fed-batch simulation procedure will be given in Section 4.1.

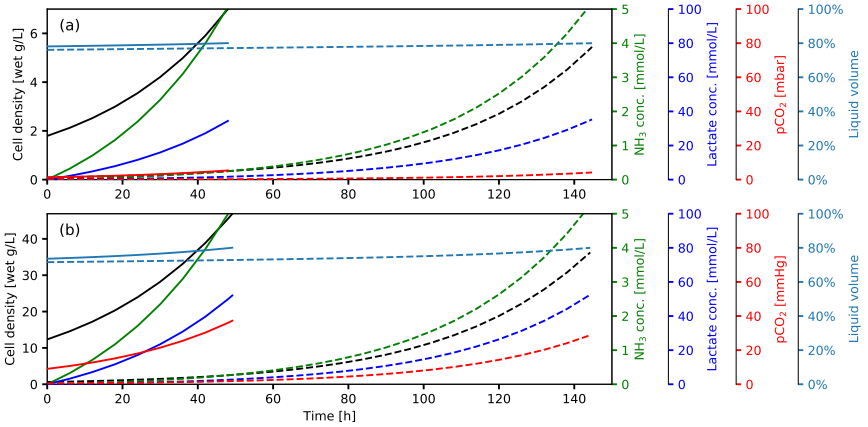

FIGURE 2.7: Fed-batch simulations in an air-sparged 20 m^3 bioreactor with 80% max working volume and 5 mmol/L max NH_3 concentration. Dashed lines represent 6 doublings; solids lines represent 2 doublings. (a) Lac/Glc=1.77 and Gln/Glc=0.13. (b) Lac/Glc=0.94 and Gln/Glc=0.047.

Gln/Glc=0.047. Figure 2.8c shows a fed-batch simulation with this enhanced metabolism, which begins at ~14.3 m^3 and a cell density of 0.2×10^6/mL (0.6 g/L). After 6 doublings, the final cell density is 12×10^6/mL (36.3 g/L). If the number of doublings is likewise limited to two, a final density of 16×10^6/mL (47 g/L) can be reached. In this case, the batch endpoint is reached simultaneously with the O_2 mass transfer limit.

These simulations can be extended to find the maximum cell density that meets all above constraints at the end of a fed batch.[64] Figure 2.8a presents this maximum supported cell density in air-sparged STRs from 1–200 m^3. At the baseline volume of 20 m^3, the O_2- and mixing-limited densities are roughly equal at ~50 g/L.[65] In fact, the catabolic parameters above (Lac/Glc=0.94 and Gln/Glc=0.047) were selected to ensure that the NH_3 constraint would not be incurred before this point. These are the maximum catabolic inefficiencies that permit a 20 m^3 fed batch to stay under the likely inhibition levels of lactate and ammonia such that the inhibitor-limited cell density is reached simultaneously with another limitation (mixing, in this case). At smaller volume, the O_2 and NH_3 limits dominate; at larger volume, the mixing time dominates.

The pCO_2 limit is not incurred when sparging with air, though from Figure 2.8a it is noted to have a strong dependence on bioreactor volume. This is due to the constraint that was placed on the superficial velocity of the sparge gas (0.006 m/s) in the constant-OTR approach. In sparged batch or fed-batch culture, CO_2 is only removed by stripping into the bioreactor exhaust. A constant-vvm scale-up approach can enhance stripping to mitigate the pCO_2 limitation but may lead to excessive bubble-induced shear at very large volume. In any event, the maximum supported cell density in an air-sparged STR is only a fraction of the viscosity-limited density of 258 g/L.

[64] Constraints summary:

- Volume fraction $\phi<0.25$
- k_La such that OTR=OUR at $u_s=0.006$ m/s and $\lambda_K\geq20$ μm
- $pCO_2<100$ mbar
- Mixing time $t_m<1/k_La$
- $NH_3<5$ mmol/L
- Lac<50 mmol/L

[65] For a 1,500 pg CHO cell, this mass density would be equivalent to $\sim30\times10^6$/mL.

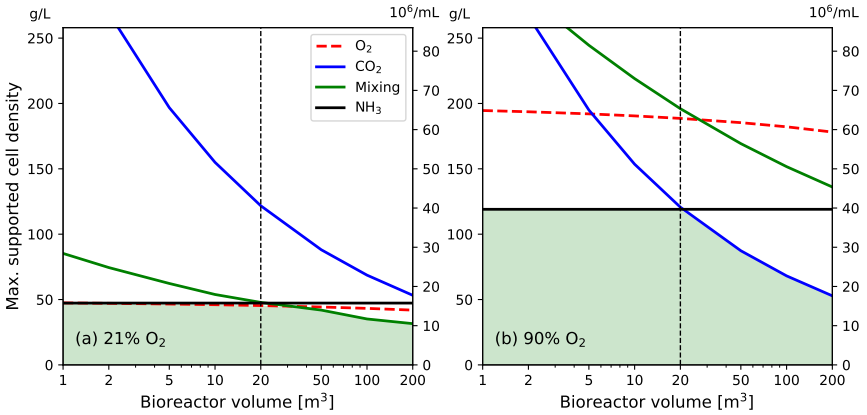

FIGURE 2.8: Maximum cell density achievable in fed-batch suspension culture at various bioreactor sizes and with various limitations. The limiting density for each constraint was computed independently of the others, and the density axis is truncated at the viscosity limit (Table 2.2). (a) 21% O_2 sparge; Lac/Glc=0.94 and Gln/Glc=0.047. (b) 90% O_2 sparge; Lac/Glc=0.50 and Gln/Glc=0.025.

HIGH-PURITY OXYGEN

Although an OTR approaching 200 mol O_2/m^3-h is common in an air-sparged STR fermentor, the sparging and agitation limits of a cell culture bioreactor effectively limit OTR to <~25 mol O_2/m^3-h when air is used. To obtain a higher OTR (and thus a higher cell density), oxygen or O_2-enriched air must instead be sparged. In biopharmaceuticals manufacturing, the use of high-purity oxygen is a simple economic decision. With such valuable products and such small volumes, the benefits of increased cell density and product titer far outweigh the cost of gas. At the scale of cultured meat, however, the economics are less clear. Though a sufficiently large consumer (one that requires O~1,000 kTA, such as a steel mill) can contract with an industrial gas company to construct a dedicated air separation unit that provides pure O_2 at ~$0.04/kg, the demand of a cultured-meat facility would not be nearly this large. At smaller scale, high-purity merchant oxygen (delivered in trucks) is far too expensive, given that as much as 80% of it will be vented from the bioreactor. The scale of a cell-culture facility would be more consistent with on-site production of 90% O_2 in a vacuum pressure-swing adsorption (VPSA) unit, which has a size-dependent effective cost of $0.10–0.20/kg O_2 [130]. From Reaction 2.11, the stoichiometric demand of O_2 is 0.2 kg/kg wet cell mass. Even if 80% of sparged O_2 were lost through the reactor vent, a single facility producing 50 kTA of bulk cell mass could be served with a ~50 kTA (4,000 Nm^3/h) oxygen unit[66] and the cost contribution to cell mass would be <$0.20/kg.

Reaction 2.11 was cited above because, to take advantage of higher O_2 purity, the catabolic efficiency must be further enhanced to Lac/Glc=0.50 and Gln/Glc=0.025.[67] Figure 2.8b repeats the cell density calculation with 90% O_2 sparge gas and the enhanced metabolism, which was selected to cause the NH_3 limit to occur at the same cell density as the pCO_2 limit at 20 m^3. The

[66] Well within available capacity [131].

[67] These are the parameters used in Reaction 2.10. Note that the ratio of Lac/Glc to Gln/Glc must be 20 for the limits of 5 mM NH_3 and 50 mM Lac to be reached simultaneously.

maximum supported cell density at this volume is 40×10^6/mL (120 g/L). At larger volume, the pCO_2 limit is incurred, but the supported cell density with 90% O_2 remains significantly higher than with air.[68]

[68] The mixing limitation has been pushed to higher cell density because the criterion for this limit is $t_m < 1/k_La$, and k_La can be much lower when the O_2 concentration driving force is high (Equation 2.15).

Perfusion culture

Perfusion technology was developed as a higher-intensity alternative to batch or fed-batch cultures in biopharmaceuticals manufacturing. In perfusion culture (Figure 2.6b), the contents of the bioreactor are continuously cycled through a cell retention device, e.g., a filter, gravity settler, or centrifuge. Cells are returned to the bioreactor while the spent media perfuses out. Lost nutrients are replaced by fresh media. Via the perfusate stream, extracellular products are continuously harvested and inhibitors are continuously removed. In many cases, the removal of inhibitors permits higher cell densities than are achievable in fed-batch operation—in commercial perfusion cultures of CHO cells, 100×10^6/mL is not unheard of, though 50×10^6/mL is more common.

Because they are limited by the capacity and efficacy of the cell retention device, perfusion culture volumes are necessarily much smaller than the volumes discussed above for fed-batch cultures. The alternating tangential-flow (ATF) filter has near 100% cell retention and is commonly used for high cell-density applications; its capacity is limited by the residence time of cells inside the unaerated dead volume of the filter and its connecting piping [132]. The largest available can run at perfusion rates up to 1,000 L/d [133], though practical perfusion rates may be lower, depending on cell density, culture viscosity, and the desired cultured duration.[69] According to its manufacturer (Repligen), the Xcell ATF 10 is capable for bioreactors up to 2 m^3 in a dual-filter configuration, though several review papers indicate that commercial perfusion culture sizes are rather closer to the 0.5–1 m^3 range [134, 135]. If the perfusion rate is expressed in units of reactor volumes per day,[70] Table 2.4 gives some practical limits for perfusion rate in various bioreactor sizes.

[69] Filters foul faster at a higher perfusion rate.

[70] Common units are RV/d, or d^{-1}.

At steady-state operation, cells are bled from the bioreactor (see Figure 2.6b) to maintain growth rate at μ_{max} and avoid stress or senescence. At a growth rate of 0.029/h, the cell bleed increases the effective perfusion rate by 0.5–0.6/d, depending on cell density.[71] In principle, a semi-continuous cell bleed could feed downstream processing operations such as tissue culture. This downstream equipment could thus be rationally sized to the plant's average output, instead of being massively oversized to process a fed-batch harvest before it dies. With continuous inhibitor removal, it would also seem that perfusion might enable higher-density culture of metabolically inefficient cell lines.

Table 2.4: Practical maximum perfusion rates with ATF cell retention, at various bioreactor sizes.

Volume	ATF	Perf. rate
0.5 m^3	1×ATF 10	2.0/d
1 m^3	1×ATF 10	1.0/d
1 m^3	2×ATF 10	2.0/d
2 m^3	2×ATF 10	1.0/d

[71] At relatively low cell density, devices with higher throughput but lower cell retention than an ATF (e.g., a centrifuge or gravity settler) could be used for bulk cell culture if the perfusate and cell bleed streams were combined into a single outlet. However, the cell density achievable with these devices is much lower than the >100 g/L density required for economic cell production [133].

Figure 2.9 presents curves of achievable cell density in perfusion cultures as a function of perfusion rate. The wild-type Reaction 2.9 generates 2 mmol NH_3/mol DCM_a-h. If NH_3 were removed via the perfusate stream at a steady-state NH_3 concentration of 5 mmol/L, then at a perfusion rate of 2.0/d it can be computed that the inhibition limit is reached at a cell density of only 20 g/L (6.8×10^6 cell/mL). This density is significantly higher than predicted

for a fed-batch process, as shown in Figure 2.7a, but is still not high enough to be economic. With the more efficient Reaction 2.11, the O_2-limited cell density of 195 g/L (65×10^6 cell/mL; see Figure 2.8) can be achieved at a perfusion rate of 1.0/d. Furthermore, this metabolism could be scaled into a 2 m^3 bioreactor, as 1.0/d is within the acceptable range of perfusion rates at that scale (Table 2.4).[72]

Note that the performance of a given cell line in perfusion culture, i.e., its ultimate cell density and residual growth rate at this ultimate density (likely less than μ_{max}), are not predictable without some characterization; perfusion operations are thus not absolved from the development efforts cited above for fed-batch. To summarize, while perfusion generally enables a higher cell density than a fed-batch culture, it does not make a poor metabolism cost-effective. Cell-line engineering and characterization are thus equally important for either technology.

[72] Given the linear relationship between density and perfusion rate in Figure 2.9, it follows that any metabolism can be coaxed to high density with a sufficiently high perfusion rate. Indeed, in the experiments of Clincke et al. [112], which produced CHO cells at $>130\times10^6$/mL (reaching the viscosity limit of the ATF pump), the culture volume was 4 L and the perfusion rate as high as 6/d.

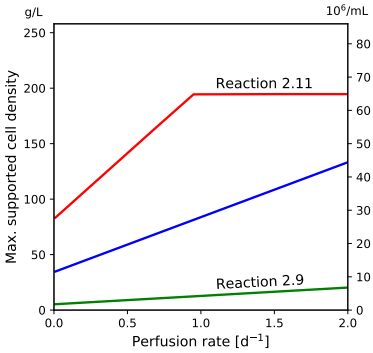

FIGURE 2.9: Maximum cell density achievable in perfusion suspension culture as a function of perfusion rate (90% O_2). The catabolisms implied in Reactions 2.9 and 2.11 are compared. The intermediate (blue) curve has Lac/Glc=0.94 and Gln/Glc=0.047, as used in Figure 2.8a.

MICROCARRIERS

To grow cells with strict anchorage dependence in a suspension-like culture, microscopic (100–300 μm) beads of, e.g., collagen, polymer, or glass known as microcarriers are used [136]. Many of the bioreactor design concepts above are not valid for microcarrier culture, however, as the hydrodynamics of microcarrier cultures in stirred tanks are significantly different from those of suspension cultures. Specifically, sparging and stirring rates are significantly lower in microcarrier cultures, where cells may be damaged by impeller-bead and bead-bead collisions [111].

In applications where cells are to be recovered, microporous microcarriers are used. Cells grow on the exterior surface of the bead and can be released with the enzyme trypsin.[73] Microporous carriers are used to produce (e.g.) influenza vaccines in STRs up to 6 m^3. To protect cells from bubbles, such cultures are not sparged and the cell density is thus very low ($<2\times10^6$/mL). When recovery of cells is not critical, macroporous carriers can be used. The cells grow inside pores on the bead where they are protected from bubble shear and collisions. Such cultures may be directly sparged to obtain a slightly higher cell density on the order of 3×10^6–5×10^6/mL. The cells in macroporous carriers cannot be released, but some bead materials can be dissolved chemically or enzymatically. In general, no more than 70–90% of the cells are recoverable in this way [137].

Microcarriers are well suited for perfusion processes where various density- and sized-based retention devices can be used. Notably, dense and rigid carriers can be used in a fluidized bed bioreactor [136] where fresh medium is circulated around a captive bed of carriers. Cell densities upwards of 200×10^6/mL have been attained for CHO cells in a fluidized bed [138],[74] though such bioreactors are not commercial scale (100 L and smaller).

Some developers have proposed the use of edible microcarrier materials that can be incorporated into a final product [139]. However, it should be noted that current low-density microcarrier cultures require 1–3 g (dry) of

[73] Typically animal-derived.

[74] Here, density is expressed as cells per volume of microcarrier. The microcarriers, however, only occupy a fraction of the culture working volume.

carrier beads to produce 1 g (wet) of cell mass. In high-density applications like the fluidized-bed case, this ratio is closer to 12 g/g, as such carriers are non-swelling.[75] The question of cell mass scale-up thus becomes a question of microcarrier production scale-up. Given the limitations cited above (which have not even addressed the added costs of beads), this analyst asserts that microcarriers are not consistent with an economic bulk cell-culture process.

[75] And definitely not edible—made from dense polyethylene and silica.

2.4 Aseptic operation

One especially pervasive metaphor in contemporary cultured-meat messaging holds that production will take place in a familiar, open facility resembling a brewery [27–30]. A brewery, however, is a sanitary facility, not an aseptic one. Beer is fermented anaerobically, at low pH (which kills most bacteria), and at inoculation rates high enough for the production strain to crowd out small numbers of competing organisms that may enter the system after pasteurization of the wort.[76] Failure to follow good sanitation practices merely results in (subjectively) bad beer, caused by the formation of lactic acid and "off" flavor compounds. In animal cell culture, by contrast, failure to maintain asepsis results in culture collapse and batch loss.

[76] Primarily harmless *Lactobacillus* and wild yeast.

Some definitions: *Sterile* implies the absence of all life, desired or undesired. *Aseptic* implies life in the absence of foreign pathogens. A bioreactor is sterile before a batch starts, and is operated aseptically after inoculation. Piping and connected equipment outside the aseptic bioreactor remain sterile.[77] *Sanitary* implies that pathogens may be present, but have been reduced to levels where they cannot cause disease. Within these definitions, there exists an important distinction between aseptic industrial fermentation and aseptic animal cell culture: While industrial fermentation of a commodity bioproduct can generally be carried out in the presence of small numbers of foreign organisms—as long as these are not pathogenic to the production cells or users of the end product—*any* stray microbial life is functionally pathogenic to animal cells in culture. At neutral pH, elevated temperature, and (according to cultured-meat messaging) in the absence of antibiotics,[78] a cell-culture bioreactor will readily harbor and be overcome by the contaminating microbe, which proliferate much faster than animal cells (Table 1.1). Typically, animal cell cultures can thus be further classified as *axenic*, i.e., free of any foreign organisms.

[77] The so-called sterile envelope [140].

[78] At the R&D level, antibiotics and fungistatics are sometimes used to clean up stray microbes in media and on equipment [141], even though these may be detrimental to the culture [142, 143]. Antibiotics are generally *not* used in large-scale upstream cell culture [144].

In upstream biopharmaceuticals manufacturing, axenic culture is compulsory, otherwise no harvest can be delivered downstream [145].[79] This does not mean that sterility in upstream cell culture can be considered a solved problem. It would be more accurate to state that typical modes of contamination have been identified over decades and mitigated, at great expense, to acceptable levels of batch loss and product quality/safety lapse. Consider the basic biopharmaceutical process flow sketched in Figure 2.10. In upstream cell culture, media, gases, and water are minimally filtered to 0.2 μm to remove bacteria and usually to 0.1 μm to remove mycoplasma. Virus

[79] To the extent that the U.S. FDA provides guidance on managing foreign organism ingress (bioburden) in biologics production, it is limited to downstream purification and packaging of the drug substance [146].

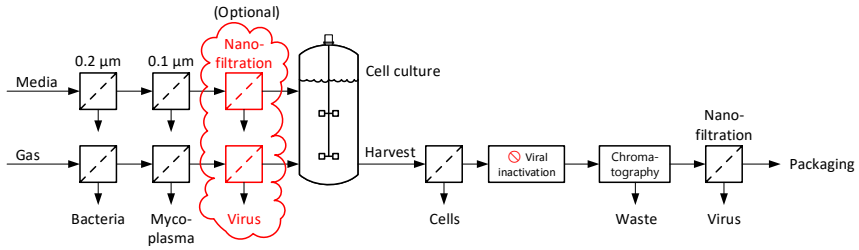

FIGURE 2.10: Basic flowsheet for the production of biopharmaceuticals from cell culture.

removal from cell-culture media is a recommended practice nowadays but is not always performed, as it is an added expense. Any virus used deliberately in the cell-culture process and/or endogenous retrovirus shed by the host cells is dealt with in multiple inactivation and filtration steps in downstream processing after cell removal.[80]

The risk of a viral infection event in upstream cell culture is rather low when animal-free chemically defined media are used.[81] Nevertheless, virus particles surviving in raw materials [147, 148] have caused plant shutdowns and drug shortages [149, 150]. If cells are the product, any virus introduced by raw materials will end up in said product if not removed upstream. Any retrovirus generated during culture (whether or not it is shed externally) cannot be removed at all, at least not without significantly altering or perhaps killing the cells. So, just as the errant mouse virus particle carried over from the field or warehouse might have the potential to infect an entire culture of CHO (rodent) cells, a cultured-meat bioreactor full of, e.g., chicken cells would require protection against all manner of avian viruses, particularly those that may subsequently infect the humans handling or consuming those cells, such as coronaviruses [151]. Protection will be especially challenging when the production of raw media components including glucose and plant hydrolysates is likely to be agriculture adjacent.

Media sterility safeguards include high-temperature/short-time (HTST) treatment and retention filters. The former is more cost-effective than the latter and is compatible with microbial fermentation media (sugars and mineral salts), but heat treatment may degrade the amino acids and growth factors required in animal cell-culture media. In particular, amino acids and glucose cannot be heated together or they will undergo Maillard reactions, potentially forming carcinogenic or mutagenic compounds [152]. Equipment sterility safeguards include frequent cleaning and steam sterilization of bioreactors and piping, surface treatments such as electropolishing and acid passivation, highly trained operators (no tourists), and extreme automation [153]. Sterility assurance also imposes a practical limit on bioreactor size. Although the largest practical stirred-tank bioreactor is ~1,000 m^3 [38],[82] current designs of such large bioreactors, their associated piping and valves, and their heat removal equipment (internal coils or external loop through a heat exchanger) are not practicably cleaned and sterilized to a level suitable for

[80] Endogenous retroviruses in cell lines are usually very well characterized in process qualification.

[81] Viruses are also highly species-specific and contamination does not necessarily result in infection.

[82] For reference, lysine fermentation is carried out at 500 m^3 [154].

animal cell culture. Rather, these are reserved for so-called non-sterile fermentations, in which aseptic inoculum is prepared in sterile bioreactors up to ~200 m^3 and the final production fermentor is run with a low level of contamination, possibly controlled with antibiotics or chemical agents like chlorine dioxide [60].

Finally, the efficacy of all these engineering and administrative controls is only assured when the facility environment is already relatively contaminant-free, so animal cell culture is usually carried out in clean rooms and laminar-flow hoods. Considering the potential for virus propagation mentioned above, in some cases the risk of contamination egress is equal to or greater than the risk of ingress, leading to biosafety containment requirements.[83] The cost implications of these safeguards is addressed in later sections.

[83] A cGMP clean room is generally sufficient for BSL-2 containment.

3

Economic aspects

This section provides background on major economic assumptions made in the TEA models that follow. Aspects that warrant further discussion include: capital cost development, costs of media components at scale, and fixed operating costs such as labor. Conceptual configurations of fed-batch and perfusion processes will be examined in Section 4 for the purposes of production cost estimation. Any process-specific economic assumptions will be discussed in that context.

3.1 Capital costs

In conceptual techno-economic analysis, the capital cost of a future process facility is typically estimated from the bare equipment costs of its most important items. From this purchased equipment cost (PEC), a total capital investment (TCI) is obtained through the application of one or more cost escalation factors. This factored approach is usually attributed to Lang [155], and the overall ratio of TCI/PEC is known as the Lang factor.[84] For conventional process-industry projects (e.g., a chemical plant or refinery), the overall Lang factor generally falls between 4 and 6, depending on process complexity.

The Lang factor of a conceptual bulk animal cell-culture process is unknown. Suitably sterile bioprocessing equipment is highly specialized and is today only available from a limited number of vendors.[85] As discussed in previous sections, sterility assurance and diminishing returns on cell density keep the overall size of equipment *much* smaller than the chemical plant or refinery equipment for which the factored approach was intended. Furthermore, cost factors in TEA are usually based on experience with similar and projects and processes. In the case of bulk animal cell culture, no similar processes exist. For more conventional bioprocesses, Petrides [67] proposed ranges on the cost factors to capture different classes of facility with different levels of sterility assurance, automation, biosafety containment, etc. Table 3.1 reviews the cost factors from some of Petrides's example facilities, included with SuperPro Designer software [56]. As presented, most of the differentiation happens in the direct-cost factor for buildings, which Petrides explains is

[84] For TEA, the overall Lang factor is generally divided into direct-cost or installation factors that are applied to the PEC for erection, piping, instrumentation, etc., and indirect-cost factors applied to the total direct cost (TDC) for engineering/design and construction fees [78, 156, 157].

[85] Who are under no obligation to provide quotes to a curious analyst.

TABLE 3.1: Lang factors for bioprocess facilities, as multipliers on equipment cost. Adapted from Petrides [56, 67].

Process	Non-sterile outdoors (lysine)	Sanitary indoors (beer)	Aseptic indoors (lactase[a])	cGMP microbe (insulin)	cGMP cell culture (mAb)
Applied to purchased equipment cost (PEC)					
Equipment	1.00	1.00	1.00	1.00	1.00
Installation	0.29	0.41	0.43	0.56	0.51
Process piping	0.38	0.38	0.38	0.38	0.38
Instr. + Elec.	0.40	0.50	0.50	0.60	0.50
Buildings	0.10	0.45	1.00	1.50	3.00
Site improv.	0.10	0.15	0.15	0.15	0.15
Aux. facilities	0.30	0.40	0.40	0.60	0.40
Applied to total direct cost (TDC)					
Engineering	0.25	0.25	0.25	0.25	0.25
Construction	0.35	0.35	0.35	0.35	0.35
Applied to total direct+indirect (TPC)					
Contractor's fee	0.05	0.05	0.05	0.05	0.05
Contingency	0.10	0.10	0.10	0.10	0.10
Overall Lang factor	4.7	6.1	7.1	8.8	10.9
Final vessel (m^3)	500	135	90	50	20
Cost of final vessel	$747k	$470k	$1.59M	$1.30M	$1.96M
Cost of 20 m^3 vessel	$133k	$168k	$1.01M	$1.01M	$1.96M

[a] β-galactosidase

lowest for primarily outdoor installations and highest for processes requiring cGMP clean room suites and special considerations for air/water purity, waste treatment, and so on. The overall Lang factor varies widely between classes, from ~5–11.

Hidden in this range, however, is the fact that the purchased cost of key equipment also varies widely between classes, as further shown in Table 3.1. Using SuperPro to estimate the cost of a 20 m^3 vessel consistent with each technology, a 15× variation is noted, from $133k for a basic lysine fermentor (bare equipment) to $1.96M for a fully customized, cGMP-compliant skid bioreactor. The latter is delivered piped, instrumented, and ready to be connected to the facility's process, utilities, and CIP systems—in other words, the purchased cost already includes many features that are typically captured by direct-cost factors.[86] Furthermore, with such inflated equipment costs, it is hard to reconcile the extravagant "buildings" implied by a direct-cost factor of, say, 3.0 with any reasonable estimate of equipment footprint, given the published clean room costs in Table 3.2.[87] More likely, then, that Petrides's factor for buildings was floated on the high end to match the costs of biologics facilities reported in press releases [158], and that it actually captures many extra costs that are not immediately apparent from a conceptual understanding of the process. These could include bespoke sterile design and construction for, e.g., drainage assurance and dead-leg elimination, orbital welding with full X-ray inspection, encapsulation of porous insulation materials, sterile seals on rotating equipment, cGMP compliance costs,[88] and perhaps a simple willingness to pay more for over-engineered or pre-certified systems.

Such characteristics, however, are surely incompatible with cultured meat's ostensible future as an affordable commodity bioproduct. For such a future

TABLE 3.2: Building costs and electric loads by class, 2018$. From Petrides [67] and ACCE.

Building class	$/$m^2$-level	W/m^2
Outdoors	$0	0
Slab only	$140	0
Warehouse	$1,130	5
Maint. shop	$1,250	43
Compressor	$1,290	43
Office	$1,660	54
Sanitary	$1,980	50
Laboratory	$2,640	54
Class 8	$3,760	410
Class 7	$4,990	500
Class 6	$8,750	1,000
Class 5	$11,700	1,520

[86] The unintended application of direct-cost factors to an installed or partially installed (skid) equipment cost in TEA is known as "double-dipping."

[87] Consider that a 20 m^3 bioreactor has a footprint of ~4 m^2.

[88] Compliance mainly adds indirect costs for, e.g., documentation requirements, supply-chain tracing, and testing.

to be realized, the equipment, design, and regulation of eventual cultured-meat facilities will have to be commodities in their own right. Consider the maximum achievable cell densities indicated in Figure 2.8b: 150 g/L in a 20 m^3 bioreactor and 70 g/L in a 200 m^3 bioreactor. In Section 4, it will be demonstrated that a modest production volume of 100 kTA cell mass in 20 m^3 fed-batch bioreactors would require a global installed bioreactor volume of ~10,000 m^3 (Figure 3.1a).[89] In 200 m^3 bioreactors, the global installed volume would be 20,000 m^3. Without making a serious dent in global meat consumption,[90] either of these new industries would already be biotechnology legend. In terms of installed volume, 10,000 m^3 of ≤20 m^3 bioreactors would be quite a bit larger than the entire biopharmaceuticals industry [60]; one hundred 200 m^3 fermentors would be roughly enough to supply all the baker's yeast in Europe (30% of the world) [55]. As shown in Figure 3.1b, on the path to full displacement of conventional meat at ~10^5 kTA, these bulk cell-culture processes would surpass all existing bioproducts in volume, ultimately becoming even larger than fuel ethanol—an anaerobic, antibiotic, non-sterile, low cell-density process that bears no resemblance to animal cell culture or food production in general.

To reflect commoditized equipment and facility costs consistent with this future, cost estimation software for the chemical process industry can be leveraged. Humbird et al. [38] presented general methods for estimating the costs of industrial fermentation equipment with Aspen Capital Cost Estimator (ACCE) [159]. For pressure vessels, ACCE computes weight and material cost as a function of metallurgy, geometry, and design pressure, then estimates the cost to fabricate the vessel, resulting in a total purchased cost. As it is designed for chemical and refining applications, the software assumes rather low rates of shop profit and no custom design services in its estimated fabrication costs.[91] It can thus be assumed that equipment costs estimated with ACCE reflect the discounts expected with bulk orders, off-the-shelf designs, and the elimination of cGMP compliance.

In the case of steam-sterilizable cell-culture equipment, the ASME standard for bioprocessing equipment (BPE-2016) requires 316L stainless steel and full vacuum design [140, 160]. Assuming that sterility and safety requirements remain constant at scale, Figure 3.2 presents a sketch of a jacketed STR with geometry as specified in Figure 2.5, fully piped and instrumented to a configuration suitable for aseptic animal cell culture: sterilizable media inputs, gas supply to headspace and sparger, heating and cooling on the jacket, CIP and SIP throughout the system, etc. The reactor is highly automated, with instrumentation for pH, DO, and pCO_2 monitoring.[92] At 20 m^3, ACCE estimates the cost of a bare vessel and agitator with this geometry and the ASME specifications above as ~$330k, as indicated in Table 3.3. The costs of the piping and instrumentation features can further be estimated with ACCE. With additional allowances for surface treatment (electropolishing, acid passivation), internals (sparger, spray balls) and externals (exhaust heater, double mechanical impeller seal), the total estimated cost of a 20 m^3 system

[89] Including large seed reactors.

[90] 100 kTA is ~0.03% of global meat production.

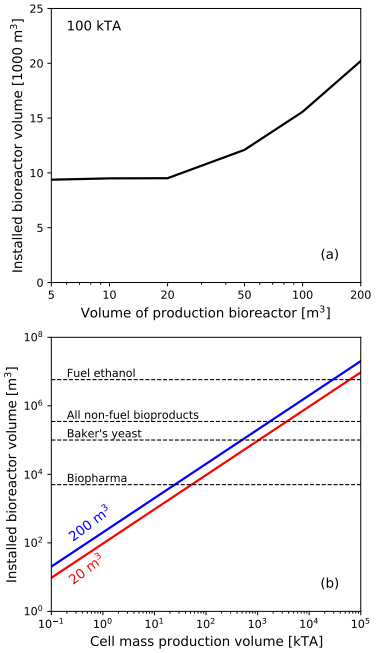

FIGURE 3.1: (a) Global bioreactor volume required to produce 100 kTA of cell mass in bioreactors of varying size. The increase at >20 m^3 is due to reduced cell density (Figure 2.8). (b) Required global volume to produce a varying amount of cell mass, using the cell densities observed in Figure 2.8b for 20 m^3 and 200 m^3 bioreactors. Horizontal lines indicate the estimated installed volumes of key biotechnology sectors.

[91] With default settings.

[92] Probes are 3× redundant, though only one of each is shown.

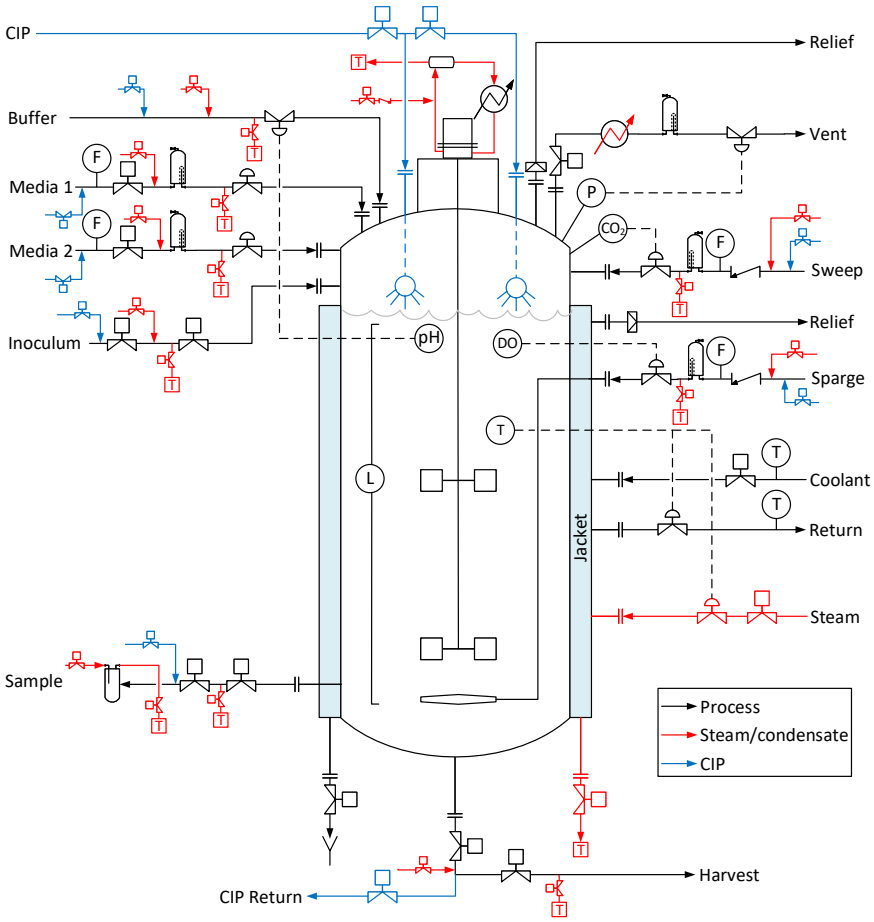

FIGURE 3.2: Piping and instrumentation sketch for an aseptic bioreactor with sterile envelope. Based on ASME BPE-2016 [140].

TABLE 3.3: Detailed costs for the sterile configuration in Figure 3.2 at 1 m^3 and 20 m^3. For volumes 1–200 m^3, the bare equipment and total direct costs are shown.

1 m^3	
ACCE vessel + agitator	$59k
ACCE piping	$201k
ACCE instr. + elec.	$454k
ACCE other direct cost	$3k
Add for internals/externals	$29k
Add for surface treatment	$28k
Total	$774k

20 m^3	
ACCE vessel + agitator	$330k
ACCE piping	$360k
ACCE instr. + elec.	$476k
ACCE other direct cost	$22k
Add for internals/externals	$164k
Add for surface treatment	$132k
Total	$1.5M

All volumes

	Bare	Installed	DCF [a]
1 m^3	$59k	$774k	12.1
2 m^3	$93k	$856k	8.2
5 m^3	$138k	$966k	6.0
10 m^3	$217k	$1.2M	4.4
20 m^3	$330k	$1.5M	3.5
50 m^3	$722k	$2.6M	2.6
100 m^3	$1.3M	$4.0M	2.2
200 m^3	$2.4M	$6.8M	1.8

[a]Direct cost factor (Installed/Bare-1)

is $1.5M, or about 25% lower than the packaged skid in the mAb analysis above (Table 3.1).[93]

ACCE can be further be used to estimate the cost of the aseptic configuration in Figure 3.2 at larger volumes up to 200 m^3. The estimated bare equipment (vessel and agitator) and total system costs are shown in Table 3.3, along with a factor describing the direct costs relative to the vessel.[94] At small bioreactor volume, the direct costs estimated in ACCE are much higher than implied by the cumulative factors for installation, piping, and instrument/electrical offered in Table 3.1. At large volume, the relative direct costs begin to flatten out and approach parity with these factors. As illustrated in Figure 3.3, installation costs dominate the system cost at small volume and remain relatively constant as volume increases, becoming roughly equal to the equipment cost (including internals and surface treatment) at the 100 m^3 scale.

Thus, much as the overall Lang factors in Table 3.1 are not strictly transferable between facility classes due to the variation in individual equipment costs,[95] it appears that a one-size-fits-all approach to direct costs is not ideal

[93] The same is true for the 1 m^3 bioreactor cost of $774k given in Table 3.2; Petrides gives ~$1M for a 1.2 m^3 system in the mAb analysis.

[94] Sizing performed by keeping the same relative vessel geometry and scaling pipe diameters and lengths by vessel diameter.

[95] In other words, it will not cost $12M to brew beer in a $2M bioreactor.

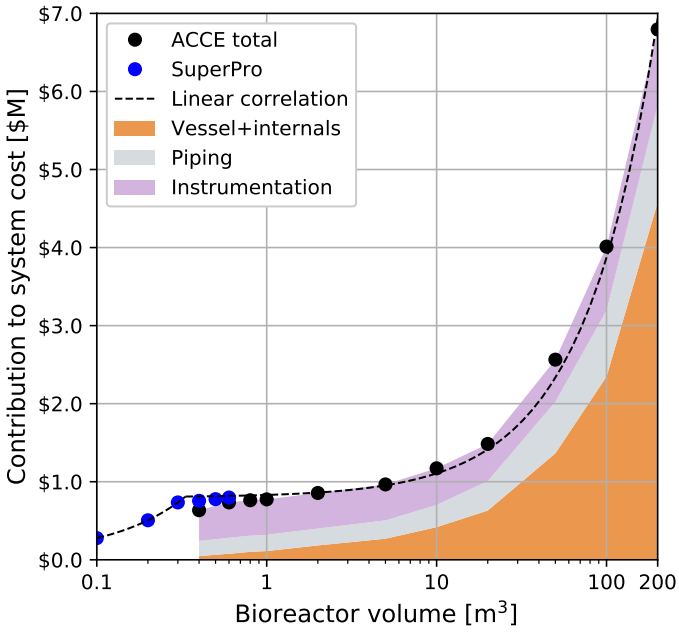

FIGURE 3.3: Total purchased cost of equipment, piping, and instrumentation/electrical for the packaged aseptic bioreactor system in Figure 3.2. Dashed line: piecewise linear correlation used for analysis purposes (Equation 3.1).

for TEA of a bulk cell-culture process, which is expected to have a relatively small maximum bioreactor volume. Instead, the following points are used to guide the development of capital costs of specific configurations in Section 4:

1. As the most significant contributors to equipment cost, the total direct costs of production and seed bioreactors is taken from ACCE (large vessels) or SuperPro (small vessels).[96] For rapid analysis of arbitrary vessel sizes, the piecewise linear correlation shown in Figure 3.3 is proposed, which matches the ACCE and SuperPro estimates (with a 25% discount, as described above). The two pieces are equivalent at 0.33 m^3. No additional installation costs are applied.

$$\text{Cost (\$k)} = \begin{cases} 30.7 \times V + 800 & V \geq 0.33\ \text{m}^3 \\ 2285 \times V + 49.5 & V < 0.33\ \text{m}^3 \end{cases} \tag{3.1}$$

2. Appropriate costs for minor ISBL[97] process equipment items like media storage tanks, HTST sterilizers, filter housings, etc. are estimated with ACCE, SuperPro, or the correlations in Couper et al [161]. Installation costs of ISBL equipment are taken as 1.3× the bare equipment cost, following Table 3.1. A 10% correction is added to account for minor equipment not included in the abbreviated equipment list (e.g., pumps) [67].
3. Similarly, OSBL facilities for utilities, O_2 generation, etc. are estimated independently (not factored from the equipment cost), or represented

[96] ACCE is less accurate at predicting the installed costs of bioreactors <0.5 m^3, which have unique fabrication and plumbing methods (e.g., tubing in place of pipe) that fall outside of the software's fit space.

[97] ISBL and OSBL designate equipment located inside or outside of the process battery limits.

with an operating cost. Installation costs of 1.3× and the 10% correction are likewise applied to the OSBL equipment.

4. Building costs are computed from an estimate of equipment footprint and the costs in Table 3.2.
5. The sum of the above represents the total direct cost (TDC) of the facility. Per Table 3.1, the indirect cost factors appear constant across facility types; in fact, this is a fairly accurate representation of how engineering and construction companies charge for process-industry projects, regardless of novelty or complexity.[98] These are applied as shown in the table to compute the total capital investment (TCI).

[98] These should increase the total direct cost first, resulting in higher absolute fees to the E&C firm via a flat percentage.

Finally, to represent the TCI of a facility as an annual charge ($/y),[99] a capital charge factor (CCF) is often used in high-level TEA [162]:

$$\text{CCF}\ [\%\ \text{of TCI/y}] = \frac{i}{(1-(1+i)^{-n})} \tag{3.2}$$

[99] And, if divided by annual production, a contribution to total COP ($/kg).

where i is an internal rate of return reflecting a hypothetical alternative investment and n is the lifetime of the facility. Note that i is independent of any instantaneous interest rate and varies by sector; typically, the weighted-average cost of capital (WACC) for the sector can be used. In 2019, the WACC of the pharmaceutical and biotechnology sectors was 8.5% and that of the food processing sector was 5.4% [163]. The WACC of plant-based meat company Beyond Meat, Inc. in the same year was 7.5% [164]. For the present analysis, i is thus taken as 7.5% and n as 10 years (common for food manufacturing facilities [165]), giving a capital charge factor of 15% TCI/y.

3.2 Costs of media components

A general observation in TEA for the process industries is that products with smaller market volumes must cost more. Referring to Figure 1.3, this price-volume relationship is less a function of scarcity than of scale. Products with small demands will forever be produced using small equipment located in small facilities with high overhead. Indeed, catalog prices for research-grade cell-culture media components, which are packaged at extremely high purity and in sub-kilogram quantities, are liable to evoke a degree of "sticker shock." Even at the biopharmaceuticals scale, where media components are routinely purchased in 10–1,000 kg quantities, these can cost much more than food- or feed-grade formulations of the same material, especially if they are produced and/or packaged in a cGMP facility to comply with regulations. To predict the costs of commodity and certain specialty chemicals at scale for TEA purposes, some exponential methods have been proposed to extrapolate, e.g., price per ton from a known price per gram or kilogram [79, 166]. Such methods presuppose, of course, that there exists a ton available for purchase. Yet, many important cell-culture media components are not currently produced at scales consistent with food production. It is therefore important to consider actual

demand levels when estimating future price, and to think about where these raw materials might come from.

▸ GLUCOSE

As the primary carbon and energy source in Reaction 2.11, glucose is required at 0.36 kg per kg of wet cell mass. Commercial D-glucose (dextrose) is produced in the U.S. at corn wet mills and sold as corn syrup with a market volume of >4,000 kTA. While current output is fully contracted, the mills are almost certainly operating under capacity. A new wet mill has not been commissioned in the U.S. for decades, and some have closed as a result of low demand [167]. Spot prices for glucose in the range of $0.50–$1.00/kg are inflated by a vanishingly small spot market: about 34 kTA/y (40 jumbo rail cars). Although the cost and availability of spot glucose present significant barriers to entry for new bioproducts developers today, contract prices for more established industries are closer to ~$0.25/kg [168]. Emerging corn fractionation technologies also offer opportunities to produce refined glucose at ethanol dry mills, at a smaller scale but a similar cost.[100] In the short term, glucose is thus not anticipated to be a bottleneck to scale-up, nor a significant contributor to cost: From the stoichiometry of Reaction 2.11, glucose at $0.26/kg would only contribute $0.24/kg wet cell mass. In the long term, 4,000 kTA of dextrose is (in principle) enough to make 11,400 kTA of animal cell mass. Wet mills process slightly more than 10% of the corn in the U.S. to make this dextrose. New or alternative sugar sources may thus be required to reach an ultimate production volume of 10^5 kTA.

[100] One developer claims $0.26/kg [169].

▸ AMINO ACIDS

Organic nitrogen sources (i.e., amino acids) may present a challenge even in the short term. Each essential and non-essential amino acid is currently produced at some commercial scale [170], with production volumes ranging from thousands of kTA for certain animal-feed supplements to <1 kTA for aminos with primarily pharmaceutical uses including cell-culture media. As shown in Table 3.4, if the amino acids in Reaction 2.11 were purchased individually to produce cultured-meat media, even at the modest scale of 100 kTA cell mass, the new demand created would exceed several of their existing market volumes. In other words, there can be no cultured meat scale-up without concomitant and dramatic scale-up of amino acid production.

Investigating the scale-up potential of each amino acid is beyond the scope of this analysis, but there are reasons to be dubious. Figure 3.4a presents available price-volume data for individual amino acids. An average selling price is shown, i.e., global market (in dollars) divided by global production volume (in kg) [171–173]. Although Figure 3.4a clearly indicates that aminos with smaller market volumes cost more, the high-volume/low-cost data points for the major amino acids (O~1,000 kTA) reflect feed-grade formulations unsuitable for cell-culture media. DL-methionine (Met), for instance, is produced by chemical synthesis as a racemic mixture that can be metabolized by humans

TABLE 3.4: Amino acid demands at 100 kTA cell mass production versus current market size. Based on the stoichiometry of Reaction 2.11. Prices estimated with Equation 3.3 at the given demand are also shown.

	Stoich. demand (g/g wet)	Demand at scale (kTA)	Current volume (kTA)	Est. price at scale ($/kg)[a]	Contrib. to cell mass ($/kg wet)
Glucose[b]	0.362	36.2	4,000	$0.26	$0.10
Essential amino acids					
L-arginine	0.016	1.6	1.5	$70	$1.12
L-cysteine	0.005	0.5	10	$137	$0.67
L-glutamine[b]	0.044	4.4	3.0	$40	$1.74
L-histidine	0.006	0.6	0.4	$118	$0.75
L-isoleucine	0.012	1.2	0.4	$83	$0.98
L-lysine	0.020	2.0	2,317	$62	$1.23
L-methionine	0.004	0.4	1,172	$156	$0.60
L-phenylalanine	0.011	1.1	30	$85	$0.96
L-threonine	0.014	1.4	684	$76	$1.05
L-tryptophan	0.004	0.4	14	$146	$0.64
L-tyrosine	0.012	1.2	0.2	$81	$1.00
L-valine	0.016	1.6	2.0	$71	$1.11
Total EAA					$11.84
Non-essential amino acids					
L-alanine	0.016	1.6	1.2	$71	$1.11
L-asparagine	0.011	1.1	0.1	$85	$0.96
L-aspartic acid	0.014	1.4	10	$75	$1.06
L-glutamic acid[c]	–	–	145	–	–
Glycine	0.011	1.1	23	$87	$0.95
L-leucine	0.019	1.9	0.5	$63	$1.21
L-proline	0.010	1.0	0.4	$90	$0.92
L-serine	0.015	1.5	0.2	$74	$1.07
Total NAA					$7.29
Total Macronutrients					**$19.23**

[a]As pure-formula AA (no hydrate/HCl).
[b]Includes catabolism at μ=0.029/h.
[c]Glu requirement satisfied by RNA production.

and animals without separation, though the same is not guaranteed for cells in culture [174]. L-threonine (Thr), the lowest-cost amino in Figure 3.4a, is produced commercially in *E. coli*, which leaves behind relatively high levels of lipopolysaccharide(LPS) endotoxin.[101] Costs associated with LPS removal generally preclude the use of *E. coli* in low-volume food- or pharma-grade aminos [175], but LPS is not a concern for feed-grade formulations,[102] as livestock are already exposed to high environmental levels of *E. coli* and LPS does not cross the intestinal barrier to accumulate in edible tissue [177]. L-lysine (Lys), the highest-volume amino in Figure 3.4a, is primarily produced by *C. glutamicum*, which does not have an LPS problem.[103] However, feed-grade formulations of lysine have less stringent specifications on foreign matter and metal content (e.g., arsenic and lead) than food- or pharma-grade formulations. Even if these contaminants did not directly inhibit cell growth or development in cell-culture media, they would very likely be left behind in the product.

There is much uncertainty. To project a cost for an amino acid at scale, this analysis recognizes that the price-volume relationship observed across all amino acids must also exist in some form across formulations of an individual amino acid. Furthermore, developers aiming to design formulations that

[101]A component of the cellular membrane in Gram-negative bacteria.

[102]Apart from safety precautions to prevent inhalation when handling bulk powders [176].

[103]*C. glutamicum* is a Gram-positive bacterium. Note, however, that in some parts of the world, lysine demand exceeds the availability of high-quality sugar suitable for *C. glutamicum* fermentation, and *E. coli* is being pursued as a host that can be engineered to produce feed-grade lysine from lower-grade sugars like beet molasses [178].

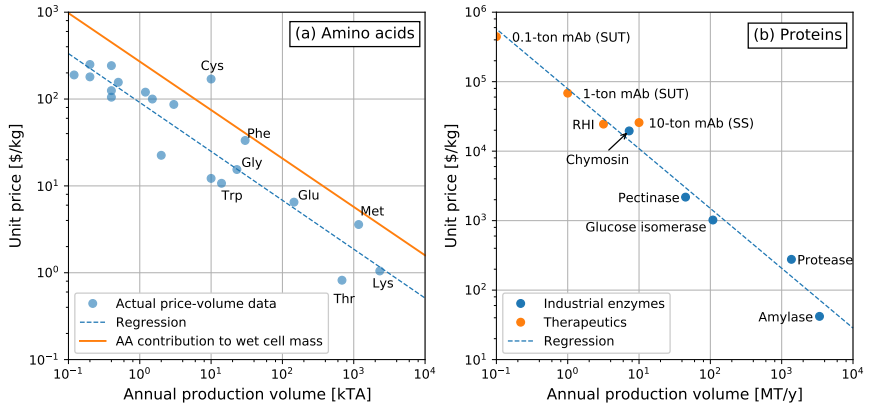

FIGURE 3.4: (a) Unit cost versus production rate for individual amino acids and their cost contribution to wet cell mass at scale (stoichiometry of Reaction 2.11). (b) Price-volume relations for industrial enzymes and therapeutics. Adjusted to 2018$. (SS=stainless steel; SUT=single-use technology; RHI=recombinant human insulin)

strike a balance between price and suitability for cell culture are, in a sense, designing a new product: a "cultured meat-grade" formulation. This product must have its own production and purification process, quality specifications, and market size. The metrics associated with manufacture of these formulations, e.g., yield, titer, fermentor size, and recovery costs, must certainly influence their ultimate price, but not by multiple orders of magnitude as observed in Figure 3.4a. For these reasons, the market volume of a novel amino acid formulation is probably a more reliable predictor of its price at scale than tenuous assertions about its ease of microbial expression or similarity to existing products.[104] As a function of demand, prices for individual amino acids at scale are therefore correlated to the market data with the following regression:

$$\log(\text{Price } [\$/\text{kg}]) = -0.563 \log(\text{Prod. volume } [\text{MT/y}]) + 3.65 \qquad (3.3)$$

The regression in Equation 3.3 captures the price dynamics both at very low demand (small reactors in small facilities, campaign production, high overhead, and strict product certification requirements) and at very high demand (large, dedicated facilities with relaxed or nonexistent regulation). The amino acid prices estimated at a scale of 100 kTA cell mass and their contributions to the cell mass production cost (given the stoichiometry of Reaction 2.11) are presented in Table 3.4. Out of a macronutrient cost of $19/kg wet cell mass, ~$12/kg derives from essential amino acids. In principle, the non-essential remainder could be provided by a variable composition of other amino acids. As further shown in Figure 3.4a (orange line), Equation 3.3 also causes the macronutrient cost contribution to cell mass to have the same slope as amino acids, as a function of production volume. Given that the dry mass of an animal cell primarily derives from amino acids [94], a significantly different slope would be unexpected.

[104] Other reasons to be dubious about the scale-up potential of high-quality amino acids include: a fairly high water footprint due to recovery operations with ion exchange and crystallization, and recombinant holdouts like L-cysteine (Cys). A notable Figure 3.4a outlier, cysteine is challenging to over-express in microorganisms due to toxicity [179]. Lower grades of cysteine are produced by hydrolysis of animal byproducts, with food/pharma-grade formulations produced by chemical synthesis and racemic separation.

TABLE 3.5: Hydrolysate and supplemental amino acid demands at 100 kTA cell mass production, based on the stoichiometry of Reaction 2.13.

	Stoich. demand (g/g wet)	Demand at scale (kTA)	Est. price at scale ($/kg)	Contrib. to cell mass ($/kg wet)
Glucose	0.362	36.2	$0.26	$0.10
Soy hydrolysate	0.337	33.7	$2.00	$0.67
Supplemental amino acids				
L-glutamine	0.044	4.4	$40	$1.74
L-tyrosine	0.009	0.9	$95	$0.88
Total Macronutrients				**$3.39**

PLANT PROTEIN HYDROLYSATE

Soybean hydrolysate was discussed in Section 2.2 as a potential alternative source of amino acids. In animal-free media formulations for cell culture, enzymatic hydrolysates and peptones of plant proteins are sometimes used as supplements and serum replacements, but only at low levels (2–20 g/L) in otherwise chemically defined media [180]. Even at such low levels, Hartshorn et al. [181] demonstrated (albeit without any process details) that the hydrolysate preparation process can have a marked effect on cell growth. At a minimum, the hydrolysate must be ultrafiltered to remove all protein (including the hydrolyzing enzyme) and variable-molecular weight peptides, pasteurized, and spray-dried for storage [182]. As a result, the production process can be fairly expensive.

As a macronutrient source, the suitability of plant protein hydrolysates is less clear. Hydrolysis is not generally favored for the production of single amino acids, in part because the concentration of any one amino is too low for it to be cost effectively isolated from the rest.[105] Considering the amino-acid distribution of soy protein in Figure 2.4, enzymatic hydrolysates of whole plant protein fractions could be designed that provide all amino acids with the probable exception of glutamine.[106] Engineering controls to reduce variability and overfeeding[107] might include aggregation and blending at the species or producer level, enzyme cocktail design, or ion-exchange separations. Perhaps toleration of variable amino acid compositions could also be implemented at the cell level.

To speculate on a future price of enzymatic hydrolysates,[108] consider that current soybean meal pricing for animal feed is about $300/U.S. ton ($0.33/kg) [183]. Subtilisin protease enzyme at $15/kg (see Figure 3.4b) and 2% loading would further add $0.30/kg of meal processed. If meal is 48% protein, protein is 88% soluble, and hydrolysis conversion is 80%, then a formulation of mixed amino acids from hydrolysis (correcting for water) could cost as little as $1.60/kg, plus processing, purification, and packaging costs. Assuming that soy meal is not likely to be in shortage[109] and that an ultimate price of ~$2/kg mixed amino acids is feasible, then a new raw material contribution of $3.40/kg total cell mass can be computed using Reaction 2.13, as shown in Table 3.5.[110]

[105] Even though soybean meal is considered a lysine-rich animal feed, there are barely enough soybeans in the world to produce the 2,300 kTA of lysine made by fermentation.

[106] Monomeric glutamine is not likely to survive the process, but some glutamine may remain in low-MW peptides.

[107] Overfeeding, as proposed in Reaction 2.13, may lead to accumulation of unused aminos and peptides, particularly in fed-batch operations. Excessive accumulation can then lead to precipitation or osmolality constraints. It is unknown whether such constraints would be incurred before those studied in Section 2.3.

[108] The neutralization and desalting of acid hydrolysates at scale would be a sustainability non-starter.

[109] With reference to the corn discussion above, it also happens that the annual U.S. soybean crop would be *just* enough to support 10^5 kTA of cell mass.

[110] 77% of this is contributed by supplemental glutamine and tyrosine, with prices estimated by Equation 3.3. As mentioned in Note 50, it is possible that the tyrosine requirement could be supplied with a designer hydrolysate, but probably not the glutamine.

Protein micronutrients

The various hormones, cytokines, vitamins, etc. (growth factors) that must be provided in cell-culture media to regulate cell growth and metabolism are responsible for a great deal of criticism and speculation among cultured-meat developers and the media who cover them. Much of this stems from the observation that, at the bench scale, growth factors are typically supplied in complex sera extracted from animal blood. Notably, Fetal Bovine Serum (FBS) is a common research serum that tends to work very well for most mammalian cell lines and therefore appears in many published laboratory protocols. FBS is indeed an animal product with a rather objectionable production method; it is also incredibly expensive and has known supply-chain problems, even at the research scale [184]. Due to the potential for adventitious contamination by viruses and prions, FBS has largely been eliminated from large-scale biopharmaceuticals manufacturing, and it has no future chance of ever becoming an approved ingredient in anything intended for general human consumption. Pledges by cultured-meat developers to eliminate or replace FBS and other animal sera [185–187] are thus somewhat beside the point—without animal-free sera (or serum-free culture), there will be no cultured meat.

Some serum alternatives have been developed that are plant-based in the sense that they comprise highly processed and purified extracts of plant proteins as discussed above, and/or recombinant proteins made in, e.g., *E. coli* or *Pichia pastoris* hosts grown on glucose, glycerol, or methanol. All of these products are likewise understood to be very expensive in today's market.[111] In fact, commercial protein products from cell culture and fermentation have a price-volume relationship that is quite similar to that noted for amino acids. Figure 3.4b presents market data for protein bioproducts, including antibodies [188],[112] recombinant human insulin (RHI) [189],[113] and high-volume hydrolytic enzymes for industrial use [192]. Given the low end of the cost range in Figure 3.4b, one might be tempted to forecast a future price of recombinant growth factors on the order of $1,000/kg. From the regression of the market data in Equation 3.4, however, it can be seen that such a low cost would only be consistent with a protein having a production volume of ~160 MT/y.

$$\log(\text{Price [\$/kg]}) = -0.861 \log(\text{Prod. volume [MT/y]}) + 4.90 \qquad (3.4)$$

Demands of protein micronutrients, which do not appear in the growth stoichiometry, can be estimated on a concentration basis. Consider the four protein components in Essential 8 stem-cell medium: insulin at 19.4 mg/L, transferrin at 10.7 mg/L, fibroblast growth factor (FGF) at 0.1 mg/L, and transforming growth factor (TGF-β) at 0.002 mg/L [193]. If it can be assumed that the proteins are not consumed or degraded during the cell growth process, then the amount required is simply equal to the amount lost from the bioreactor. In perfusion culture, losses occur over time and depend on perfusion rate; in batch or fed-batch culture, losses occur when the bioreactor

[111] Research quantities of human TGF-β from the Sigma catalog cost about $29k/mg.

[112] This reference provides estimates for stainless-steel (SS) and single-use technology (SUT) facilities; the lower of the two is used. Further note that a "10-ton mAb" does not exist today. Rather, this point represents a hypothetical contract manufacturer making a total of 10 MT/y of varied mAb products.

[113] Gotham et al. [189] estimated the API production cost of RHI as $24.5k/kg. Global insulin Rx in 2018 were 5.16×10^{11} IU [190], about 18% of which was RHI (0.0347 mg/IU) [191]. The global production of RHI can thus be estimated as ~3.2 MT/y protein.

TABLE 3.6: Growth factor demands and estimated costs from Equation 3.4 at final fed-batch cell densities of 50 and 150 g/L.

	Demand at scale (kg/y)	Est. price at scale ($/kg)	Cost per kg cell mass ($/kg)
50 g/L cell density, 2.0×10^9 L/y			
Insulin	39,000	$3.4k	$1.31
Transferrin	21,000	$5.6k	$1.21
FGF	200	$316k	$0.63
TGF-β	4.0	$9.2M	$0.37
	Total per kg cell mass		$3.52
150 g/L cell density, 6.7×10^8 L/y			
Insulin	13,000	$8.7k	$1.13
Transferrin	7,100	$15k	$1.04
FGF	67	$812k	$0.54
TGF-β	1.3	$24M	$0.31
	Total per kg cell mass		$3.02

is emptied. In either case, losses are in turn a function of cell density, which is estimated in Figure 2.8 to be in the range of 50–150 g/L. In a fed-batch process with 50 g/L final cell density, the annual bioreactor turnover for 100 kTA cells is 2×10^9 L/y. At 150 g/L, the annual turnover is 6.7×10^8 L/y. At these limits, Table 3.6 computes the annual demand for growth factors as, e.g., 13–39 MT/y of cell culture-grade insulin and 1–4 kg/y of TGF-β.[114] Although the unit prices for growth factors estimated by Equation 3.4 are relatively high, the usages are so small that these components do not contribute a significant operating expense—only $3–3.50 per kg of wet cell mass at the modest scale of 100 kTA.

[114]Much less than the 160 MT/y volume required for $1,000/kg.

Ultimately, some assumptions above may not be satisfactory. Growth factors will almost certainly be consumed or at least degraded over time.[115] It is also very likely that the required concentrations also depend on cell density. Absent scientific data, such uncertainties are not resolvable at this level of analysis. Nevertheless, due to the price-volume effects inherent to Equation 3.4, attempts to correct for them did not result in a significantly larger overall cost of growth factors. It can thus be assumed that growth factors contribute about $3–4/kg wet cell mass at the 100 kTA scale. At much larger scale, their contribution vanishes entirely.

[115]The micronutrient concentrations in Essential 8 generally assume that the entire medium is replaced every 1–2 days, as determined by the macronutrient consumption rate.

NUTRIENT RECOVERY AND RECYCLE

A common research target among bioproducts developers reacting to high feedstock/media costs (real or perceived), spent media recycling has always proven impractical in this analyst's experience and is not considered here.[116] Concentrating separations like affinity chromatography would be impractical at food scale, and scale-appropriate separations like simulated moving-bed chromatography would produce refined product streams even more dilute than the feed.[117] Attempting to reconcentrate with heat would degrade many of the more coveted species, like growth factors. If nutrients remain in spent media at concentrations high enough for cost-effective recovery, then they were probably being used inefficiently in the first place.

[116]There may, however, be opportunities in re-purposing spent animal cell-culture media as fermentation media. These will be discussed briefly in Section 5.

[117]"Purity" in chromatography is measured on a water-free basis.

- WATER

A critical raw material in any fermentation or cell-culture process, the water used in pharmaceuticals manufacturing (synthetic or biologic) is of an ultrapure quality known as Water for Injection (WFI), implying water pure enough to be injected into a patient along with the drug. In upstream cell culture, where dissolved solids, microbes, and virus particles must be tightly controlled, WFI is typically used throughout the process to mix cell-culture media and CIP chemicals, raise steam for SIP, etc. There are several technologies available for USP-grade WFI systems. Most involve a distillation step, which is fairly energy-intensive. Membrane- and resin-based systems[118] use much less steam but have higher consumables and maintenance costs.

[118] Reverse osmosis, deionization, ultrafiltration.

Selection and sizing of an appropriate water treatment unit is beyond the scope of this analysis. Instead, the total water demand is estimated for the process (in, e.g., m^3/batch or m^3/y) and represented as an operating expense. The WFI supplier MECO advises that the average cost of water from any of the technologies above is ~\$20/m^3 [194]. Compared to a fermentation process, which uses minimally processed potable water (~\$0.26/m^3 [130]), water is a significant operating cost in cell culture.

3.3 Fixed operating costs

The fixed operating costs of a process facility include overhead and labor. Overhead is dominated by equipment maintenance costs and annual insurance premiums, usually taken to be a percentage of the TCI. Annual maintenance is here taken to be 4% TCI/y, which is assumed to include CIP chemicals in addition to the repair and preventative maintenance of rotating equipment, etc. Annual insurance is taken to be 5% TCI/y.

Estimating staff levels and labor costs for industrial biotechnology processes, which are typically batch-based, tends to be a more subjective exercise. Although correlations to the number of processing steps are sometimes proposed [195], these do not scale satisfactorily to many fermentors/bioreactors. Reisman [196] presents a labor-estimation method more specific to fermentation processes, using a table of FTE requirements for typical unit operations. Reisman's method is practical for continuous or nominally continuous parts of the process like media prep, dewatering, air compression, and utilities, but less useful for cyclic, batch-based labor. The latter is highly dependent on batch cycle time, and an accurate estimate requires a detailed batch schedule, including pre-batch activities in cell bank, seed train, and media prep areas.

Without a detailed scheduling exercise, labor can be reasonably quantified in terms of operator attention per batch, based on a series of task/time assumptions.[119] For example, the model baker's yeast facility in Appendix A has six production fermentors operating with 24-hour turnaround. In this process design, a single slant from the cell bank is eventually propagated to all six fermentors (Figure A.4a). For every six batch starts, there are 4 passage steps in the lab, requiring 60 minutes of attention each, followed by transfers

[119] I developed this approach for biotech startups to validate labor quotes from contract manufacturing operations.

into increasingly large fermentors. The attention paid to seed and production fermentors can be expressed as percentages of their online time and offline (drain/clean/fill) time. For small seed fermentors ($<1 m^3$), this is taken as 25% each to allow for some manual dis/assembly. For larger seed and production fermentors, this attention is taken as 10% each. An efficiency of 80% is further imposed on these time estimates to account for breaks and administrative activities. As shown in Table 3.7, this calculation leads to two FTE/shift on fermentor duty.[120]

In the yeast example, the six fermentors are viewed as a single train with a shared operations crew. In the process designs offered in Section 4, larger numbers of bioreactors are divided logically into parallel trains. FTEs for continuous operations, maintenance, and utilities are accounted for on a per-train basis. One supervisor is added per 10 regular FTE, and all shift hours are multiplied by 4.5 hires per position to account for 24×7 operation with 8-hour shifts [197]. For the yeast example, the total staff requirement is 24.

Scheduling and labor considerations for specific process configurations will be discussed below in context. In all cases, a baseline non-supervisory salary of $50,000/y is taken from the U.S. Bureau of Labor Statistics—Chemical Plant Operator. The supervisor's salary is taken as 140% of this. A labor burden (overhead) of 100% is added to the total labor cost. This includes employee training and benefits as well as administrative functions (payroll, HR) that may be outsourced.

[120] If a third FTE is included for media prep, the estimate is consistent with Reisman's own guidance of three FTE in the fermentation area for $N_{ferm}=6$.

TABLE 3.7: Labor hours summary for the fed-batch yeast process in Appendix A.

Batch	Attention	h/batch	FTE/shift
Lab	1 h/step	0.8	0.2
Small seed	25% time	2.5	0.6
Large seed	10% time	1.5	0.4
Production	10% time	3.0	0.8
Total batch workers			2.0

Continuous	FTE/shift
Media prep	0.5
Dewatering	0.8
Utilities	1.0
Maintenance	0.5
Total continuous workers	2.8
Supervisor	0.5
Total labor per shift	5.3
Total labor (all shifts)	24

4

Production cost studies

This section examines the cost of bulk cell mass production using TEA models developed for both fed-batch and perfusion processes. General discussion of the major economic assumptions made in these models was provided in Section 3. Process-specific details of equipment sizing, labor estimation, etc. will be discussed here along with sensitivity analyses. These models are relatively complex and only limited details are included here. The reader is invited to view the supplemental information for further details.

4.1 Fed-batch operation

A process flow diagram (PFD) of a conceptual fed-batch cell-culture process is given in Figure 4.1. For the detailed example given below, the model cell-culture facility is designed with 24×20 m^3 production bioreactors and is assumed to exist as part of a larger industry producing 100 kTA of animal cell mass, as proposed in Section 1.3. Cells are propagated from the lab through increasingly large bioreactors, ultimately inoculating the 20 m^3 production bioreactors. When the production culture reaches an 80% working volume, the cell mass is harvested and dewatered in a disk-stack centrifuge to 20% solids. To prepare sterile media for cell culture, two large media tanks attached to HTST sterilizers are assumed for separate preparation and heat treatment of glucose and amino acids or hydrolysate. These large tanks are shared among bioreactors to provide the initial fill before inoculation. A smaller, dedicated makeup tank is provided on each bioreactor to contain the media that will be added during the batch. It is assumed that the makeup medium is pre-mixed at batch start and that it contains a defined composition of glucose, amino acids, and protein growth factors. These components cannot be co-sterilized with heat, so a battery of 0.2 μm, 0.1 μm, and virus retention filters is provided on the makeup tank only. This media prep configuration is provided on all bioreactors >100 L (0.1 m^3).

A fed-batch simulation much like those shown in Figure 2.7 is used to compute the required number and size of seed bioreactors and shared media tanks. Integration of the simulation results further provides estimates of media

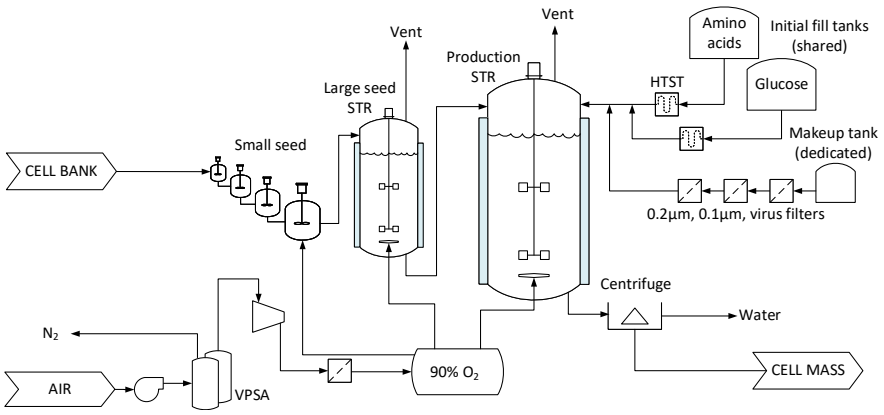

FIGURE 4.1: Process flow diagram of a conceptual fed-batch process for bulk cell culture.

and utility use per batch.[121] The simulation is performed in Excel as follows: At t=0, the bioreactor volume is set to 13.2 m^3 (66% working volume) with 482 kg (wet) of inoculum.[122] The bioreactor conditions are 37 °C and 1.33 bar (5 psig) back pressure at the top. The bottom pressure varies with the head exerted by the culture volume. The growth rate is initially set to μ=0.029/h. At regular time intervals, a new amount of cell mass (DCM_a) is computed with a growth reaction:

$$DCM_{t+\Delta t} = DCM_t \exp(\mu \Delta t) \tag{4.1}$$

and the corresponding stoichiometric requirements (q-rates) of glucose, amino acids, and O_2 in each interval are computed using the process reaction 2.11. A volume of makeup medium is computed from the nutrient q-rates in each interval and added to the bioreactor such that its volume increases with time. At the instantaneous reactor volume, the q-rate of oxygen is expressed as a volumetric oxygen uptake rate (OUR). If the bioreactor is operating normally, this OUR is in balance with the OTR from Equation 2.15.

$$\text{OUR} = \frac{q_{O_2}}{\text{cell-free liquid volume}} \approx \text{OTR} = k_L a \Delta C_{O_2} \tag{4.2}$$

The aeration and agitation rates are manipulated at each time interval as described in Section 2.3 to ensure both that k_La computed by Equation 2.16 is equal to or greater than the required k_La, and that a sufficiently low mixing time is maintained (Equation 2.18). The simulation proceeds with μ=0.029/h until one of the design constraints is no longer satisfied (see Note 64). Beyond this point, the constraint is enforced by reducing μ with Excel Solver or Goal Seek.[123] In this case, the process reaction is designed to cause the batch to reach an NH_3 limit simultaneously with a pCO_2 limit. The simulation stops after ~48 h (two doublings), as shown in Figure 4.2. The final conditions of the fed batch are 16 m^3 (80% working volume) and 1,850 kg of DCM_a.[124]

Adding 2 h to drain, 4 h to CIP/SIP, and 4 h to re-fill the bioreactor through the HTST sterilizers, the total turnaround time can be taken as 57 h. If it can be

[121] The earlier simulations assumed air sparging; in this section, a new simulation will be generated for 90% O_2.

[122] Equivalent to 12×10^6/mL or 36.5 g/L wet cells.

[123] Kinetic limitations on μ are usually represented with attenuation factors f:

$$\mu = \mu_{max} f([\text{Glc}]) f([O_2]) \ldots$$

where $f([X])$ varies between 0 and 1 with the concentration of component X according to the Monod relation:

$$f([X]) = \frac{[X]}{[X] + K_X}$$

Without knowledge of K_X, the limitation can be enforced by manipulating the growth rate down such that the reactor simulation fits within some known constraint.

[124] 39×10^6/mL or 120 g/L wet cells.

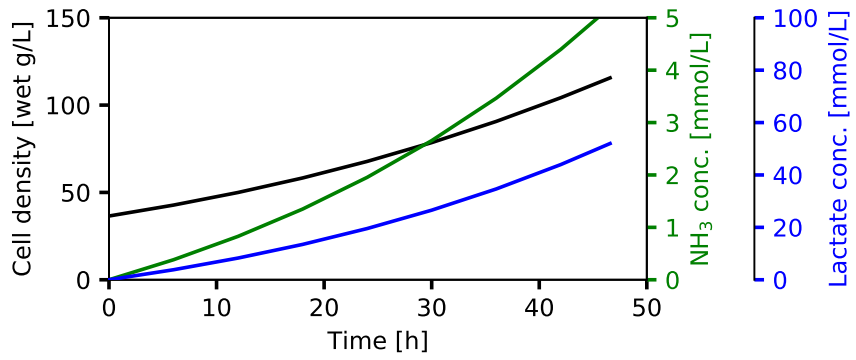

FIGURE 4.2: Fed-batch simulation in an O_2-sparged 20 m^3 bioreactor with 80% max working volume and the stoichiometry of Reaction 2.11.

assumed that the seed bioreactors operate with the same number of doublings, same endpoint, and same turnaround as the production bioreactor, then the 24×20 m^3 production fermentors could be serviced by 24 final seeds of 4 m^3 each. However, volumetric economies of scale dictate that it is more cost-effective to split a larger seed batch into multiple production fermentors [58, 198]. Figure 4.3 shows an optimized set of splits: four identical trains ending with 6×F5 (the production bioreactors) having ~1,850 wet kg each. These batches can be back-cast to F0, a single 150 L seed bioreactor inoculated with 3 kg of cells prepared in the lab.[125] With 24 production bioreactors, this facility is estimated to run 3,600 batches per year, producing 6.8 kTA of wet cell mass (assuming no failures). To meet a modest global production scale of 100 kTA, 15 such facilities comprising 352×20 m^3 bioreactors running 54,000 batch/y would be required. Including large seeds, the total volume of installed bioreactors would be 9,500 m^3.

[125] F*x*-notation is borrowed from baker's yeast production, where F5 is the final production fermentor, and seed fermentors are counted backwards from F4.

CAPITAL COSTS

Bioreactor costs are estimated with Equation 3.1, while costs for the remaining equipment are estimated with ACCE or SuperPro Designer. To compute the size and number of shared media-prep tanks at the F5 level, it is assumed that sterility assurance dictates the F4 seeds must be emptied immediately into ready F5s, the F3 seed immediately into ready F4s, and so on, with the result that all 6×F5 on each train start and end at the same time. For flexibility, it is further assumed that three F5s are filled simultaneously from amino and glucose media prep tanks each containing half of the initial batch volume, as shown in Figure 4.3.[126] HTST sterilizers are sized based on the prep tank volume and the 4 h fill time cited above. The trains are assumed to be staggered such that the four tanks and sterilizers can be shared between them. For each production and seed bioreactor, a dedicated tank holds the makeup medium for the entire batch. Filters and housings are sized for a flux of 500 L/m^2-h at the maximum makeup rate, which occurs at the end of the batch.

[126] The number and volume of media-prep tanks in the seed train (not depicted in Figure 4.3) are computed similarly.

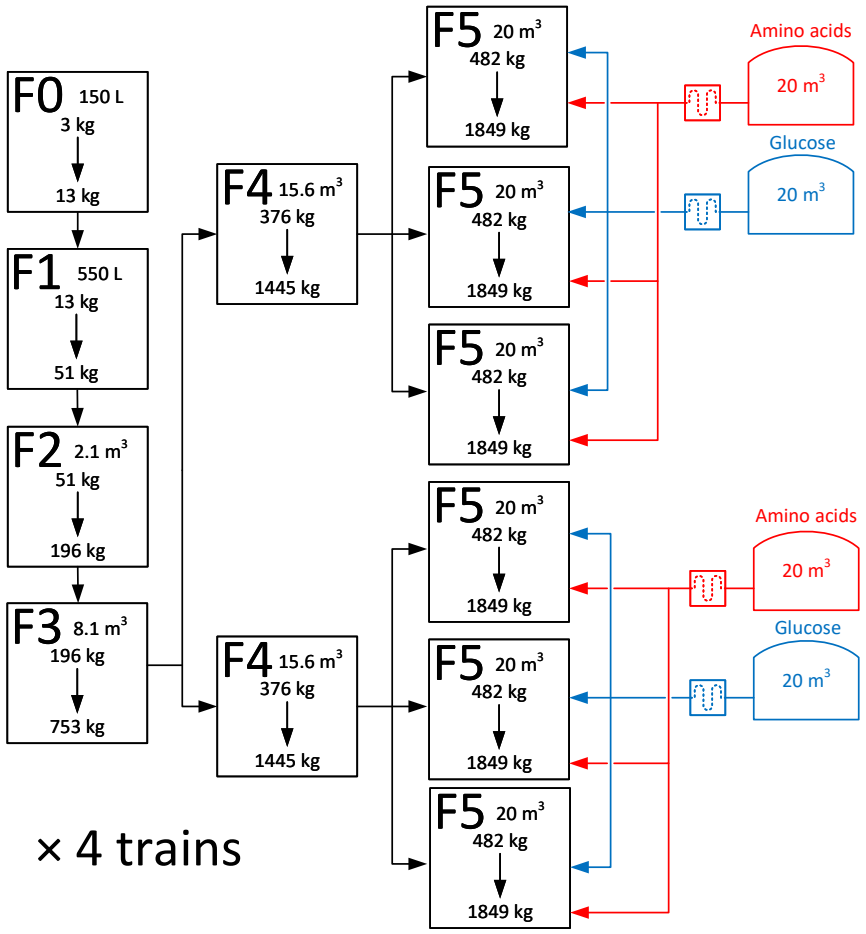

FIGURE 4.3: Seed splits for a fed-batch bulk cell-culture process with 24×20 m^3 production bioreactors. The final production bioreactor is referred to as F5 and seeds are counted backwards from F4.

Significant items on the OSBL equipment list include the VPSA unit for O_2 generation and the CIP system. The VPSA is sized for the O_2 feed rate from the fed-batch simulation multiplied by the number of online bioreactors. A cost for the VPSA is developed from information in the IHS Chemical PEP Yearbook [130]. The CIP system is taken to be 3 large tanks (for acid/caustic/sanitizer) on each train, sized for 20% of the total bioreactor and media-tank volume on that train. The abbreviated equipment lists and total direct costs of ISBL/OSBL equipment are given in Table 4.1.

Building footprints are estimated as shown in Table 4.2. An equipment occupancy fraction of 15% in the cell-culture area derives from floorplans of upstream biopharmaceutical clean rooms [145, 199, 200]. All bioreactors, media tanks, and CIP tanks are included in this fraction, leaving the remainder for pumps, panels, piping, and personnel access. Footprints for the other areas are estimated as described in the table, though these are much smaller than the cell-culture area. The bare costs of the buildings are estimated from these

footprints and Table 3.2. A Class 8 clean room is selected for the cell-culture area and Class 6 for the laboratory areas.

The sum of the ISBL/OSBL direct costs and building costs gives a total direct cost (TDC) of $94M. Indirect costs are factored from the TDC as shown in Table 4.3 to give a total capital investment (TCI) of $328M for this facility. As an annual capital charge (Equation 3.2), this is equivalent to an operating expense of $47.8M/y. Dividing the TCI by the total bare equipment cost gives an overall Lang factor of 7.2 for this analysis.[127]

[127] Bare equipment costs for bioreactors of volume V are estimated with a correlation based on the costs shown in Table 3.3:

$$\text{Cost (\$k)} = 51 \times (V[\text{m}^3])^{0.69}$$

Variable operating costs

Macro/micronutrients, consumables, and utilities costs are summarized in Table 4.4. Total consumptions of glucose and individual amino acids per batch are computed by integrating the q-rates from the fed-batch simulation.[128] The price of glucose is fixed at $0.26/kg and the global demand (i.e., for 54,000 batches per year) of each amino acid and growth factor is used to estimate its unit price, as described in Section 3.2. Consumables in the fed-batch process comprise membranes for the sterile retention filters sized above, which are assumed to be replaced at every batch start. Power demands for the VPSA, compressor, and bioreactor agitator are all estimated from the fed-batch simulation. The only significant power user, however, is the clean room facility, with power estimated from Tables 3.2 and 4.2. Water is also an important utility; bioreactor water is straightforward to estimate, while CIP and SIP usages are estimated from pharmaceutical plant design rules [201, 202], resulting in a total of 52 m^3 of water used per 20 m^3 batch at$20/cum.

[128] Additional nutrients and utilities required in the seed train are ratioed to the net cell mass made in the production bioreactor.

Fixed operating costs

As discussed in Section 3.3, labor hours are quantified in terms of operator attention per batch. Given the slower and more delicate nature of animal cell culture, the attention assumed for cell-bank steps is doubled in comparison to the yeast example given in Table 3.7. In addition to the %-online/offline attention assigned to each bioreactor, a fixed-hour task is added to each bioreactor step to capture filter replacements and preparation of the makeup medium. The continuous media-prep position is retained for the shared media tanks (Figure 4.1). The fixed operating costs are summarized in Table 4.5. They include annual overhead rates of 4% TCI/y for maintenance and 5% TCI/y for insurance.

Model results and sensitivities

The overall cost of production estimated for a fed-batch cell-culture process is $37/kg. This estimate uses 24×20 m^3 bioreactors and the stoichiometry found in Reaction 2.11. The estimate is summarized in Table 4.6. Table 4.7 restates the production cost summary by decomposing it into variable OPEX, labor, and capital cost contributions from bioreactors, buildings, and the rest of the plant.[129] Figure 4.4 presents various sensitivity analyses for the fed-batch process.

[129] Capital contributions in Table 4.7 include the annual capital charge and maintenance/insurance overhead, which are all factored on TCI.

The fed-batch production cost exceeds the affordability target of $25/kg asserted in Section 1.3 for a market volume of 100 kTA. Macronutrients, i.e., amino acids, contribute the most to the production cost estimate, as dictated by the stoichiometry of Reaction 2.11. In Figure 4.4a, nutrient costs vanish at extremely large production volume, due to the price-volume relationship inherent to Eqs. 3.3 and 3.4. An asymptotic cost of ~$16/kg is predicted at the ultimate scale of 10^5 kTA. At 100 kTA, substituting hydrolysate at $2/kg of mixed amino acids and repeating the fed-batch simulation with Reaction 2.13 reduces the macronutrient contribution by almost $16/kg, bringing the total cost to $22/kg, as shown in Table 4.7.

Further opportunities for cost reduction are limited. Figure 4.4b indicates that 24 production bioreactors (as shown in Figure 4.3) is an optimum within the parameters of this model. The modeled production cost increases at >24 bioreactors because the clean room area grows faster than the process volume it contains. At 48×20 m^3, the clean room costs more than the bioreactors; at 96×20 m^3, it costs more than the entire equipment list. From Table 4.7, at the optimum of 24 bioreactors, buildings only contribute $3/kg. Even if this were cut in half by assuming a sanitary cell-culture area (Table 3.2) or eliminated entirely by assuming outdoor operation, the COP would remain above target.[130]

As shown earlier in Figure 3.3, larger bioreactors have lower direct costs relative to the bare equipment cost—in terms of $/$m^3$, bigger is better. However, while Figure 2.8b indicates that reasonably high cell densities are (in principle) attainable in bioreactors larger than 20 m^3, such equipment has not been tested for animal cell culture. Figure 4.4c presents the sensitivity associated with the production bioreactor size, indicating that a (still-hypothetical) volume of 50 m^3 may be optimal. At larger volume, the reduction in final cell density due to pCO_2 limitations outweighs the cost benefits of larger reactors.[131]

Fill-and-draw operation, in which a fraction of the bioreactor is harvested and the remaining cells are allowed to multiply again in fresh medium, improves capital utilization by reducing bioreactor downtime and the frequency of seed starts. The optimized seed splits in Figure 4.3 hint at a preference for this operating mode, given that the F4 and F5 bioreactors are reasonably similar in volume.[132] Noting that the bioreactor offline time is ~18% in the example above, fill-and-draw operation might offer (as a best case) a similar reduction in the total CAPEX per kg, i.e., $2–3/kg.[133]

Recall that Reactions 2.11 and 2.13 assumed significant enhancements over the wild-type metabolisms in Reactions 2.9 and 2.12. The latter were dismissed in Section 2.3 because it was difficult to reach a high cell density with an ammonia accumulation limit of 5 mmol/L. To prove the point, Table 4.7 further presents the results of the fed-batch TEA calculations above for the wild-type metabolisms, with amino acids and hydrolysate. Compared to the enhanced-metabolism process described in detail above, a wild-type process with roughly the same CAPEX, bioreactor volume, and number of FTE

[130] Assuming outdoor operation does push the (very weak) optimum out to 48 bioreactors.

[131] As shown above in Figure 3.1a, the total installed bioreactor volume required to produce 100 kTA of cell mass is relatively constant up to 20 m^3 but increases above this volume as a result of lower cell density.

[132] In other words, F5 is nearly the same operation as F4, split three times and run again. An extreme example of this is observed in Figure A.4b for the constrained baker's yeast process.

[133] Note that fill-and-draw operation is very common in wastewater treatment and somewhat common in industrial bioproducts. It is *not* common when live cells are the product (e.g., baker's yeast) or when the number of contaminating organisms must be tightly controlled. Its applicability to bulk cell culture is therefore not guaranteed.

produces only 6% as much cell mass. Figure 4.5a presents the COP sensitivity to metabolism (Lac/Glc ratio[134]) and cell doubling time (i.e., growth rate). At the baseline metabolism of Lac/Glc=0.5, the modeled COP roughly doubles as the doubling time increases from 24 to 48 hours. This economic disadvantage is much more pronounced at lower metabolic efficiency. However, even as the metabolism approaches maximum efficiency at full respiration (Lac/Glc=0), the estimated COP does not fall below $30/kg at any growth rate. From a target-setting perspective, the TEA model thus predicts that high metabolic efficiency is more important than high growth rate.

Finally, the fed-batch TEA model can be used to probe COP sensitivity to the fundamental assumption of cell size. On a mass basis, smaller cells are less efficient with respect to energy and oxygen usage; as shown in Figure 4.5b, the model indeed predicts a relatively weak sensitivity to this parameter. The cost to bulk-produce 5,000 pg cells is estimated to be ~5% lower than the 3,000 pg cells modeled above.

[134]The Gln/Glc ratio in Figure 4.5 is fixed at 0.05×Lac/Glc, as discussed in Note 67.

TABLE 4.1: Abbreviated equipment list and direct costs for bulk cell mass production by a fed-batch process.

Equipment	Qty/Capacity	Cost
ISBL: Bioreactors[a]		
Production (F5)	24×20 m^3	$33,922,000
Seed bioreactors	24×16 m^3 and smaller	$22,673,000
ISBL: Other		
Initial fill tanks	14×20 m^3 and smaller	$1,660,000
HTST sterilizers	14×4,950 L/h and smaller	$702,000
Makeup tanks	72×2.8 m^3 and smaller	$3,370,000
Filter housings	216×0.7 m^2 and smaller	$1,481,000
Centrifuge, disk stack	4×35 gpm	$1,744,000
Missing capital	10%	$7,284,000
Installation	1.3× PEC[b]	$21,113,000
ISBL: Total Direct Cost		**$93,949,000**
OSBL		
O_2 vacuum PSA	25 kTA	$8,840,000
O_2 compressor	2,977 ACMH	$295,000
NG boiler	3,612 kg/h	$154,000
CIP tanks	12×42 m^3	$4,136,000
Chiller	959 kW	$551,000
Cooling tower	12 L/s	$24,000
Missing capital	10%	$1,556,000
Installation	1.3× PEC	$20,223,000
OSBL: Total Direct Cost		**$35,779,000**

[a]Estimated bare equipment cost: $13,794,000

[b]Only to applied to "ISBL: Other"

TABLE 4.2: Building costs for the fed-batch process.

Building	Area (m^2)	Levels	Cost	Remark
Cell culture (Class 8)	5,268	2	$39,607,000	15% occupied by major equipment
Cell lab (Class 6)	294	1	$2,575,000	10 m^2 per active seed in the lab
QC lab (Class 6)	147	1	$1,287,000	50% of the cell lab
Office	318	1	$527,000	15 m^2/FTE on a single shift
Compressor	63	2	$162,000	Based on fresh air feed to VPSA
Shop	1,317	1	$1,648,000	25% of the cell-culture area
Warehouse	1,317	1	$1,491,000	25% of the cell-culture area
Slab	8,724		$1,185,000	Entire developed area
Buildings total			**$48,482,000**	

TABLE 4.3: Indirect costs and total capital investment (TCI) summary for the fed-batch process.

ISBL direct cost		$21,113,000
OSBL direct cost		$35,779,000
Buildings		$48,482,000
Total Direct Cost (TDC)		$178,210,000
Engineering & Construction	0.6× TDC	$106,926,000
Total Plant Cost (TPC)		$285,136,000
Fees & Contingency	0.15× TPC	$42,770,000
Total Capital Investment (TCI)		**$327,907,000**
Annual capital charge	14.6% TCI/y	$47,771,000/y
Overall Lang factor estimate (TCI/PEC)		7.2

TABLE 4.4: Variable operating cost summary for the fed-batch process.

Macronutrients	Unit	Per batch	Unit cost	$/batch	$/kg
Glucose	kg	687	$0.26	$177	$0.10
L-arginine	kg	30	$70	$2,050	$1.11
L-cysteine	kg	9	$136	$1,220	$0.66
L-glutamine	kg	82	$39	$3,184	$1.72
L-histidine	kg	12	$117	$1,371	$0.74
L-isoleucine	kg	22	$83	$1,794	$0.97
L-lysine	kg	37	$61	$2,260	$1.22
L-methionine	kg	7	$154	$1,105	$0.60
L-phenylalanine	kg	21	$85	$1,761	$0.95
L-threonine	kg	26	$75	$1,932	$1.04
L-tryptophan	kg	8	$144	$1,165	$0.63
L-tyrosine	kg	23	$81	$1,845	$1.00
L-valine	kg	30	$70	$2,039	$1.10
L-alanine	kg	29	$70	$2,032	$1.10
L-asparagine	kg	21	$84	$1,765	$0.95
L-aspartic acid	kg	27	$74	$1,953	$1.06
Glycine	kg	21	$86	$1,741	$0.94
L-leucine	kg	36	$63	$2,222	$1.20
L-proline	kg	19	$89	$1,695	$0.92
L-serine	kg	27	$73	$1,969	$1.06
Total macronutrients				$35,300	$19.08
Micronutrients	Unit	Per batch	Unit cost	$/batch	$/kg
Insulin	g	310	$7	$2,161	$1.17
Transferrin	g	171	$12	$1,989	$1.08
FGF	g	1.6	$649	$1,039	$0.56
TGF-β	g	0.032	$18,837	$603	$0.33
Total micronutrients				$5,800	$3.13
Consumables	Unit	Per batch	Unit cost	$/batch	$/kg
0.2-μm filter	m^2	0.9	$200	$186	$0.10
0.1-μm filter	m^2	0.9	$500	$464	$0.25
Virus filter	m^2	0.9	$1,000	$929	$0.50
Total consumables				$1,600	$0.85
Utilities	Unit	Per batch	Unit cost	$/batch	$/kg
Process water	kg	52,467	$0.02	$1,049	$0.57
VPSA power	kWh	2,139	$0.05	$101	$0.05
Compressor power	kWh	156	$0.05	$7	$0.00
Agitator power	kWh	47	$0.05	$2	$0.00
Chiller power	kWh	257	$0.05	$12	$0.01
Dewatering power	kWh	22	$0.05	$1	$0.00
Facility power	kWh	11,511	$0.05	$543	$0.29
Natural gas	MMBtu	10	$2.90	$29	$0.02
Municipal WWT	m^3	52	$0.40	$21	$0.01
Total utilities				$1,700	$0.94
Total variable operating costs				**$44,400**	**$24.01**

TABLE 4.5: Fixed operating cost summary for the fed-batch process.

Batch labor	Attention	h/batch	FTE/shift	$/y	$/kg
Lab	120 min/step	2.5	1.1	$55,000	$0.01
Small seed	2 h prep + 25% time	10.2	4.3	$215,000	$0.03
Large seed	4 h prep + 10% time	6.1	2.6	$130,000	$0.02
Production	8 h prep + 10% time	12.4	5.2	$260,000	$0.04
Total batch workers		31.2	13	$660,000	$0.10
Continuous labor	Positions/shift				
Media prep	0.5/train		2.0	$100,000	$0.01
Dewatering	0.25/train		1.0	$50,000	$0.01
Utilities	1		1.0	$50,000	$0.01
Maintenance	0.5/train		2.0	$100,000	$0.01
Supervisor	1 per 10 FTE		2.0	$140,000	$0.02
Total continuous workers			8	$440,000	$0.06
Total workers per shift			21	$1,100,000	$0.16
Total workers (all shifts)			95	$4,950,000	$0.73
Labor burden (100%)				$4,950,000	$0.73
Total labor				**$9,900,000**	**$1.45**
Annual maintenance (4% of TCI/y)				$13,116,000	$1.92
Annual insurance (5% of TCI/y)				$16,395,000	$2.40
Total fixed operating costs				**$39,412,000**	**$5.78**

TABLE 4.6: Total cost of production summary for the fed-batch process.

	$/batch	$/y	$/kg
Macronutrients	$35,300	$130,130,000	$19.08
Micronutrients	$5,800	$21,364,000	$3.13
Consumables	$1,600	$5,825,000	$0.85
Utilities	$1,700	$6,437,000	$0.94
Total variable OPEX	$44,400	$163,755,000	$24.01
Burdened labor cost	$2,700	$9,900,000	$1.45
Annual maintenance	$3,600	$13,116,000	$1.92
Annual insurance	$4,400	$16,395,000	$2.40
Total fixed OPEX	$10,700	$39,412,000	$5.78
Annual capital charge	$13,000	$47,771,000	$7.00
Total cost of production	**$68,000**	**$250,938,000**	**$36.79**

TABLE 4.7: TEA estimates for the fed-batch production of bulk cell mass from individual amino acids or from plant hydrolysate. Wild-type and enhanced metabolisms are compared.

	Reaction 2.11 Enhanced Amino acids	Reaction 2.13 Enhanced Hydrolysate	Reaction 2.9 Wild-type Amino acids	Reaction 2.12 Wild-type Hydrolysate
Production rate (kTA)	6.8	6.9	0.41	0.41
Total CAPEX	$328M	$330M	$286M	$288M
Total bioreactor volume (m^3)	649	644	633	637
Total FTE	95	94	81	81
Water usage L/kg	45	44	720	738
Cost contributors, $/kg				
Macronutrients	$19.08	$3.39	$18.24	$4.27
Micronutrients	$3.13	$3.12	$4.60	$4.62
Consumables	$0.85	$0.81	$12.56	$13.05
Utilities	$0.94	$0.93	$14.52	$14.81
Labor	$1.45	$1.42	$20.70	$20.86
Bioreactor CAPEX	$3.60	$3.56	$55.09	$55.43
Buildings CAPEX	$3.08	$3.11	$43.37	$43.78
Rest of plant CAPEX	$4.65	$4.66	$67.48	$68.22
Total cost of production	$36.79	$21.00	$236.58	$225.03

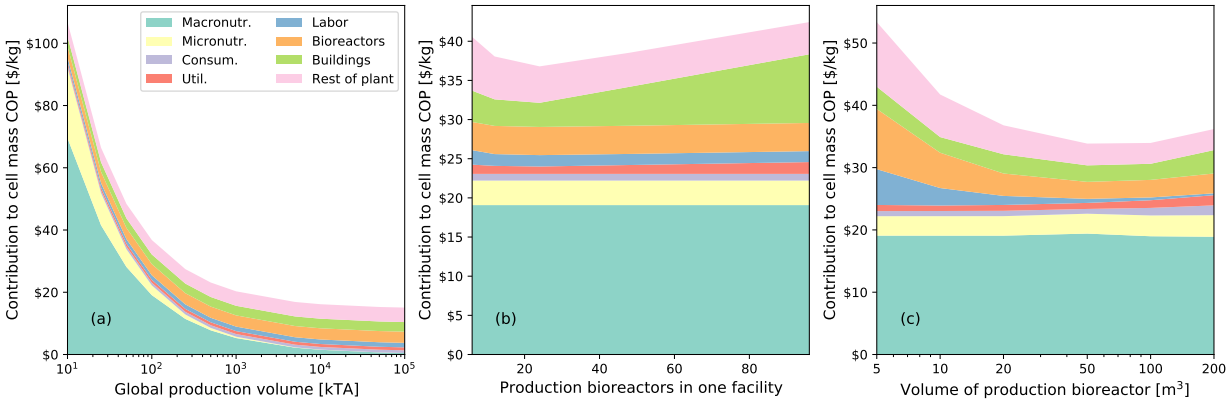

FIGURE 4.4: COP sensitivities predicted by the fed-batch TEA model. (a) 24×20 m^3 bioreactors at increasing global production volume. (b) Varying number of 20 m^3 bioreactors in a single facility, at 100 kTA. (c) Varying volume of the production bioreactor (24×).

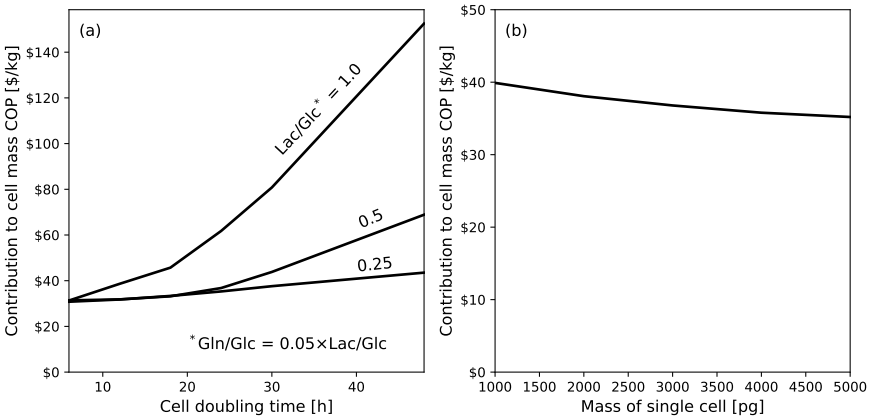

FIGURE 4.5: COP sensitivity to basic modeling assumptions. (a) Cell doubling time (i.e., growth rate) and Lac/Glc ratio. Note that Gln/Glc=0.05×Lac/Glc. The baseline model uses a 24-hour doubling time and Lac/Glc=0.5. (b) Wet mass of a single cell. The baseline model uses 3,000 pg.

4.2 Perfusion operation

A PFD of a conceptual cell-culture process based on perfusion technology is given in Figure 4.6. For the detailed example given below, the facility will be designed for a cell mass production rate of 6.9 kTA, which roughly matches the 24×20 m^3 fed-batch process from the previous section. The perfusion facility is likewise assumed to exist as part of a 100 kTA market. The production bioreactor is 2 m^3 in volume and operates with a perfusion rate of 1.0/d with 2×ATF 10 filters, as proposed in Table 2.4. The production bioreactor is inoculated by expanding cells from the lab through 125 L and 500 L seed bioreactors, which are operated in fed-batch mode with a final cell density of 120 g/L wet cells. Upon inoculation, the production bioreactor also operates in fed-batch mode up to 120 g/L. At this point, perfusion begins and the retained cell density rises to 195 g/L,[135] per Figure 2.9 and Reaction 2.11. At steady state, 9 kg/h of wet cell mass is harvested from the bioreactor. As in the fed-batch example, bulk amino-acid and glucose tanks are shared for initial filling of all bioreactors. Additionally, each production bioreactor gets two dedicated day tanks to hold 24 h of makeup media each. These are switched and re-filled on alternate days.

[135] 65×10^6/mL

Capital costs

The perfusion process is analyzed with shortcut scheduling calculations, much as described above in Section 4.1. The actual schedule implied by these calculations would be rather aggressive compared to upstream biopharmaceutical processes that use perfusion, but should help to examine the projected economics of this configuration at a very large and mature scale. To compute the required number of bioreactors, it is assumed that each one operates with continuous cell harvest except during 10 scheduled turnarounds per

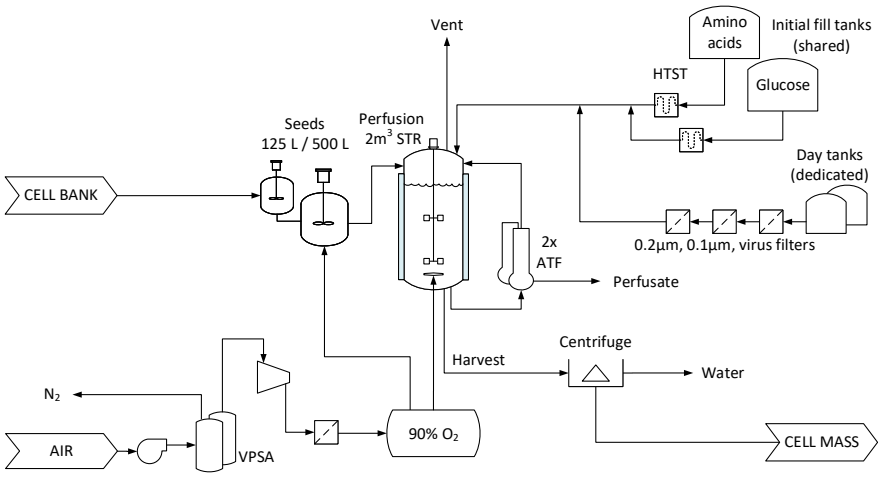

FIGURE 4.6: Process flow diagram of a conceptual perfusion process for bulk cell culture.

year. At each turnaround, the bioreactor is offline for 10 hours for CIP/SIP and re-filling,[136] then immediately reinoculated from a ready 500 L seed bioreactor. To increase the cell density to 195 g/L after inoculation requires 2.7 cell doublings (24 h each) or 65 h. The average annual uptime (at steady state) of each bioreactor is thus ~91%, and 96 production bioreactors are required to produce 6.9 kTA. These can be serviced with eight fed-batch seed trains. Centrifuges, sterilizing equipment, and CIP tanks are sized as above for the fed-batch process. A cost for the ATF 10 perfusion devices is taken from Pollock et al [134].

[136] 2 h drain, 4 h CIP/SIP, 4 h fill.

At a global production scale of 100 kTA, 14 such facilities would be required, comprising an installed bioreactor volume of 1,400×2 m^3. The total volume of installed bioreactors would be 2,850 m^3. Abbreviated equipment lists and total direct costs for ISBL/OSBL equipment are given in Table 4.8, and building footprints and costs are shown in Table 4.9. As for the fed-batch process discussed above, a Class 8 clean room is selected for the cell-culture area and Class 6 for the laboratory areas. The TDC developed in Table 4.10 is $360M and the factored TCI is $663M, giving an annual capital charge of $97M/y. The overall Lang factor for the perfusion process is estimated as 6.9.

Variable operating costs

In addition to cellular consumption, nutrient losses are included in total usage, assuming a perfusion rate of 1/d (1,600 L/d) at residual concentrations of 1 g/L glucose and 0.5 g/L total amino acids. Consumables in the perfusion process comprise the sterile retention filters (described above for the fed-batch process) and ATF 10 membranes at $16k each [134]. All of these are assumed to be replaced at every turnaround. Power demands for the VPSA, compressor, and bioreactor agitator are estimated from the steady-state bioreactor conditions. Facility power demand is estimated as described previously. Bioreactor water is estimated from the perfusion rate and CIP/SIP water is estimated as above. The total variable operating costs are summarized in Table 4.11.

Fixed operating costs

For the perfusion process, which is nominally continuous, operator attention hours are estimated somewhat differently from the fed-batch process. Each inoculation (10 per bioreactor per year) is assigned an 8-hour effort from lab to steady state and each bioreactor is assigned a monitoring effort equivalent to 10% of the online time. Every change of the media day tanks is also assigned a fixed 2-hour effort and the continuous media prep position is eliminated. These total hours are converted to FTE equivalents with a factor of 2,080 FTE-h/y. Positions per shift for the remainder of the process are estimated as in the fed-batch example above. Total fixed operating costs are summarized in Table 4.12.

Model results and sensitivities

The overall cost of production estimated for a perfusion-based cell-culture process is \$51/kg. This estimate uses 96×2 m^3 bioreactors and the stoichiometry found in Reaction 2.11. The estimate is summarized in Table 4.13. Table 4.14 presents a decomposed production cost summary, and Figure 4.7 presents various sensitivity analyses for the perfusion process.

As discussed above for the fed-batch process, the modeled cost of production exceeds the affordability target of \$25/kg for a market volume of 100 kTA. Opportunities for cost reduction are limited. Given the aggressive scheduling assumed above (91% uptime), capital utilization is nominally maximized. However, the limited volume, the relatively high direct costs of small bioreactors (Figure 3.3), and the extra CAPEX and consumables associated with the perfusion device present significant disadvantages. Indeed, in contrast to the fed-batch analysis above, capital costs are a much more significant contributor to production cost—almost 50% of the total. Nutrient costs can be minimized by assuming a much larger global production volume, as shown in Figure 4.7a, or reduced \$15–16/kg by substituting low-cost hydrolysate for the amino acids. Neither affects the capital cost, however, so the total COP remains above the target.

In Figure 4.7b, bioreactor number is expressed in terms of the total cell mass production for one facility. A very weak minimum is found at around 3.5 kTA, though the COP is only 2.5% lower than that estimated for the 7 kTA facility above. The issue with divergent clean room cost noted above for fed-batch bioreactors is also present for perfusion, but to a much smaller degree. Given the independence of production cost on total output, the 2 m^3 perfusion process approaches a true scale-out facility. Figure 4.7b further presents the facility-scale behavior (total COP only) of 1 m^3 bioreactors operating at 1/d with a single ATF 10. Roughly twice as many vessels are required in this case, causing the clean room costs (and thus the total COP) to grow faster than with 2 m^3 bioreactors.

Figure 4.7c examines the sensitivity of the perfusion production cost to retained cell density. Recall that Figure 2.9 and Table 2.4 indicate either a retained wet cell density of 195 g/L at a perfusion rate of 1.0/d (dual ATF 10) or 140 g/L at a perfusion rate of 0.5/d (single ATF 10). From ~100 g/L (i.e., no perfusion) to 140 g/L, a reduced production cost is largely a function of better capital utilization. Above 140 g/L, however, the extra capital and consumables costs associated with the second ATF device eliminate this benefit, such that the production cost at 195 g/L is hardly any better than at 140 g/L.[137]

As above for the fed-batch process, the wild-type metabolism fails miserably in the perfusion process. With a retained cell density of 13 g/L, a wild-type process with roughly the same CAPEX, bioreactor volume, and number of FTE produces only 6.5% as much cell mass, as shown in Table 4.14. Metabolic enhancement is thus equally important for either technology.

[137] Specifically, \$51.84/kg at 140 g/L and 0.5/d versus \$51.29/kg at 195 g/L and 1.0/d.

TABLE 4.8: Abbreviated equipment list and direct costs for bulk cell mass production by a perfusion process.

Equipment	Qty/Capacity	Cost
ISBL: Bioreactors[a]		
Production	96×2 m^3	$82,686,000
Seed bioreactors	16×1 m^3 and smaller	$9,203,000
ISBL: Other		
Cell retention	192×ATF 10	$38,530,000
Initial fill tanks	16×3 m^3 and smaller	$1,457,000
HTST sterilizers	16×667 L/h and smaller	$533,000
Makeup tanks	192×1.5 m^3 and smaller	$13,345,000
Filter housings	288×0.1 m^2 and smaller	$2,663,000
Centrifuge	2×24 gpm	$721,000
Missing capital	10%	$16,571,000
Installation	1.3× PEC[b]	$95,967,000
ISBL: Total Direct Cost		**$261,676,000**
OSBL		
O_2 vacuum PSA	21 kTA	$7,963,000
O_2 compressor	2,296 ACMH	$275,000
NG boiler	1,946 kg/h	$142,000
CIP tanks	24×10 m^3	$4,059,000
Chiller	571 kW	$445,000
Cooling tower	16 L/s	$30,000
Missing capital	10%	$1,435,000
Installation	1.3× PEC	$18,654,000
OSBL: Total Direct Cost		**$33,002,000**

[a]Estimated bare equipment cost: $8,243,000
[b]Only to applied to "ISBL: Other"

TABLE 4.9: Building costs for the perfusion process.

Building	Area (m^2)	Levels	Cost	Remark
Cell culture (Class 8)	13,073	1	$49,143,000	15% occupied by major equipment
Cell lab (Class 6)	368	1	$3,223,000	10 m^2 per active seed in the lab
QC lab (Class 6)	184	1	$1,611,000	50% of the cell lab
Office	440	1	$728,000	15 m^2/FTE on a single shift
Compressor	56	2	$144,000	Based on fresh air feed to VPSA
Shop	3,268	1	$4,091,000	25% of the cell-culture area
Warehouse	3,268	1	$3,700,000	25% of the cell-culture area
Slab	20,657		$2,805,000	Entire developed area
Buildings total			**$65,445,000**	

TABLE 4.10: Indirect costs and total capital investment (TCI) summary for the perfusion process.

ISBL direct cost		$95,967,000
OSBL direct cost		$33,002,000
Buildings		$65,445,000
Total Direct Cost (TDC)		$360,124,000
Engineering & Construction	0.6× TDC	$216,074,000
Total Plant Cost (TPC)		$576,198,000
Fees & Contingency	0.15× TPC	$86,430,000
Total Capital Investment (TCI)		**$662,628,000**
Annual capital charge	14.6% TCI/y	$96,536,000/y
Overall Lang factor estimate (TCI/PEC)		6.9

TABLE 4.11: Variable operating cost summary for the perfusion process.

Macronutrients	Unit	Per year	Unit cost	$/y	$/kg
Glucose	MT	40,320	$260	$672,000	$0.10
L-arginine	MT	1,760	$66k	$7,384,000	$1.07
L-cysteine	MT	540	$130k	$4,392,000	$0.64
L-glutamine	MT	4,830	$38k	$11,467,000	$1.66
L-histidine	MT	700	$111k	$4,936,000	$0.71
L-isoleucine	MT	1,300	$79k	$6,462,000	$0.94
L-lysine	MT	2,200	$59k	$8,140,000	$1.18
L-methionine	MT	430	$147k	$3,981,000	$0.58
L-phenylalanine	MT	1,240	$81k	$6,342,000	$0.92
L-threonine	MT	1,540	$72k	$6,958,000	$1.01
L-tryptophan	MT	480	$137k	$4,196,000	$0.61
L-tyrosine	MT	1,370	$77k	$6,604,000	$0.96
L-valine	MT	1,740	$67k	$7,342,000	$1.06
L-alanine	MT	1,730	$67k	$7,317,000	$1.06
L-asparagine	MT	1,250	$80k	$6,357,000	$0.92
L-aspartic acid	MT	1,580	$71k	$7,031,000	$1.02
Glycine	MT	1,210	$82k	$6,269,000	$0.91
L-leucine	MT	2,120	$60k	$8,001,000	$1.16
L-proline	MT	1,140	$85k	$6,104,000	$0.88
L-serine	MT	1,610	$70k	$7,090,000	$1.03
Total macronutrients				$127,044,000	$18.39

Micronutrients	Unit	Per year	Unit cost	$/y	$/kg
Insulin	kg	13,667	$8	$7,173,000	$1.04
Transferrin	kg	7,538	$14	$6,603,000	$0.96
FGF	kg	70	$775	$3,447,000	$0.50
TGF-β	kg	1.4	$22,482	$2,001,000	$0.29
Total micronutrients				$19,225,000	$2.78

Consumables	Unit	Per year	Unit cost	$/y	$/kg
ATF filter membrane	ea	1,920	$16,300	$31,296,000	$4.53
0.2-μm filter	m^2	122	$200	$24,300	$0.00
0.1-μm filter	m^2	122	$500	$60,800	$0.01
Virus filter	m^2	122	$1,000	$121,600	$0.02
Total consumables				$31,503,000	$4.56

Utilities	Unit	Per year	Unit cost	$/y	$/kg
Process water	kg	183,020,000	$0.02	$3,660,000	$0.53
VPSA power	kWh	6,838,000	$0.05	$323,000	$0.05
Compressor power	kWh	348,000	$0.05	$16,000	$0.00
Agitator power	kWh	79,000	$0.05	$3,700	$0.00
Chiller power	kWh	4,598,000	$0.05	$217,000	$0.03
Dewatering power	kWh	66,000	$0.05	$3,100	$0.00
Facility power	kWh	53,414,000	$0.05	$2,521,000	$0.36
Natural gas	MMBtu	1,000	$2.90	$2,500	$0.00
Municipal WWT	m^3	183,000	$0.40	$73,000	$0.01
Total utilities				$6,747,000	$0.98

Total variable operating costs				**$184,518,000**	**$26.70**

TABLE 4.12: Fixed operating cost summary for the perfusion process.

Batch labor (all shifts)	Attention	h/y	FTE/y	$/y	$/kg
Inoculum prep	8 h	9,600	4.6	$231,000	$0.03
Media prep	2 h at every change	80,069	38.5	$1,925,000	$0.28
Production monitoring	10% time	105,120	50.5	$2,527,000	$0.00
Total batch workers		194,789	94	$4,682,000	$0.68
Continuous labor	Positions/shift		FTE/shift		
Dewatering	0.25/train		0.5	$25,000	$0.00
Utilities	1		1.0	$50,000	$0.01
Maintenance	0.5/train		4.0	$200,000	$0.03
Supervisor	1 per 10 FTE		3.0	$210,000	$0.03
Total continuous workers			9	$485,000	$0.07
Total workers (all shifts)			132	$6,865,000	$0.99
Labor burden (100%)				$6,865,000	$0.99
Total labor				**$13,730,000**	**$1.99**
Annual maintenance (4% of TCI/y)				$26,505,000	$3.84
Annual insurance (5% of TCI/y)				$33,131,000	$4.79
Total fixed operating costs				**$73,366,000**	**$10.62**

TABLE 4.13: Total cost of production summary for the perfusion process.

	$/y	$/kg
Macronutrients	$127,044,000	$18.39
Micronutrients	$19,225,000	$2.78
Consumables	$31,503,000	$4.56
Utilities	$6,747,000	$0.98
Total variable OPEX	$184,518,000	$26.70
Burdened labor cost	$13,730,000	$1.99
Annual maintenance	$26,505,000	$3.84
Annual insurance	$33,131,000	$4.79
Total fixed OPEX	$73,366,000	$10.62
Annual capital charge	$96,536,000	$13.97
Total cost of production	**$354,420,000**	**$51.29**

TABLE 4.14: TEA estimates for the perfusion process with wild-type or enhanced metabolism.

	Reaction 2.11 Enhanced Amino acids	Reaction 2.9 Wild-type Amino acids
Production rate (kTA)	6.9	0.45
Total CAPEX	$663M	$663M
Total bioreactor volume (m^3)	197	197
Total FTE	132	132
Water usage kg/kg	26	423
Cost contributors, $/kg		
Macronutrients	$18.39	$20.48
Micronutrients	$2.78	$4.08
Consumables	$4.56	$69.50
Utilities	$0.98	$15.20
Labor	$1.99	$30.26
Bioreactor CAPEX	$5.77	$87.88
Perfusion CAPEX	$5.56	$84.75
Buildings CAPEX	$4.11	$62.10
Rest of plant CAPEX	$7.17	$110.12
Total cost of production	$51.29	$484.37

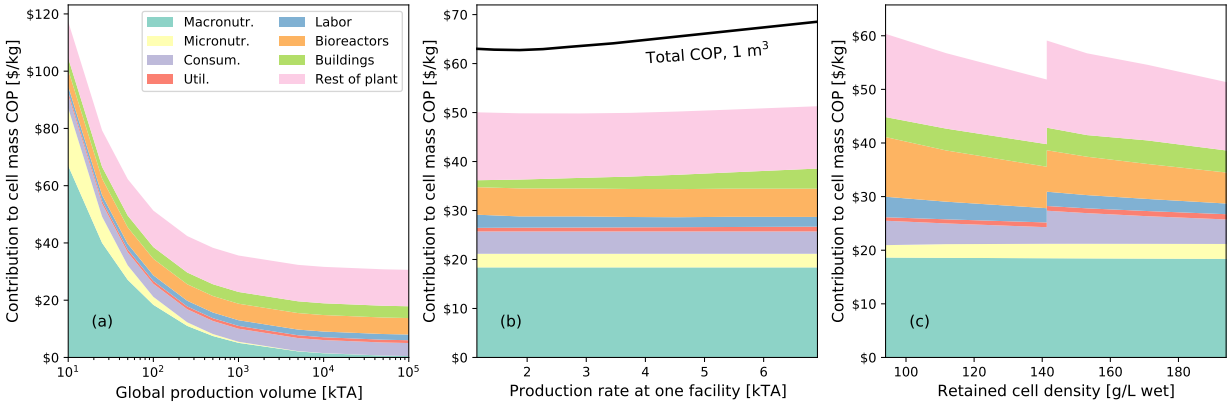

FIGURE 4.7: COP sensitivities predicted by the perfusion TEA model. (a) 6.9 kTA production in a single facility at increasing global production volume. (b) Varying production rate (i.e., number of bioreactors) at a single facility, at 100 kTA. (c) Increasing perfusion rate and cell density, per Figure 2.9. At >1.0/d (140 g/L), a second ATF filter is added.

4.3 Economic sustainability metrics

This section discusses how the analysis fares against metrics of price acceptance and resource efficiency, i.e., its economic sustainability. It should be recognized that the analysis clearly carries many uncertainties. The scope of the following discussion is therefore limited by the results of the modeling above and this analyst's perspective. In the end, judgment is left to the reader.

Affordability

Section 1.3 proposed a target of $25/kg (wet basis) for bulk animal cell culture at a global production volume of 100 kTA. It was asserted that this should resolve to ~$50/kg for a finished product at the supermarket, i.e., something that ten million people might buy regularly. Although both of the baseline estimates detailed above exceed this target, the fed-batch process could potentially be brought under $25/kg through the use of low-cost plant protein hydrolysates as cell-culture media. The same is not true of the perfusion process, which has baseline capital costs and capital-dependent fixed costs that are well in excess of the target.

The bioreactor cost estimates (Section 3.1) assumed 316L stainless steel construction, as dictated by the ASME standard for bioprocess equipment. Though not analyzed here, some cost reduction may be possible by assuming that cultured-meat equipment will be made primarily from high-grade plastic and lower-grade steel—something like a commercial kitchen. While such materials are probably not consistent with the ultimate sterility requirements of cultured meat, these are presently unknown. Nor is their use necessarily a guarantee of significantly lower capital costs. As addressed in the discussions surrounding Table 3.1 and Figure 3.1, direct and indirect plant costs (as understood by a Lang factor on purchased equipment cost) are very much a function of facility size and the general size of the equipment in that facility, regardless of its materials of construction. The effective Lang factors of ~7 computed in Tables 4.3 and 4.10 are reflective of this.[138] Without more detailed design, a lower Lang factor is not justified.

Indeed, at this level of detail, too much speculation on cost reductions is ill-advised, for many cost *increases* could easily be justified in the TEA model. For instance:

- Product loss associated with batch failure is not considered. Usually modeled as a linear reduction of yield, losses could be expected to increase with, e.g., fewer engineering controls on equipment and plant design, or the reduced sterility assurance of lower-grade materials of construction and lower-quality media components.
- Salary assumptions of $50k per operator and $70k per supervisor may be consistent with chemical and food production facilities, but they are decidedly *in*consistent with the skills required of cell-culture practitioners in the contemporary biopharmaceuticals industry.[139]

[138] This is not to say that the Lang factor must necessarily be lower with larger equipment. As shown in Table 4.15, the effective Lang factor is not a monotonic function of bioreactor size. Rather, it has jumps associated with an increase in the number of levels required in the clean room.

Table 4.15: Effective Lang factors for the fed-batch TEA model at various bioreactor volumes.

Production bioreactor	Clean room levels	Eff. Lang
5 m^3	1	7.4
10 m^3	1	6.8
20 m^3	2	7.2
50 m^3	2	7.0
100 m^3	2	7.0
200 m^3	3	8.0

[139] Location also plays a role here. Compared to a U.S. biotechnology hub like Boston or San Francisco, engineering and construction costs as well as utilities and labor could be reduced by ~25% if the facility were sited in Raleigh or Austin, or 75% if sited in Bangalore [203]. The latter, of course, obviates any arguments of increased food security from cultured meat. It would also likely result in a product that might be deemed affordable by U.S. consumers but not by the people who made the item.

- The costs of R&D associated with the fairly heroic feats of cell-line engineering that were assumed in order to even approach affordability in the previous models must ultimately be amortized to the product price. In TEA, this cost is typically modeled with a licensing fee, on an annual or per-kg basis.

From the modeling above, it can be concluded that metabolic efficiency and low-cost hydrolysate media development can both be taken as necessary but insufficient conditions of affordability. Capital cost reduction is a secondary condition at best.

▸ RETURN ON HUMAN INVESTMENT

At 25 MT/y, the hypothetical cultured-meat factory of van der Weele and Tramper [4] is sized to feed ~2,500 people annually at some fraction of their total diet (10 kg/y each), while employing "three to four highly educated and well-trained" individuals, and (one presumes) a number of less-technical staff to maintain the facility. Up and down the supply chain, the factory's revenues must fractionally employ other individuals as well, at media suppliers, power and wastewater facilities, logistics and shipping companies, etc. For argument's sake, say 10 FTE in total, or an eater:worker ratio of 250. In the present models, this ratio is also a function of metabolic efficiency, as presented in Table 4.16. With the enhanced metabolism of Reaction 2.11, the ratios computed in the TEA models above are much better than 250. With the wild-type metabolism of Reaction 2.9, they are significantly worse.[140]

This eater:worker ratio invites a troubling corollary, for labor estimates in TEA (including the present analysis) are based on many assumptions about productivity and automation that may not be achievable. As performance falls short relative to these assumptions, there are several conceivable outcomes. At the extreme ($\leq$1) is a factory that doesn't make enough food to feed its workers. Shy of this extreme, one should expect shifts in the economy as cultured-meat consumption scales, causing significant numbers of workers to move out of other sectors and into food manufacturing and its support industries. An imbalance between the number of jobs created by cultured meat and the number eliminated in conventional meat would ultimately create market pressures that resist the displacement of the former by the latter. Perhaps the most likely outcome, however, is simply a factory that produces food which its workers cannot afford.

That is certainly the outcome of the present analysis, at least when the wild-type metabolism is used. Even with a rather meager salary assumption of $50k/y, labor still contributes $20–30/kg to the modeled cell mass production cost in such cases, as shown in Tables 4.7 and 4.14. Raising the salary assumption does not resolve the situation, as it causes the production cost to increase. If retail cost is double the production cost, and a worker should spend no more than 2% of their gross salary on 10 kg/y, then this function reaches parity at a salary of about $350k/y for the wild-type fed-batch case

[140] Assuming three total workers per plant staff computed in the models.

TABLE 4.16: Eater:worker ratios computed by TEA. Enhanced and wild-type metabolisms are compared.

20 m^3 fed-batch, enhanced	2,400
20 m^3 fed-batch, wild-type	170
2 m^3 perfusion, enhanced	1,700
2 m^3 perfusion, wild-type	115

or $1.1M/y for the wild-type perfusion case.[141] Again, without the significant metabolic engineering effort assumed throughout this analysis, high labor costs associated with large numbers of workers will probably preclude bulk animal cell-culture processes from scaling to levels consistent with measurable displacement of conventional meat.

[141] Nice work, if you can get it.

Return on resource investment

Values of plant-to-animal calorie conversion are frequently cited in cultured-meat presentations. These figures vary by source: One summary reports that pork has a 10% calorie conversion,[142], poultry 9%, and aquacultured fish 8% [204]. Recognizing that cell cultures are also "fed" more processed versions of the same plants that are fed to animals, a similar conversion can be computed here. Assuming 4 cal/g for carbohydrate, 4 cal/g for protein, and 9 cal/g for lipids, Table 4.17 presents calorie conversions predicted by the various stoichiometries for individual amino acids and soy hydrolysate.[143]

[142] In other words, ten calories of plants are consumed to make one human-edible calorie of pork.

[143] Assuming fermentative production, the individual amino acid demands are converted to a glucose demand as follows. The theoretical conversion of one molecule to another can be computed with the degree of reduction γ. For an organic molecule with formula $C_aH_bO_cN_d$, $\gamma = 4a + b - 2c - 3d$. The ratio of $\gamma_{glucose}/\gamma_{product}$ gives the theoretical molar conversion. TEA of industrial lysine [130] indicates a practical conversion of ~50% theoretical. This is applied to the other amino acids as well.

Assuming soy hydrolysate feed, a calorie conversion efficiency of 26–33% is predicted, i.e., 3–4 calories of raw plants are used to make one calorie of cell mass. This ratio does improve with more efficient metabolism. The efficiencies predicted for individual amino acid feeds are significantly higher; these gains are primarily due to the relatively large plant-matter losses associated with milling and hydrolysis (about 80% of soybeans versus 30% of corn). Note that the calculation in Table 4.17 assumes that this remainder is wasted at no value. In practice, something would have to be done with this material. The sustainability of cultured-meat supply chains thus requires further investigation.

The water footprint of conventional meat is understood to be very high, though the vast majority of this footprint is natural rainwater that falls on feed crops like corn and soybeans, i.e., the same plants that would be processed to feed cultured meat. Considering the improved plant-calorie efficiencies discussed above, cultured meat may indeed offer environmental benefits with respect to water usage. In the TEA models above, water usage of the process is estimated at a high level only: media, CIP/SIP, and an allowance for cell washing. With a detailed analysis accounting for additional water and steam demands for, e.g., impeller seals, equipment washdown, and heating/cooling, the actual usage could be significantly higher. For an RO-based system, a 66% WFI recovery is assumed, i.e., one liter of water is rejected for every two liters of WFI used in the process [194]. Hydrolysis and processing of plants for cell-culture media would contribute an additional water footprint as well. As shown in Tables 4.7 and 4.14, the expected usage of raw water in the bulk cell-culture process is estimated as 45 L/kg of wet cells in the fed-batch process or 26 L/kg in the perfusion process, both with enhanced metabolism. A small amount of this water ends up in the product; the rest is wastewater. The water demand of future cultured-meat processes thus remains a key area of uncertainty.

Table 4.17: Calorie conversions of cultured animal cell mass.

Lipid/Protein/Carb. per g		cal/g
Cell mass	0.05/0.21/0.03	1.4
Corn	0.02/0.03/0.21	1.1
Soybeans	0.09/0.18/0.08	1.8

Plant-equivalent inputs per g wet cells		
Reaction 2.9		
0.82 g glucose	1.4 g corn	1.5 cal/g
0.69 g aminos	1.2 g corn	1.3 cal/g
		2.8 cal/g
Conversion	2.1 cal/cal	48%
Reaction 2.12		
0.82 g glucose	1.4 g corn	1.5 cal/g
0.12 g aminos	0.4 g corn	0.4 cal/g
0.34 g soy hyd.	1.8 g soy	3.2 cal/g
		5.2 cal/g
Conversion	3.8 cal/cal	26%
Reaction 2.11		
0.36 g glucose	0.6 g corn	0.7 cal/g
0.58 g aminos	1.0 g corn	1.1 cal/g
		1.8 cal/g
Conversion	1.3 cal/cal	78%
Reaction 2.13		
0.36 g glucose	0.6 g corn	0.7 cal/g
0.05 g aminos	0.2 g corn	0.2 cal/g
0.34 g soy hyd.	1.8 g soy	3.2 cal/g
		4.1 cal/g
Conversion	3.0 cal/cal	33%

Water usage is not a function of metabolism per se, but it is a function of cell density. Processes simulated with the wild-type metabolisms are noted to have significantly higher water demand, and perfusion processes are predicted to have much lower water demand than fed-batch processes. As modeled, the water losses (per kg of cell mass produced) associated with continuous perfusion from a 2 m^3 bioreactor at 1.0/d are lower than those associated with dumping a 20 m^3 bioreactor every 57 hours. The same is true of nutrient losses, assuming the same residual concentrations. Furthermore, from an installed-volume perspective (i.e., steel usage), the perfusion processes modeled here only require about a third as much bioreactor volume as the fed-batch processes, given the same production volume. As modeled above, perfusion processes have a fairly substantial economic disadvantage relative to fed-batch processes, due to bioreactor size limits and cell retention CAPEX. If these could be overcome, perfusion might indeed offer significant sustainability advantages.

5

Concluding discussion

5.1 Summary

This analysis was commissioned to investigate cultured meat's potential to measurably displace conventional meat consumption. Noting that the scalability of such products must in turn depend on the scalability of bulk animal cell growth, this analysis examined the extent to which an animal cell culture could be scaled like an industrial fermentation process such as baker's yeast. The result is a transparent scale-up projection of a bulk cell-mass process designed to produce a new, commoditized starting material for further processing through flavoring, texturization, and possibly tissue culture into an array of meat substitutes.

An investigation of cell growth and metabolism indicated that animal cells grow much more slowly than microbial cells. Compared to, say, a ton of yeast cells, the analysis found that significantly more bioreactor volume would be required to make a ton of animal cells, driving up capital costs. Furthermore, metabolically unregulated wild-type cells in culture outside the animal body tend to exhibit inefficiencies that cause them to produce growth-inhibiting catabolites such as lactate and ammonia at relatively high rates. The analysis found that accumulation of such inhibitors in cell culture would severely limit the attainable cell density in suspension fed-batch culture. Theoretically, at least, metabolic inefficiency and catabolite inhibition could be addressed with cell-line characterization and engineering. However, even with enhanced metabolic efficiency, other cell-density limitations are reached in fed-batch culture, most notably gas-liquid mass transfer of O_2 and CO_2. The latter is more prevalent in desirably large bioreactors (>20 m^3), where gas sparging is limited by the potential for bubble-induced shear damage to animal cells, which lack a rigid cell wall. Catabolite inhibition can also be mitigated, to a degree, with the use of perfusion culture, but appropriate bioreactor volumes are much smaller than in fed-batch culture.

Animal cell cultures are highly susceptible to microbial contamination, but an examination of likely facility CAPEX indicated that the costs of pharma-grade engineering and equipment would be inconsistent with the food-scale

commoditization of animal cell culture. Process-industry software was used instead to estimate the installed costs of bioreactors with appropriate sterility safeguards for animal cell culture, but without the overhead of custom design services or regulatory compliance. Larger bioreactors were shown to have lower direct costs relative to their bare equipment cost, though bioreactors larger than 20 m^3 have not been tested for animal cell culture and their consideration was somewhat speculative. Clean room construction costs were developed from estimates of equipment footprint, and direct/indirect costs for the remainder of the cell-culture facility were adequately estimated with cost-escalation factors appropriate for industrial fermentation.

An investigation into the cost and availability of amino acids for cell-culture media indicated that suitable formulations are not currently produced at scales that would be consistent with food production. Noting a strong price-volume relationship in amino-acid market data, a correlation was proposed to forecast prices consistent with the global demand of a new formulation of each. A similar price-volume relationship was also noted for protein bioproducts including therapeutics and industrial enzymes. A related correlation was proposed to forecast demand-consistent prices of recombinant growth factors.

From these observations, production cost estimates and sensitivities were developed for conceptual fed-batch and perfusion processes to produce bulk animal cell mass. Both processes were examined with a baseline cellular metabolism significantly enhanced relative to a wild-type cell line, implying extensive characterization, process development, and metabolic engineering. To set a global demand for media component costs, the facilities so modeled were assumed to exist within a larger market producing a modest (but measurable) 100 kTA of wet animal cell mass—similar to the current production volume of ascendant plant-based meat replacements. To be consistent with the level of consumption implied at this volume (10M people consuming 10 kg/y), the present analysis asserted a production-cost target of $25/kg wet cell mass.

A bulk cell-culture process comprising 24×20 m^3 fed-batch bioreactors was estimated to produce 6.8 kTA of wet cell mass at a production cost of $37/kg. Amino acids contributed the largest share of this cost ($19/kg), followed by capital and facility overhead. Clean rooms and other buildings contributed $3/kg to the baseline production cost, and the analysis found that increasing the number of production bioreactors caused this cost to grow faster than any benefits offered by more bioreactors: a 24-bioreactor configuration was optimal. Increasing the size of the final production bioreactor to 50 m^3gave a slight reduction in the modeled production cost. Above this volume, a reduction in final cell density (associated with CO_2 accumulation) and an increase in the number of levels in the clean room (associated with taller vessels) outweighed the scale benefits.

A perfusion process designed to produce the same output of bulk animal cell mass (6.9 kTA) required 96×2 m^3 bioreactors operating with a perfusion rate of 1.0/d through dual ATF 10 perfusion devices. With scheduling

assumptions resulting in a rather aggressive steady-state uptime of 91%, the estimated cost of wet cell mass production was $51/kg. The relatively high installation costs of small bioreactors and the extra capital and consumables costs associated with the perfusion device were significant economic disadvantages. At the 2 m^3 scale, the perfusion process approached a true scale-out facility, i.e., the modeled cost of production (including the clean room cost) was relatively insensitive to the number of bioreactors assumed.

U.S. soybean hydrolysate was considered as a potentially lower cost and more sustainable source of amino acids for cell culture. At a proposed $2/kg mixed amino acids, low-cost hydrolysates could potentially provide a $15–16/kg reduction in the modeled production costs. Hydrolysates appropriate for whole, unsupplemented cell-culture media do not exist today and the redirection of plant protein to make them would displace significant amounts of animal feed. The assertions of hydrolysate suitability and price made here are thus somewhat speculative. Nevertheless, a fed-batch process with this modification was the only scenario considered in the analysis that would fall below a $25/kg threshold.

Even a theoretically efficient metabolism (i.e., full respiration) and a drastically increased growth rate did not cause any of the models to fall below $25/kg when amino-acid media was assumed. On the other hand, when the assumed enhanced metabolism was replaced by one more consistent with a wild-type cell line, the cell mass production of both designs fell by 95%, while keeping the same capital and labor costs. Moreover, these wild-type processes begin to fail other basic metrics of sustainability as the inefficiency propagated through the power and water used per kg of product and the number of workers required to grow cells process relative to the number of people potentially fed by these. The analysis thus concludes that metabolic efficiency improvements and low-cost hydrolysate media development can both be taken as necessary but insufficient conditions of cultured meat's potential to displace conventional meat.

5.2 Recommendations

Animal cells can indeed be cultured in vitro. Without doubt of this fact, ascendant technologies should be judged on the metabolic efficiency of their cell lines and their approach to achieving high fed-batch cell densities in conventional bioreactor volumes up to 20 m^3 and perhaps slightly larger. These aspects are more likely to be indicative of future success than "novel" process intensification techniques or specific tissue-culture innovations. Early developers hoping to build pioneer cultured-meat facilities (presumably with small, pilot-scale bioreactors) should not underestimate the capital costs associated with appropriate sterility assurance. Development of sustainable and scalable cell-culture media that leverage low-cost plant protein hydrolysates will be of benefit to all technologies. Discussion of some possible areas for future research follows.

- CELL-LINE ENGINEERING
  This analysis demonstrated that inefficient cellular metabolisms with high levels of inhibitor formation will not achieve high cell densities in a large bioreactor, even with inhibitor removal via perfusion. Development of highly efficient, immortal cell lines capable of repeatable culture at high density will be required. This effort should not be underestimated—even an industrial cell line like CHO, which has enjoyed 60+ years of characterization and optimization, is probably not efficient enough for low-cost production of bulk cell mass. There are several potential areas of study: toleration of plant protein hydrolysates, transfection of glutamine synthetase genes (or wholesale knockout of amino acid catabolism), reduced CO_2 and catabolite inhibition, lower susceptibility to bubble damage, and of course higher growth rate and attainable cell density.

- PLANT PROTEIN HYDROLYSIS
  This analysis further demonstrated that metabolic engineering alone is an insufficient condition of affordability. As modeled here, even theoretically efficient cells will encounter media costs that preclude the affordability of cultured animal cells as food. Reduction of media costs through the use of low-cost plant hydrolysates was shown to be a necessary condition of such affordability. In the present analysis, however, the assertions of hydrolysates' price and suitability as cell-culture media are speculative and introduce a significant degree of uncertainty. Hydrolysis and cell-culture studies at the academic level could provide guidance on hydrolysis enzymes and processes, acceptable levels of ionic and organic contaminants, achievable cell density, and appropriate blends of plants to eliminate supplemental amino acids.

- HEAT-STABLE MEDIA FORMULATION
  In both of the process designs presented here, HTST sterilization was assumed for bulk media sterilization, with sterile filtration assumed for makeup media only. At HTST temperature, however, many components of cell-culture media will be degraded. Furthermore, both models were relatively aggressive with respect to the replacement rate of sterile filters, which resulted in a fairly low consumables cost. As actual productivity falls short of either assumption, filtration consumables costs may become prohibitive. Studies on the formulation of heat-stable media and characterizations of its degradation products are thus warranted.

- ASEPTIC BIOREACTOR DESIGN
  In the fed-batch cell-culture process modeled above, the optimum facility was characterized by a relatively low number of relatively small bioreactors. This was due to both a decline in achievable cell density in bioreactors >20 m^3 and the geometric scaling of the clean room area. The density issue was in turn caused by poor CO_2 stripping at the recommended limits of sparging and agitation in bioreactors for cell culture—recommendations that generally

exceed the requirements of typical cell-culture processes in, e.g., upstream biopharmaceuticals. Thus, much as the extremes of large-bioreactor/high-density culture have not been tested, these operating limits are also dubious and some investigators suspect that they are needlessly conservative [111]. Recent advances in the physical simulation of large fermentors (e.g., computational fluid dynamics) can be leveraged to study the hydrodynamics expected at these extremes. Such simulations can also be validated with practical equipment using real cells in so-called "scale-down simulators" [205, 206]. For fed-batch processes, computational and practical simulations can be used to comment on the potential for cell culture to be carried out in significantly larger bioreactors, perhaps located in a less controlled environment like a warehouse or indeed a brewery.[144] For perfusion processes, simulations can point to potential technological advances: co-harvesting of cells and spent media, high-throughput and consumables-free retention devices, and mitigation of genetic drift at indefinite culture duration.

[144] A de-escalation of facility class (e.g., clean room→sanitary→outdoors) assumes that sterility measures are self-contained on the equipment such that it can be taken out of a clean room and still maintain a very low rate of batch failure from contamination (the state of the art is about 2% [207, 208]). This is already true of most cell culture-grade equipment; the clean room is a risk-reduction measure that is justified by the regulation and extremely high value of biopharmaceutical products [60]. De-escalation further assumes that biosafety containment measures are not required. Given the earlier discussion on infectious virus propagation, this may be dubious.

- NITROGEN INTEGRATION

Considering Figure 2.3, nitrogen (specifically ammonia) in animal cell culture presents a problem on both the front end and the back end of a speculative cultured-meat process. Whether cells are cultured on plant hydrolysate or fermentative amino acids, much of the nitrogen ultimately derives from fossil ammonia produced from natural gas by the Haber process.[145] Metabolically inefficient cells will then turn much of this nitrogen back into ammonia during metabolism. Though wastewater treatment was not explicitly addressed in the present analysis, it should be mentioned that excessive ammonia in wastewater is not easily treated, requiring either dilution with partially treated "gray" water or additional treatment by nitrifying bacteria. There appear to be integration opportunities here, including perhaps the design of microbial fermentation media from spent cell culture media, or the development of an immobilized glutamine synthetase reactor to produce glutamine from the spent ammonia and low-cost glutamic acid. Colocation of cultured-meat manufacturing with corn/soybean mills, which are predominantly found in the U.S. Midwest, would facilitate such integration while offering labor cost reductions as discussed in Note 139.

[145] Not all soybeans are fertilized with ammonia; guidance varies by crop yield and soil type [209].

5.3 Related topics

To close this report, some thoughts on select related topics are offered below.

- DOWNSTREAM TISSUE CULTURE

The economics of producing a bulk animal cell slurry were examined here, but it must be noted that cell slurry is not a product [210]. At a minimum, it is two steps away from becoming a product: flavoring and forming. As long as conventional meat still exists, unstructured products made in this way are likely to have a relatively low price ceiling, as speculated in Section 1.3.

For a structured product, the acceptable price is probably much higher, and could be expected to increase boundlessly with its degree of resemblance to an actual cut of meat. It thus stands to reason that the proprietary efforts of many developers are ultimately focused on structured, whole-tissue products, even if these are unlikely to reach the market before unstructured ones.

In the context of the present analysis, it can be stated that if tissue culture adds no additional cell mass, then it can only increase the cost of cultured meat products beyond the $30–50/kg range estimated here. If intracellular mass is accumulated (e.g., by hypertrophy of muscle cells) at roughly the same efficiencies of media, capital, and labor, then the cost should remain the same.

In the larger context of process design, structured products might benefit from individual small bioreactors to facilitate heat/mass transfer. The economics of such a facility would fall somewhere between those modeled here and a cell-therapy production facility. Recent cost estimates of the latter indicate that a facility producing 10,000 doses per year (1.8 kg/y total cell mass) in parallel single-use STRs with final cell density 7×10^6/mL would have a fixed capital investment of ~$10M [200].[146] At a 15%/y charge factor (Section 3.1), this would resolve to $833k/kg of cells for facility capital only. Assuming an intensification of 3 orders of magnitude (cells in tissue are O~10^9/mL), the cost of cell mass would likely still be in the thousands of dollars per kg after labor, media, and fixed costs were considered. The scale limitations of individual single-use technology thus appear to be inconsistent with the production of food.

[146]The cost of a facility using hollow-fiber bioreactors was estimated to be 6×higher.

FIGURE 5.1: ABEC single-use bioreactor bag, packaged for sterilization and shipping [211].

SINGLE-USE TECHNOLOGY

The use of larger-scale single-use technology (SUT) has recently gained enough popularity and acceptance in the biopharmaceutical industry that some find themselves arguing whether or not stainless steel even has a future in manufacturing [212]. For the production of therapeutics with small patient populations, SUT is a valid strategy for reducing risk associated with equipment cleaning/sterilization and cross-contamination in facilities with multiple products. Sustainability analyses of SUT claim reduced usages of water, chemicals, and energy due to the elimination of in-house cleaning and sterilization, as SUT equipment is pre-sterilized by gamma irradiation [213].[147]

Sterile irradiation is performed in modular aluminum totes that are (e.g.) 120 cm×100 cm with a depth of 60 cm [216]. Tote width and height are variable depending on the configuration of the tote conveying system but the depth is non-negotiable, as it is determined by the penetration depth of gamma radiation from a cobalt-60 source. When single-use bioreactor bags are packaged for sterilization (Figure 5.1), the rigid impeller blades inside the bag can therefore be no wider than ~50 cm in diameter. With the geometry specified in Figure 2.5 (vessel:impeller diameter ratio of 3 and vessel height:diameter ratio of 2), the largest possible bag has ~4 m^3 of working volume.[148]

[147]The sustainability of the gamma-sterilization industry is another matter. Current facilities are at capacity and supply of cobalt-60 isotope has become tight [214, 215]. A capacity expansion consistent with the scale-up of cultured meat (if produced in SUT) would be out of the question today.

[148]The applicability of this geometry to extremely high-density cell culture is still speculative and relatively larger impellers may be required at higher OUR. For microbial fermentors, which can have a vessel:impeller diameter ratio as low as 2, the maximum working volume is rather closer to 1 m^3. Though single-use bioreactors up to 6 m^3 are now available [217], these appear to be aimed at lower cell-density processes.

In the fed-batch process modeled here, bioreactors <4 m^3 only comprise about 35% of the seed train CAPEX, or 5% of the total CAPEX. SUT bioreactors might be better suited for the 2 m^3 perfusion process, though the economics are still dubious. Even in biopharmaceuticals, the economic benefits of SUT vanish at ~10 MT/y of mAb production (see Figure 3.4b and Note 112). At this stage in the technology, SUT does not appear to be an enabling alternative for large-scale animal cell culture.

▸ ECTOTHERMIC (COLD-BLOODED) CELL CULTURE

Cultured seafood from the cells of fish, crustaceans, and mollusks is a commonly proposed alternative to cultured beef, pork, or poultry [218, 219]. Perceived benefits of fish cell culture over mammalian cell culture include an increased ammonia tolerance, growth at lower pH (leading to increased CO_2 tolerance), and perhaps growth at a lower temperature. Regarding temperature, Section 2.2 discussed the basal metabolic rate of a single mammalian cell as a function of size. Thermodynamics dictates that this quantity must also be a function of temperature, but mammalian cells do not function outside a narrow range around ~37 °C so this effect can be ignored. In principle, a lower rate of cellular maintenance catabolism (known as standard metabolic rate in ectotherms) at a lower temperature could reduce the costs of non-anabolic media consumption. However, the cellular *growth* rate must also be a function of temperature: If cells are not metabolizing, then they are not growing. As demonstrated for baker's yeast in Table 1.3, a reduced growth rate requires more bioreactors (i.e., higher CAPEX) for the same production rate. Ultimately, assuming similar growth rates and attainable cell densities,[149] it is not clear that the economics of cultured seafood should be any different from those presented here.

[149] Which, it should be noted, are also speculative for mammalian cells.

▸ SINGLE-CELL PROTEIN

Finally, no biotechnology scale-up discussion is complete without mention of the Pruteen fermentor. Pruteen was a single-cell protein (SCP) animal feed developed by ICI in the 1970s in response to rising soybean prices. The development of Pruteen led to the construction of a 1,500 m^3 airlift—the world's largest aerobic fermentor at the time and ever since [220]. This scale was necessary if Pruteen was to compete with soy protein on price, but problems became evident immediately. After startup in 1979, the fermentor's foaming and sterility control systems had to be redesigned in 1980. By 1983, Pruteen was selling for double the price of European soybean meal. By 1987, the facility had been decommissioned.

The technology behind Pruteen later reemerged as the meat replacement Quorn, which is produced from cell mass of the filamentous microfungus *F. venenatum*.[150] Other SCP products for animal feed are still being developed today [222], though these primarily aim to use advantaged feedstocks, including natural gas and waste streams from food or biodiesel production. As with biofuels, the SCP experience indicates that good biology always needs better engineering. The same will be true for cultured meat.

[150] In more modestly sized fermentors (150 m^3) [221].

Acknowledgments

This analysis was funded by Open Philanthropy, San Francisco, California. The final report was edited by Kat Eschner. Special thanks to Alex Baker, Melisa Carpio, Jeff Lievense, David Lubertozzi, Brian Maiorella, Henk Noorman, Neil Renninger, and Benjamin Wurgaft. The author acknowledges free software leveraged in the analysis and in this document: Jupyter Lab [223], xlrd [224], Matplotlib [225], WebPlotDigitizer [226], and the LaTeX template of Friedrich Wiemer [227].

Bibliography

[1] The Good Food Institute. (Sep. 6, 2016). "'Clean Meat': The 'Clean Energy' of Food," The Good Food Institute, [Online]. Available: *https://www.gfi.org/clean-meat-the-clean-energy-of-food*.

[2] The Good Food Institute. (Sep. 27, 2018). "'Clean Meat,' 'Cell-Based Meat,' 'Slaughter-Free Meat': How We Talk About Meat Grown without Animals," The Good Food Institute, [Online]. Available: *https://www.gfi.org/how-we-talk-about-meat-grown-without-animals*.

[3] The Good Food Institute. (Sep. 13, 2019). "Cultivated Meat: Why GFI Is Embracing New Language," The Good Food Institute, [Online]. Available: *https://www.gfi.org/cultivatedmeat*.

[4] C. van der Weele and J. Tramper, "Cultured meat: Every village its own factory?" *Trends in Biotechnology*, vol. 32, no. 6, pp. 294–296, Jun. 2014. DOI: *10.1016/j.tibtech.2014.04.009*.

[5] W. Dufresne. (2011). "Proteins & Enzymes: Transglutaminase," [Online]. Available: *https://youtu.be/McjrzC6KNSo?t=1948*.

[6] BCC Research, "Synthetic (Cultured) Meat: Technologies and Global Markets," BIO174A, 2019.

[7] J. R. Anthis, "Survey of US Attitudes Towards Animal Farming and Animal-Free Food," Sentience Institute, Nov. 20, 2017. [Online]. Available: *https://sentienceinstitute.org/animal-farming-attitudes-survey-2017*.

[8] World Wildlife Fund, "Appetite for Destruction," 2017. [Online]. Available: *https://www.wwf.org.uk/updates/appetitefordestruction*.

[9] P. J. Gerber, H. Steinfeld, B. Henderson, A. Mottet, C. Opio, J. Dijkman, A. Falcucci, and G. Tempio, *Tackling Climate Change through Livestock: A Global Assessment of Emissions and Mitigation Opportunities*. Rome: Food and Agriculture Organization of the United Nations (FAO), 2013, 115 pp., ISBN: 978-92-5-107920-1.

[10] N. Chestney and S. Nebehay. (Aug. 2019). "The UN says we need to reduce our meat consumption to fight climate change and improve food security," World Economic Forum, [Online]. Available: *https://www.weforum.org/agenda/2019/08/global-meat-consumption-reduce-mitigate-effects-global-warming/*.

[11] B. A. Wurgaft, *Meat Planet: Artificial Flesh and the Future of Food*. Oakland, California: University of California Press, 2019, ISBN: 978-0-520-29553-7.

[12] J. Lynch and R. Pierrehumbert, "Climate Impacts of Cultured Meat and Beef Cattle," *Frontiers in Sustainable Food Systems*, vol. 3, no. 5, Feb. 2019. DOI: *10.3389/fsufs.2019.00005*.

[13] L. Specht, "An analysis of culture medium costs and production volumes for cultivated meat," Feb. 2020. [Online]. Available: *https://www.gfi.org/files/sci-tech/clean-meat-production-volume-and-medium-cost.pdf*.

[14] H. L. Tuomisto and M. J. Teixeira de Mattos, "Environmental Impacts of Cultured Meat Production," *Environmental Science & Technology*, vol. 45, no. 14, pp. 6117–6123, Jul. 2011. DOI: *10.1021/es200130u*.

[15] Foodspark. (Oct. 25, 2019). "Food Futures Lab's Max Elder," Foodspark, [Online]. Available: *https://www.foodspark.com/Trends-People/Food-Futures-Lab-s-Max-Elder-You-really-can-t-think-about-the-future-of-food-unless-you-re-thinking-about-the-future-of-technology*.

[16] M. J. Post, "Cultured beef: Medical technology to produce food," *Journal of the Science of Food and Agriculture*, vol. 94, no. 6, pp. 1039–1041, Apr. 2014. DOI: *10.1002/jsfa.6474*.

[17] I. Datar. (Nov. 3, 2015). "Mark Post's Cultured Beef," New Harvest, [Online]. Available: *https://www.new-harvest.org/mark_post_cultured_beef*.

[18] D. Schwartz. (Mar. 27, 2015). "NT Cattlemen's Association to hear that 'cultured meat' could end their industry within decades," [Online]. Available: *http://www.abc.net.au/am/content/2015/s4205857.htm*.

[19] J. Nason. (Mar. 29, 2015). "Lab grown meat pioneer meets Territory cattle producers," Beef Central, [Online]. Available: *https://www.beefcentral.com/features/ntca-conferences/lab-grown-meat-pioneer-meets-territory-cattle-producers/*.

[20] B. Crew. (Apr. 2, 2015). "Cost of Lab-Grown Burger Patty Drops From $325,000 to $11.36," ScienceAlert, [Online]. Available: *https://www.sciencealert.com/lab-grown-burger-patty-cost-drops-from-325-000-to-12*.

[21] D. Coffey. (May 11, 2020). "Don't look now, but we could soon be growing steaks and pork loins in a lab," Massive Science, [Online]. Available: *https://massivesci.com/articles/bioreactor-animal-muscle/*.

[22] N. Pai. (Jul. 8, 2019). "Non-veg without the violence or the guilt that come with it," Livemint, [Online]. Available: *https://www.livemint.com/opinion/columns/opinion-non-veg-without-the-violence-or-the-guilt-that-come-with-it-1562513069549.html*.

[23] A. Peters. (May 2, 2018). "Lab-Grown Meat Is Getting Cheap Enough For Anyone To Buy," Fast Company, [Online]. Available: *https://www.fastcompany.com/40565582/lab-grown-meat-is-getting-cheap-enough-for-anyone-to-buy*.

[24] M. Griffin. (Oct. 15, 2019). "UK startup's new method drastically reduces the cost of clean meat," By Matthew Griffin Futurist and Keynote Speaker, [Online]. Available: *https://www.fanaticalfuturist.com/2019/10/uk-startups-new-method-drastically-reduces-the-cost-of-clean-meat/*.

[25] A. Cocan. (Oct. 2, 2017). "Talk About Disruption — Lab-Grown Meat Has Arrived!" PlanetSave, [Online]. Available: *https://planetsave.com/2017/10/02/talk-about-disruption-lab-grown-meat-has-arrived/*.

[26] D. Humbird. (Oct. 1, 2018). "Expanded Technology Readiness Level (TRL) Definitions for the Bioeconomy," Biofuels Digest, [Online]. Available: *https://biofuelsdigest.com/bdigest/2018/10/01/expanded-technology-readiness-level-trl-definitions-for-the-bioeconomy/*.

[27] J. Splitter. (Dec. 20, 2019). "Please Don't Call This Cultured Nugget 'Lab Meat'," Popular Mechanics, [Online]. Available: *https://www.popularmechanics.com/science/a30221344/cultured-lab-meat/*.

[28] O. Khazan. (Apr. 16, 2019). "The Coming Obsolescence of Animal Meat," The Atlantic, [Online]. Available: *https://www.theatlantic.com/health/archive/2019/04/just-finless-foods-lab-grown-meat/587227/*.

[29] G. Mammoser. (Oct. 5, 2016). "Why the Meat Factories of the Future Will Look Like Breweries," Vice, [Online]. Available: *https://www.vice.com/en_us/article/nzk43b/why-the-meat-factories-of-the-future-will-look-like-breweries*.

[30] C. Purdy. (May 13, 2020). "Cultured meat startups want to build a better US meat supply chain," Quartz, [Online]. Available: *https://qz.com/1856344/cultured-meat-startups-want-to-fix-the-broken-meat-supply-chain/*.

[31] D. Dugar and G. Stephanopoulos, "Relative potential of biosynthetic pathways for biofuels and bio-based products," *Nat Biotech*, vol. 29, no. 12, pp. 1074–1078, Dec. 2011. DOI: *10.1038/nbt.2055*.

[32] J. D. Keasling, "Synthetic biology and the development of tools for metabolic engineering," *Metabolic Engineering*, vol. 14, no. 3, pp. 189–195, May 2012. DOI: *10.1016/j.ymben.2012.01.004*.

[33] C. M. Agapakis, "Designing Synthetic Biology," *ACS Synth. Biol.*, vol. 3, no. 3, pp. 121–128, Mar. 21, 2014. DOI: *10.1021/sb4001068*.

[34] A. Burgard, M. J. Burk, R. Osterhout, S. Van Dien, and H. Yim, "Development of a commercial scale process for production of 1,4-butanediol from sugar," *Current Opinion in Biotechnology*, vol. 42, pp. 118–125, Dec. 2016. DOI: *10.1016/j.copbio.2016.04.016*.

[35] C. E. Nakamura and G. M. Whited, "Metabolic engineering for the microbial production of 1,3-propanediol," *Current Opinion in Biotechnology*, vol. 14, no. 5, pp. 454–459, Oct. 2003. DOI: *10.1016/j.copbio.2003.08.005*.

[36] U.S. Energy Information Administration, *Cushing, OK WTI Spot Price FOB*. [Online]. Available: *https://www.eia.gov/dnav/pet/hist/RWTCD.htm*.

[37] U.S. Department of Agriculture, Economic Research Service. (2019). "Historical monthly price spread data for beef," [Online]. Available: *https://www.ers.usda.gov/data-products/meat-price-spreads/*.

[38] D. Humbird, R. Davis, and J. McMillan, "Aeration costs in stirred-tank and bubble column bioreactors," *Biochemical Engineering Journal*, vol. 127, pp. 161–166, Nov. 2017. DOI: *10.1016/j.bej.2017.08.006*.

[39] H. J. Noorman, W. van Winden, J. J. Heijnen, and R. Van der Lans, "Intensified Fermentation Processes and Equipment," in *Intensification of Biobased Processes*, A. Górak and A. Stankiewicz, Eds., Cambridge: Royal Society of Chemistry, 2018, ISBN: 978-1-78262-855-2.

[40] H. Noorman, "An industrial perspective on bioreactor scale-down: What we can learn from combined large-scale bioprocess and model fluid studies," *Biotechnology Journal*, vol. 6, no. 8, pp. 934–943, Aug. 2011. DOI: *10.1002/biot.201000406*.

[41] U. S. Government Accountability Office, "Renewable Fuel Standard: Program Unlikely to Meet Production or Greenhouse Gas Reduction Targets," GAO-17-94, Dec. 1, 2016. [Online]. Available: *https://www.gao.gov/products/GAO-17-264T*.

[42] J. Lane. (Jul. 18, 2016). "Abengoa's Hugoton cellulosic ethanol project goes on the block," Biofuels Digest, [Online]. Available: *http://www.biofuelsdigest.com/bdigest/2016/07/18/abengoas-hugoton-cellulosic-ethanol-project-goes-on-the-block/*.

[43] J. Lane. (Oct. 30, 2017). "Beta Renewables in cellulosic ethanol crisis, as Grupo M&G parent files for restructuring," Biofuels Digest, [Online]. Available: *https://www.biofuelsdigest.com/bdigest/2017/10/30/beta-renewables-in-cellulosic-ethanol-crisis-as-grupo-mg-parent-files-for-restructuring/*.

[44] E. Voegele, "Verbio to buy DuPont cellulosic ethanol plant, convert it to RNG," *Biomass Magazine*, Nov. 9, 2018.

[45] J. Lane. (Apr. 29, 2015). "Cargill acquires OPX Biotechnologies," Biofuels Digest, [Online]. Available: *http://www.biofuelsdigest.com/bdigest/2015/04/29/cargill-acquires-opx-biotechnologies/*.

[46] Renewable Energy Group. (Jan. 4, 2014). "Renewable Energy Group acquires biochemical company LS9," Biomass Magazine, [Online]. Available: *http://biomassmagazine.com/articles/9952/renewable-energy-group-acquires-biochemical-company-ls9*.

[47] M. Chatsko. (Aug. 2, 2017). "TerraVia Announces Bankruptcy and Asset Sale," The Motley Fool, [Online]. Available: *https://www.fool.com/investing/2017/08/02/terravia-announces-bankruptcy-and-asset-sale.aspx*.

[48] Wikipedia, *Mascoma Corporation*, in *Wikipedia*, Sep. 30, 2019. [Online]. Available: *https://en.wikipedia.org/w/index.php?title=Mascoma_Corporation&oldid=918878303*.

[49] J. Mohorčich, "What can biofuel commercialization teach us about scale, failure, and success in biotechnology?" Sentience Institute, Aug. 2019. [Online]. Available: *https://www.sentienceinstitute.org/biofuels*.

[50] J. Bjarre, "Aeration in fed batch cultivations of Saccharomyces cerevisiae," KTH Royal Institute of Technology, Stockholm, Sweden, 2016.

[51] A. R. Lara, E. Galindo, O. T. Ramírez, and L. A. Palomares, "Living with heterogeneities in bioreactors: Understanding the effects of environmental gradients on cells," *Mol. Biotechnol.*, vol. 34, no. 3, pp. 355–381, Nov. 2006. DOI: *10.1385/MB:34:3:355*.

[52] M. Al-Rubeai, R. P. Singh, M. H. Goldman, and A. N. Emery, "Death mechanisms of animal cells in conditions of intensive agitation," *Biotechnology and Bioengineering*, vol. 45, no. 6, pp. 463–472, Mar. 20, 1995. DOI: *10.1002/bit.260450602*.

[53] A. W. Nienow, "Scale-up, stirred tank reactors," in *Encyclopedia of Industrial Biotechnology*, M. C. Flickinger, Ed., Hoboken, NJ, USA: John Wiley & Sons, Inc., Mar. 15, 2010. DOI: *10.1002/9780470054581.eib001*.

[54] S. S. Ozturk, "Engineering challenges in high density cell culture systems," *Cytotechnology*, vol. 22, pp. 3–16, 1996. DOI: *10.1007/BF00353919*.

[55] BCC Research, "Yeast, yeast extracts, autolysates and related products: The global market," CHM053C, 2017.

[56] *SuperPro Designer*, version 9.5, Scotch Plains, NJ: Intelligen, Inc.

[57] A. J. Hacking, *Economic Aspects of Biotechnology*. Cambridge: Univ. Press, 1986, 306 pp., ISBN: 978-0-521-25893-7.

[58] G. Reed and T. W. Nagodawithana, *Yeast Technology*. Dordrecht: Springer Netherlands, 1990, ISBN: 978-94-011-9771-7.

[59] A. Peña, J. Ramírez, G. Rosas, and M. Calahorra, "Proton pumping and the internal pH of yeast cells, measured with pyranine introduced by electroporation.," *Journal of Bacteriology*, vol. 177, no. 4, pp. 1017–1022, Feb. 1995. DOI: *10.1128/jb.177.4.1017-1022.1995*.

[60] H.-P. Meyer, W. Minas, and D. Schmidhalter, "Industrial-Scale Fermentation," in *Industrial Biotechnology - Products and Processes*, Volume 4, C. Wittmann and J. C. Liao, Eds., First edition, Weinheim: Wiley-VCH Verlag GmbH & Co. KGaA, 2017, ISBN: 978-3-527-80782-6.

[61] T. Ben-Arye and S. Levenberg, "Tissue Engineering for Clean Meat Production," *Frontiers in Sustainable Food Systems*, vol. 3, no. 46, Jun. 2019. DOI: *10.3389/fsufs.2019.00046*.

[62] J. A. King and W. M. Miller, "Bioreactor development for stem cell expansion and controlled differentiation," *Current Opinion in Chemical Biology*, vol. 11, no. 4, pp. 394–398, Aug. 1, 2007. DOI: *10.1016/j.cbpa.2007.05.034*.

[63] M. Hall, D. Hill, and G. Pave, "Global Pharmaceuticals: 2018 Industry statistics," Hardman & Co., Apr. 9, 2019. [Online]. Available: *https://www.hardmanandco.com/research/corporate-research/global-pharmaceuticals-2018-industry-statistics/*.

[64] Drugs.com. (Apr. 2019). "Humira Dosage Guide," Drugs.com, [Online]. Available: *https://www.drugs.com/dosage/humira.html*.

[65] ClinCalc. (2017). "Adalimumab - Drug Usage Statistics," ClinCalc.com, [Online]. Available: *https://clincalc.com/DrugStats/Drugs/Adalimumab*.

[66] EvaluatePharma, "World Preview 2018, Outlook to 2024," EvaluatePharma, Jun. 2018. [Online]. Available: *https://info.evaluategroup.com/WP2018-CS.html*.

[67] D. P. Petrides, "Bioprocess design and economics," in *Bioseparations Science and Engineering*, R. G. Harrison, P. Todd, and S. R. Rudge, Eds., Second edition, Oxford: Oxford University Press, 2015, ISBN: 978-0-19-539181-7.

[68] D. P. Petrides, D. Carmichael, C. Siletti, and A. Koulouris, "Biopharmaceutical Process Optimization with Simulation and Scheduling Tools," *Bioengineering*, vol. 1, no. 4, pp. 154–187, Sep. 29, 2014. DOI: *10.3390/bioengineering1040154*.

[69] Sartorius Stedim. (2020). "Multi-Parallel Bioreactors," Sartorius, [Online]. Available: *https://www.sartorius.com/en/products/fermentation-bioreactors/ambr-multi-parallel-bioreactors*.

[70] J. Puetz and F. M. Wurm, "Recombinant Proteins for Industrial versus Pharmaceutical Purposes: A Review of Process and Pricing," *Processes*, vol. 7, no. 476, Jul. 24, 2019. DOI: *10.3390/pr7080476*.

[71] N. E. Gregorio, M. Z. Levine, and J. P. Oza, "A User's Guide to Cell-Free Protein Synthesis," *Methods Protoc*, vol. 2, no. 1, Mar. 12, 2019. DOI: *10.3390/mps2010024*.

[72] OECD, *Meat consumption*, 2020. DOI: *10.1787/fa290fd0-en*. [Online]. Available: *https://www.oecd-ilibrary.org/agriculture-and-food/meat-consumption/indicator/english_fa290fd0-en*.

[73] C. C. M. Mody, *The Long Arm of Moore's Law: Microelectronics and American Science*. Cambridge, Massachusetts: The MIT Press, 2017, 284 pp., ISBN: 978-0-262-03549-1.

[74] R. Kurzweil, *The Singularity Is Near: When Humans Transcend Biology*. New York: Viking, 2005, ISBN: 978-0-7394-6626-1.

[75] R. Shigeta. (Oct. 22, 2020). "Lab-Grown Meat is Scaling Like the Internet," Medium, [Online]. Available: *https://rshigeta.medium.com/lab-grown-meat-is-scaling-like-the-internet-540893cbaf57*.

[76] G. E. Moore, "Cramming more components onto integrated circuits," *Electronics*, vol. 38, no. 8, 1965.

[77] U. von Stockar, "Live cells as open non-equilibrium systems," in *Biothermodynamics: The Role of Thermodynamics in Biochemical Engineering*, U. von Stockar, Ed., 2013, ISBN: 978-1-4665-8217-0.

[78] M. S. Peters, K. D. Timmerhaus, and R. E. West, *Plant Design and Economics for Chemical Engineers*, 5th ed. New York: McGraw-Hill, 2003, 988 pp., ISBN: 978-0-07-239266-1.

[79] W. Qi, R. Sathre, William R. Morrow, III, and A. Shehabi, "Unit Price Scaling Trends for Chemical Products," Aug. 1, 2015. DOI: *10.2172/1236367*. [Online]. Available: *http://www.osti.gov/servlets/purl/1236367/*.

[80] AACE International, "Cost estimate classification system: As applied in engineering, procurement, and construction for the process industries," 18R-97, Nov. 29, 2011.

[81] J. H. Tjio and T. T. Puck, "Genetics of Somatic Mammalian Cells," *Journal of Experimental Medicine*, vol. 108, no. 2, pp. 259–268, Aug. 1, 1958. DOI: *10.1084/jem.108.2.259*.

[82] K. Hosono and H. Suzuki, "Morphological transformation of Chinese hamster cells by acylpeptides, inhibitors of cAMP phosphodiesterase, produced by Bacillus subtilis.," *J. Biol. Chem.*, vol. 260, no. 20, pp. 11 252–11 255, Sep. 15, 1985.

[83] F. Wurm, "CHO Quasispecies—Implications for Manufacturing Processes," *Processes*, vol. 1, no. 3, pp. 296–311, Oct. 11, 2013. DOI: *10.3390/pr1030296*.

[84] W. G. Whitford, M. Lundgren, and A. Fairbank, "Cell culture media in bioprocessing," in *Biopharmaceutical Processing: Development, Design, and Implementation of Manufacturing Processes*, G. Jagschies, E. Lindskog, K. Łącki, and P. Galliher, Eds., Amsterdam, Netherlands: Elsevier, 2018, ISBN: 978-0-08-100623-8.

[85] R. P. Nolan and K. Lee, "Dynamic model of CHO cell metabolism," *Metabolic Engineering*, vol. 13, pp. 108–124, 2011. DOI: *doi:10.1016/j.ymben.2010.09.003*.

[86] B. Alberts, Ed., *Molecular Biology of the Cell*, 4th ed. New York: Garland Science, 2002, 1548 pp., ISBN: 978-0-8153-4072-0.

[87] A. K. Burnham, "Estimating the Heat of Formation of Foodstuffs and Biomass," Lawrence Livermore National Laboratory, UCRL-TR-464095, 2010.

[88] E. H. Battley, "An empirical method for estimating the entropy of formation and the absolute entropy of dried microbial biomass for use in studies on the thermodynamics of microbial growth," *Thermochimica Acta*, vol. 326, pp. 7–15, 1999. DOI: *10.1016/S0040-6031(98)00584-X*.

[89] Z.-L. Xiu, W.-D. Deckwer, and A.-P. Zeng, "Estimation of rates of oxygen uptake and carbon dioxide evolution of animal cell culture using material and energy balances," p. 9,

[90] L. Xie and W. Zhou, "Fed-Batch Cultivation of Mammalian Cells for the Production of Recombinant Proteins," in *Cell Culture Technology for Pharmaceutical and Cell-Based Therapies*, 30, S. S. Ozturk and W.-S. Hu, Eds., Boca Raton: Taylor & Francis, 2005, ISBN: 978-0-8247-5334-4.

[91] A. Iordan, "Rheological properties of biological materials: From cell suspensions to tissues," Université Joseph-Fourier, Grenoble, 2008. [Online]. Available: *https://tel.archives-ouvertes.fr/tel-00365542*.

[92] H. J. Noorman and J. J. Heijnen, "Biochemical engineering's grand adventure," *Chemical Engineering Science*, vol. 170, pp. 677–693, Oct. 2017. DOI: *10.1016/j.ces.2016.12.065*.

[93] L. Xie and D. I. C. Wang, "Applications of improved stoichiometric model in medium design and fed-batch cultivation of animal cells in bioreactor," *Cytotechnology*, vol. 15, pp. 17–29, 1994. DOI: *10.1007/BF00762376*.

[94] A. M. Hosios, V. C. Hecht, L. V. Danai, M. O. Johnson, J. C. Rathmell, M. L. Steinhauser, S. R. Manalis, and M. G. Vander Heiden, "Amino Acids Rather than Glucose Account for the Majority of Cell Mass in Proliferating Mammalian Cells," *Developmental Cell*, vol. 36, no. 5, pp. 540–549, Mar. 2016. DOI: *10.1016/j.devcel.2016.02.012*.

[95] L. Xie and D. I. C. Wang, "Stoichiometric analysis of animal cell growth and its application in medium design," *Biotechnology and Bioengineering*, vol. 43, no. 11, pp. 1164–1174, May 1994. DOI: *10.1002/bit.260431122*.

[96] J. J. Heijnen and J. P. Van Dijken, "In search of a thermodynamic description of biomass yields for the chemotrophic growth of microorganisms," *Biotechnology and Bioengineering*, vol. 39, no. 8, pp. 833–858, 1992. DOI: *10.1002/bit.260390806*.

[97] J. A. Roels, *Energetics and Kinetics in Biotechnology*. Amsterdam ; New York: Elsevier Biomedical Press, 1983, 330 pp., ISBN: 978-0-444-80442-6.

[98] U. von Stockar, L. Gustafsson, C. Larsson, I. Marison, P. Tissot, and E. Gnaiger, "Thermodynamic considerations in constructing energy balances for cellular growth," *Biochimica et Biophysica Acta (BBA) - Bioenergetics*, vol. 1183, no. 2, pp. 221–240, Dec. 7, 1993. DOI: *10.1016/0005-2728(93)90225-5*.

[99] R. B. Kemp, "'Gie Me Ae Spark O' Nature's Fire'. An Insight Into Cell Physiology From Calorimetry," *Journal of Thermal Analysis and Calorimetry*, vol. 60, no. 3, p. 831, Jun. 1, 2000. DOI: *10.1023/A:1010199422705*.

[100] U. von Stockar, "Biothermodynamics of live cells: A tool for biotechnology and biochemical engineering," *Journal of Non-Equilibrium Thermodynamics*, vol. 35, no. 4, Jan. 2010. DOI: *10.1515/jnetdy.2010.024*.

[101] Y. Guan and R. Kemp, "Detection of the changing substrate requirements of cultured animal cells by stoichiometric growth equations validated by enthalpy balances," *Journal of Biotechnology*, vol. 69, no. 2-3, pp. 95–114, Apr. 1999. DOI: *10.1016/S0168-1656(99)00007-3*.

[102] E. K. Lindskog, "Upstream bioprocessing: Basic concepts," in *Biopharmaceutical Processing: Development, Design, and Implementation of Manufacturing Processes*, G. Jagschies, E. Lindskog, K. Łącki, and P. Galliher, Eds., Amsterdam, Netherlands: Elsevier, 2018, ISBN: 978-0-08-100623-8.

[103] G. B. West, W. H. Woodruff, and J. H. Brown, "Allometric scaling of metabolic rate from molecules and mitochondria to cells and mammals," *Proceedings of the National Academy of Sciences*, vol. 99, pp. 2473–2478, Feb. 19, 2002. DOI: *10.1073/pnas.012579799*.

[104] H. Eagle, "Nutrition Needs of Mammalian Cells in Tissue Culture," *Science*, vol. 122, p. 5, 1955. DOI: *10.1126/science.122.3168.501*.

[105] ThermoFisher Scientific. (2020). "Cell Culture Media Formulation Tool," [Online]. Available: *https://www.thermofisher.com/us/en/home/life-science/cell-culture/mammalian-cell-culture/classical-media/gibco-media-formulation-tool.html*.

[106] Z. Xing, B. M. Kenty, Z. J. Li, and S. S. Lee, "Scale-up analysis for a CHO cell culture process in large-scale bioreactors," *Biotechnology and Bioengineering*, vol. 103, no. 4, p. 14, 2009.

[107] S. Pereira, H. F. Kildegaard, and M. R. Andersen, "Impact of CHO Metabolism on Cell Growth and Protein Production: An Overview of Toxic and Inhibiting Metabolites and Nutrients," *Biotechnology Journal*, vol. 13, no. 1700499, Mar. 2018. DOI: *10.1002/biot.201700499*.

[108] N. Freund and M. Croughan, "A Simple Method to Reduce both Lactic Acid and Ammonium Production in Industrial Animal Cell Culture," *International Journal of Molecular Sciences*, vol. 19, no. 385, Jan. 28, 2018. DOI: *10.3390/ijms19020385*.

[109] U.S. Soybean Export Council, "U.S. Soybean Meal," 2015. [Online]. Available: *https://ussec.org/wp-content/uploads/2015/10/US-Soybean-Meal-Information.pdf*.

[110] G. Jagschies and K. Łącki, "Process Capability Requirements," in *Biopharmaceutical Processing: Development, Design, and Implementation of Manufacturing Processes*, G. Jagschies, E. Lindskog, K. Łącki, and P. Galliher, Eds., Amsterdam, Netherlands: Elsevier, 2018, ISBN: 978-0-08-100623-8.

[111] A. W. Nienow, "Reactor Engineering in Large Scale Animal Cell Culture," *Cytotechnology*, vol. 50, no. 1-3, pp. 9–33, Mar. 2006. DOI: *10.1007/s10616-006-9005-8*.

[112] M.-F. Clincke, C. Mölleryd, Y. Zhang, E. Lindskog, K. Walsh, and V. Chotteau, "Very high density of CHO cells in perfusion by ATF or TFF in WAVE bioreactor™. Part I. Effect of the cell density on the process," *Biotechnology Progress*, vol. 29, no. 3, pp. 754–767, May 2013. DOI: *10.1002/btpr.1704*.

[113] T. Lawson, D. E. Kehoe, A. C. Schnitzler, P. J. Rapiejko, K. A. Der, K. Philbrick, S. Punreddy, S. Rigby, R. Smith, Q. Feng, J. R. Murrell, and M. S. Rook, "Process development for expansion of human mesenchymal stromal cells in a 50 L single-use stirred tank bioreactor," *Biochemical Engineering Journal*, vol. 120, pp. 49–62, Apr. 2017. DOI: *10.1016/j.bej.2016.11.020*.

[114] P. F. Stanbury, A. Whitaker, and S. J. Hall, *Principles of Fermentation Technology*, 3rd ed. Amsterdam: Butterworth-Heinemann, an imprint of Elsevier, 2017, 803 pp., ISBN: 978-0-08-099953-1.

[115] X. Li, G. Zhang, X. Zhao, J. Zhou, G. Du, and J. Chen, "A conceptual air-lift reactor design for large scale animal cell cultivation in the context of in vitro meat production," *Chemical Engineering Science*, vol. 211, p. 115 269, Jan. 2020. DOI: *10.1016/j.ces.2019.115269*.

[116] A. Super, N. Jaccard, M. P. C. Marques, R. J. Macown, L. D. Griffin, F. S. Veraitch, and N. Szita, "Real-time monitoring of specific oxygen uptake rates of embryonic stem cells in a microfluidic cell culture device," *Biotechnology Journal*, vol. 11, no. 9, pp. 1179–1189, Sep. 2016. DOI: *10.1002/biot.201500479*.

[117] F. Garcia-Ochoa and E. Gomez, "Bioreactor scale-up and oxygen transfer rate in microbial processes: An overview," *Biotechnology Advances*, vol. 27, no. 2, pp. 153–176, Mar. 2009. DOI: *10.1016/j.biotechadv.2008.10.006*.

[118] R. Pörtner, "Bioreactors for Mammalian Cells," in *Animal Cell Culture*, M. Al-Rubeai, Ed., New York, NY: Springer Berlin Heidelberg, 2014, ISBN: 978-3-319-10319-8.

[119] ThermoFisher Scientific, *Safety data sheet: Pluronic F-68 Non-Ionic surfactant*. [Online]. Available: *https://www.thermofisher.com/order/catalog/product/24040032#/24040032*.

[120] J. Tramper, "Oxygen gradients in animal-cell bioreactors," in *Animal Cell Technology: Developments Towards the 21st Century*, E. C. Beuvery, J. B. Griffiths, and W. P. Zeijlemaker, Eds., Dordrecht: Springer Netherlands, 1995, ISBN: 978-94-010-4195-9.

[121] A. W. Nienow, "Stirring and Stirred-Tank Reactors," *Chem. Ing. Tech.*, no. 12, p. 12, 2014.

[122] M. S. Croughan, "Hydrodynamic Effects on Animal Cells in Microcarrier Bioreactors," in *Animal Cell Bioreactors*, 17, C. S. Ho and D. I.-c. Wang, Eds., Boston: Butterworth-Heinemann, 1991, ISBN: 978-0-409-90123-8.

[123] A. W. Nienow, "Impeller selection for animal cell culture," in *Encyclopedia of Industrial Biotechnology*, M. C. Flickinger, Ed., Hoboken, NJ, USA: John Wiley & Sons, Inc., Mar. 15, 2010. DOI: *10.1002/9780470054581.eib001*.

[124] K. Van't Riet and J. Tramper, *Basic Bioreactor Design*. New York: M. Dekker, 1991, ISBN: 978-0-585-15721-4.

[125] D. R. Gray, S. Chen, W. Howarth, D. Inlow, and B. L. Maiorella, "CO2 in large-scale and high-density CHO cell perfusion culture," *Cytotechnology*, vol. 22, pp. 65–78, 1996. DOI: *10.1007/bf00353925*.

[126] P. M. Doran, *Bioprocess Engineering Principles*, 2nd ed. Amsterdam; Boston: Elsevier/Academic Press, 2013, 919 pp., ISBN: 978-0-12-220851-5.

[127] K. Van't Riet and R. Van der Lans, "Mixing in Bioreactor Vessels," in *Comprehensive Biotechnology. Vol. 2*, M. Moo-Young and C. E. Webb, Eds., Amsterdam: Elsevier, 2011, ISBN: 978-0-444-53352-4.

[128] T. Hassell, S. Gleave, and M. Butler, "Growth inhibition in animal cell culture," *Appl Biochem Biotechnol*, vol. 30, no. 1, pp. 29–41, Jul. 1, 1991. DOI: *10.1007/BF02922022*.

[129] C. Kloth, G. Maclsaac, H. Ghebremariam, and A. Arunakumari, "Inoculum expansion methods, animal cell lines," in *Upstream Industrial Biotechnology*, M. C. Flickinger, Ed., Hoboken, New Jersey: John Wiley & Sons Inc, 2013, ISBN: 978-1-118-13123-7.

[130] IHS Chemical. (2020). "PEP Yearbook."

[131] PIONEER PKU. (2020). "Vacuum pressure swing adsorption oxygen plant (VPSA-O2 technology)," [Online]. Available: *https://www.vpsatech.com/VPSA-Oxygen.html*.

[132] J. Walther, J. McLarty, and T. Johnson, "The effects of alternating tangential flow (ATF) residence time, hydrodynamic stress, and filtration flux on high-density perfusion cell culture," *Biotechnology and Bioengineering*, vol. 116, no. 2, pp. 320–332, Feb. 2019. DOI: *10.1002/bit.26811*.

[133] D. S. Kompala and S. S. Ozturk, "Optimization of High Cell Density Perfusion Bioreactors," in *Cell Culture Technology for Pharmaceutical and Cell-Based Therapies*, 30, S. S. Ozturk and W.-S. Hu, Eds., Boca Raton: Taylor & Francis, 2005, ISBN: 978-0-8247-5334-4.

[134] J. Pollock, S. V. Ho, and S. S. Farid, "Fed-batch and perfusion culture processes: Economic, environmental, and operational feasibility under uncertainty," *Biotechnology and Bioengineering*, vol. 110, no. 1, pp. 206–219, Jan. 2013. DOI: *10.1002/bit.24608*.

[135] J. Walther, R. Godawat, C. Hwang, Y. Abe, A. Sinclair, and K. Konstantinov, "The business impact of an integrated continuous biomanufacturing platform for recombinant protein production," *Journal of Biotechnology*, vol. 213, pp. 3–12, Nov. 2015. DOI: *10.1016/j.jbiotec.2015.05.010*.

[136] S. T. Sharfstein and C. Kaisermeyer, "Microcarrier Culture," in *Encyclopedia of Industrial Biotechnology*, M. C. Flickinger, Ed., Hoboken, NJ, USA: John Wiley & Sons, Inc., Mar. 15, 2010, ISBN: 978-0-470-05458-1. DOI: *10.1002/9780470054581.eib001*.

[137] GE Healthcare, "Microcarrier cell culture: Principles and methods," 2005. [Online]. Available: *https://www.sigmaaldrich.com/content/dam/sigma-aldrich/docs/Sigma-Aldrich/General_Information/1/ge-microcarrier-cell-culture.pdf*.

[138] D. Kong, S. Cardak, M. Chen, R. Gentz, and J. Zhang, "High cell density and productivity culture of Chinese hamster ovary cells in a fluidized bed bioreactor," *Cytotechnology*, vol. 29, no. 3, pp. 215–220, 1999. DOI: *10.1023/A:1008064217040*.

[139] V. Bodiou, P. Moutsatsou, and M. J. Post, "Microcarriers for Upscaling Cultured Meat Production," *Front. Nutr.*, vol. 7, 2020. DOI: *10.3389/fnut.2020.00010*.

[140] ASME, "BPE-2016," American Society of Mechanical Engineers, 2016.

[141] Millipore Sigma. (2020). "Why Use Antibiotics in Cell Culture," Sigma-Aldrich, [Online]. Available: *https://www.sigmaaldrich.com/technical-documents/articles/biology/antibiotics-in-cell-culture.html*.

[142] A. H. Ryu, W. L. Eckalbar, A. Kreimer, N. Yosef, and N. Ahituv, "Use antibiotics in cell culture with caution: Genome-wide identification of antibiotic-induced changes in gene expression and regulation," *Scientific Reports*, vol. 7, no. 7533, Dec. 2017. DOI: *10.1038/s41598-017-07757-w*.

[143] A. Skubis, J. Gola, B. Sikora, J. Hybiak, M. Paul-Samojedny, U. Mazurek, and M. Łos, "Impact of Antibiotics on the Proliferation and Differentiation of Human Adipose-Derived Mesenchymal Stem Cells," *International Journal of Molecular Sciences*, vol. 18, no. 2522, Nov. 24, 2017. DOI: *10.3390/ijms18122522*.

[144] M. Butler, *Animal Cell Culture and Technology*. Oxford, GBR: Taylor & Francis Group, 2014, ISBN: 978-0-203-42783-5.

[145] J. Joseph, "Facility design and process utilities," in *Biopharmaceutical Processing: Development, Design, and Implementation of Manufacturing Processes*, G. Jagschies, E. Lindskog, K. Łącki, and P. Galliher, Eds., Amsterdam, Netherlands: Elsevier, 2018, ISBN: 978-0-08-100623-8.

[146] U.S. Food and Drug Administration, "Guidance for Industry: Sterile drug products produced by aseptic manufacture–Current Good Manufacturing Practice," 2004, p. 63.

[147] M. Moody, W. Alves, J. Varghese, and F. Khan, "Mouse Minute Virus (MMV) Contamination–A Case Study: Detection, Root Cause Determination, and Corrective Actions," *PDA Journal of Pharmaceutical Science and Technology*, vol. 65, no. 6, pp. 580–588, Nov. 1, 2011. DOI: *10.5731/pdajpst.2011.00824*.

[148] J. Skrine, "A Biotech Production Facility Contamination Case Study–Minute Mouse Virus," *PDA Journal of Pharmaceutical Science and Technology*, vol. 65, no. 6, pp. 599–611, Nov. 1, 2011. DOI: *10.5731/pdajpst.2011.00823*.

[149] P. F. F. Dimond. (Jul. 2, 2009). "Genzyme Plant Shutdown Could Mean up to $300M in Lost Sales," GEN - Genetic Engineering and Biotechnology News, [Online]. Available: *https://www.genengnews.com/insights/genzyme-plant-shutdown-could-mean-up-to-300m-in-lost-sales/*.

[150] B. Borrell. (Jun. 2009). "Virus hits Genzyme plant, halting production of orphan drugs," Scientific American Blog Network, [Online]. Available: *https://blogs.scientificamerican.com/news-blog/virus-hits-genzyme-plant-halting-pr-2009-06-17/*.

[151] P. W. Barone, M. E. Wiebe, J. C. Leung, I. T. M. Hussein, F. J. Keumurian, J. Bouressa, A. Brussel, D. Chen, M. Chong, H. Dehghani, L. Gerentes, J. Gilbert, D. Gold, R. Kiss, T. R. Kreil, R. Labatut, Y. Li, J. Müllberg, L. Mallet, C. Menzel, M. Moody, S. Monpoeho, M. Murphy, M. Plavsic, N. J. Roth, D. Roush, M. Ruffing, R. Schicho, R. Snyder, D. Stark, C. Zhang, J. Wolfrum, A. J. Sinskey, and S. L. Springs, "Viral contamination in biologic manufacture and implications for emerging therapies," *Nature Biotechnology*, vol. 38, no. 5, pp. 563–572, May 2020. DOI: *10.1038/s41587-020-0507-2*.

[152] W. D. Powrie, C. H. Wu, and V. P. Molund, "Browning reaction systems as sources of mutagens and antimutagens.," *Environ Health Perspect*, vol. 67, pp. 47–54, Aug. 1986. DOI: *https://ehp.niehs.nih.gov/doi/10.1289/ehp.866747*.

[153] B. Junker, M. Lester, J. Leporati, J. Schmitt, M. Kovatch, S. Borysewicz, W. Maciejak, A. Seeley, M. Hesse, N. Connors, T. Brix, E. Creveling, and P. Salmon, "Sustainable reduction of bioreactor contamination in an industrial fermentation pilot plant," *Journal of Bioscience and Bioengineering*, vol. 102, no. 4, pp. 251–268, Oct. 2006. DOI: *10.1263/jbb.102.251*.

[154] L. Eggeling and M. Bott, "A giant market and a powerful metabolism: L-lysine provided by Corynebacterium glutamicum," *Applied Microbiology and Biotechnology*, vol. 99, no. 8, pp. 3387–3394, Apr. 2015. DOI: *10.1007/s00253-015-6508-2*.

[155] H. Lang, "Simplified approach to preliminary cost estimation," *Chemical Engineering*, pp. 112–113, 1948.

[156] L. R. Dysert, "Sharpen Your Cost Estimating Skills," vol. 45, no. 6, p. 9, 2003.

[157] J. Cran, "Improved factored method gives better preliminary cost estimates," *Chemical Engineering*, 1981.

[158] G. Jagschies, "Management of Process Economy—Case Studies," in *Biopharmaceutical Processing: Development, Design, and Implementation of Manufacturing Processes*, G. Jagschies, E. Lindskog, K. Łącki, and P. Galliher, Eds., Amsterdam, Netherlands: Elsevier, 2018, ISBN: 978-0-08-100623-8.

[159] *Aspen Capital Cost Estimator*, version 10.0, Burlington, MA: Aspen Technology.

[160] W. M. Huitt, *Bioprocessing Piping and Equipment Design: A Companion Guide for the ASME BPE Standard*. Hoboken, New Jersey: Wiley, 2017, 455 pp., ISBN: 978-1-119-28423-9.

[161] J. R. Couper, W. R. Penney, J. R. Fair, and S. M. Walas, *Chemical Process Equipment: Selection and Design*, 3rd ed. Amsterdam: Butterworth-Heinemann, 2012, 838 pp., ISBN: 978-0-12-396959-0.

[162] H. Stauffer, "Beware Capital Charge Rates," *The Electricity Journal*, vol. 19, no. 3, pp. 81–86, Apr. 2006. DOI: *10.1016/j.tej.2006.03.004*.

[163] A. Damodaran. (Jan. 2020). "Cost of Capital by Sector (U.S.)," [Online]. Available: *http://pages.stern.nyu.edu/~adamodar/New_Home_Page/datafile/wacc.htm*.

[164] Finbox. (2020). "WACC For Beyond Meat, Inc. (BYND)," finbox.com, [Online]. Available: *https://finbox.com/NASDAQGS:BYND/explorer/wacc*.

[165] Z. B. Maroulis and G. D. Saravacos, *Food Process Design*, 126. New York: Marcel Dekker, 2003, 506 pp., ISBN: 978-0-8247-4311-6.

[166] P. W. Hart and J. T. Sommerfeld, "Cost Estimation of Specialty Chemicals From Laboratory-Scale Prices," *Cost Engineering*, vol. 39, no. 3, p. 5, 1997.

[167] R. Sterk. (Jul. 2018). "Ingredion to trim corn wet milling as part of cost savings plan," [Online]. Available: *https://www.world-grain.com/articles/10680-ingredion-to-trim-corn-wet-milling-as-part-of-cost-savings-plan?v=preview*.

[168] USDA ERS. (2020). "Sugar and Sweeteners Yearbook Tables," [Online]. Available: *https://www.ers.usda.gov/data-products/sugar-and-sweeteners-yearbook-tables/*.

[169] N. Jakel, "Industrial glucose: Bridging the industrial sugar gap," presented at the International Fuel Ethanol Workshop and Expo, Indianapolis, Ind., 2019. [Online]. Available: *https://fluidquiptechnologies.com/wp-content/uploads/2019/07/FEW-2019-Bridging-the-Industrial-Sugar-Gap.pdf*.

[170] K. Drauz, I. Grayson, A. Kleemann, H.-P. Krimmer, W. Leuchtenberger, and C. Weckbecker, "Amino Acids," in *Ullmann's Encyclopedia of Industrial Chemistry*, WILEY-VCH, 2007, ISBN: 978-3-527-30673-2. DOI: *10.1002/14356007.a02_057.pub2*.

[171] IHS Markit, "Amino Acids, Major," Nov. 2019.

[172] BCC Research, "Commercial Amino Acids," BIO007L, Nov. 2017.

[173] S. Sanchez, R. Rodríguez-Sanoja, A. Ramos, and A. L. Demain, "Our microbes not only produce antibiotics, they also overproduce amino acids," *J Antibiot*, vol. 71, no. 1, pp. 26–36, Jan. 2018. DOI: *10.1038/ja.2017.142*.

[174] F. Zuo, Q. Gu, S. Li, H. Wei, and J. Peng. (Jul. 16, 2019). "Effects of Different Methionine Sources on Methionine Metabolism in the IPEC-J2 Cells," BioMed Research International, [Online]. Available: *https://www.hindawi.com/journals/bmri/2019/5464906/*.

[175] M. Anusree and K. M. Nampoothiri, "White Biotechnology for Amino Acids," in *Industrial Biorefineries & White Biotechnology*, Elsevier, 2015, pp. 445–471, ISBN: 978-0-444-63453-5. DOI: *10.1016/B978-0-444-63453-5.00014-8*.

[176] EFSA FEEDAP Panel, "Scientific Opinion on the safety and efficacy of L-threonine produced by Escherichia coli for all animal species based on a dossier submitted by HELM AG on behalf of Meihua Holdings Group Co. Ltd," *EFSA Journal*, vol. 13, no. 3, p. 4051, 2015. DOI: *10.2903/j.efsa.2015.4051*.

[177] R. J. Wallace, J. Gropp, N. Dierick, L. G. Costa, G. Martelli, P. G. Brantom, V. Bampidis, D. W. Renshaw, and L. Leng, "Risks associated with endotoxins in feed additives produced by fermentation," *Environ Health*, vol. 15, no. 1, p. 5, Dec. 2016. DOI: *10.1186/s12940-016-0087-2*.

[178] X. He, "Enhanced l-lysine production from pretreated beet molasses by engineered Escherichia coli in fed-batch fermentation," *Bioprocess Biosyst Eng*, p. 8, 2015. DOI: *10.1007/s00449-015-1403-x*.

[179] K. Takumi, M. K. Ziyatdinov, V. Samsonov, and G. Nonaka, "Fermentative Production of Cysteine by Pantoea ananatis," *Appl. Environ. Microbiol.*, vol. 83, no. 5, Mar. 1, 2017. DOI: *10.1128/AEM.02502-16*.

[180] J. Babcock, S. Smith, H. Huttinga, and D. Merrill, "Enhancing Performance in Cell Culture," *GEN - Genetic Engineering and Biotechnology News*, vol. 27, no. 20, Nov. 15, 2007.

[181] J. N. Hartshorn, S. McNorton, C. Hernandez, E. van der Ent, and M. V. Caple, "Soy Hydrolysate Optimization for Cell Culture Applications," in *Cells and Culture*, T. Noll, Ed., Dordrecht: Springer Netherlands, 2010, pp. 777–783, ISBN: 978-90-481-3418-2. DOI: *10.1007/978-90-481-3419-9_135*.

[182] Kerry Group, "Biotechnologies Technical Manual," Aug. 2018.

[183] USDA-IL Dept of Ag Market News Service, "Central Illinois Soybean Processor report," GX_GR117, Apr. 2020. [Online]. Available: *https://www.ams.usda.gov/mnreports/gx_gr117.txt*.

[184] D. Stanton. (Apr. 3, 2019). "Quality FBS, or just BS? Industry turning to supply chain certification," BioProcess International, [Online]. Available: *https://bioprocessintl.com/bioprocess-insider/global-markets/quality-fbs-or-just-bs-industry-turning-to-supply-chain-certification/*.

[185] Mosa Meat. (Nov. 15, 2019). "Growth Medium without Fetal Bovine Serum (FBS)," Mosa Meat, [Online]. Available: *https://www.mosameat.com/blog/2019/11/15/mosa-meat-on-netflixs-explained*.

[186] M. P. Rowland. (Jan. 22, 2020). "Memphis Meats Raises $161 Million In Funding, Aims To Bring Cell-Based Products To Consumers," Forbes, [Online]. Available: *https://www.forbes.com/sites/michaelpellmanrowland/2020/01/22/memphis-meats-raises-161-million-series-b-funding-round-aims-to-bring-cell-based-products-to-consumers-for-the-first-time/*.

[187] E. Watson. (Feb. 11, 2020). "Cell-based meat in focus: In conversation with Meatable, Finless Foods, New Age Meats," foodnavigator-usa.com, [Online]. Available: *https://www.foodnavigator-usa.com/Article/2020/02/11/Cell-based-meat-in-focus-In-conversation-with-Meatable-Finless-Foods-New-Age-Meats*.

[188] B. Kelley, "Industrialization of mAb production technology: The bioprocessing industry at a crossroads," *mAbs*, vol. 1, no. 5, pp. 443–452, Sep. 2009. DOI: *10.4161/mabs.1.5.9448*.

[189] D. Gotham, M. J. Barber, and A. Hill, "Production costs and potential prices for biosimilars of human insulin and insulin analogues," *BMJ Global Health*, vol. 3, no. 5, e000850, Sep. 2018. DOI: *10.1136/bmjgh-2018-000850*.

[190] S. Basu, J. S. Yudkin, S. Kehlenbrink, J. I. Davies, S. H. Wild, K. J. Lipska, J. B. Sussman, and D. Beran, "Estimation of global insulin use for type 2 diabetes, 2018–30: A microsimulation analysis," *The Lancet Diabetes & Endocrinology*, vol. 7, no. 1, pp. 25–33, Jan. 2019. DOI: *10.1016/S2213-8587(18)30303-6*.

[191] ClinCalc. (2017). "Insulin Glargine - Drug Usage Statistics," ClinCalc.com, [Online]. Available: *https://clincalc.com/DrugStats/Drugs/InsulinGlargine*.

[192] M. Arbige, "Industrial enzymology: A look towards the future," *Trends in Biotechnology*, vol. 7, no. 12, pp. 330–335, Dec. 1989. DOI: *10.1016/0167-7799(89)90032-2*.

[193] G. Chen, D. R. Gulbranson, Z. Hou, J. M. Bolin, V. Ruotti, M. D. Probasco, K. Smuga-Otto, S. E. Howden, N. R. Diol, N. E. Propson, R. Wagner, G. O. Lee, J. Antosiewicz-Bourget, J. M. C. Teng, and J. A. Thomson, "Chemically defined conditions for human iPSC derivation and culture," *Nature Methods*, vol. 8, no. 5, pp. 424–429, May 2011. DOI: *10.1038/nmeth.1593*.

[194] MECO, "Water for Injection: A Cost Review," Jun. 7, 2019. [Online]. Available: *https://cdn2.hubspot.net/hubfs/2145052/MECO%20Water%20for%20Injection%20-%20A%20Cost%20Review%20(002)-1.pdf*.

[195] W. A. Alkhayat and A. M. Gerrard, "Estimating Manning Levels for Process Plants," *AACE Transactions*, pp. I.2.1–I.2.4, 1984.

[196] H. B. Reisman, *Economic Analysis of Fermentation Processes*. Boca Raton, Fla: CRC Press, 1988, 235 pp., ISBN: 978-0-8493-6886-8.

[197] R. Turton, *Analysis, Synthesis and Design of Chemical Processes*, 5th edition. Boston, MA: Prentice Hall, 2018, ISBN: 978-0-13-417740-3.

[198] H. Suomalainen, "Changes in the cell constitution of baker's yeast in changing growth conditions," *Pure and Applied Chemistry*, vol. 7, no. 4, pp. 639–654, Jan. 1, 1963. DOI: *10.1351/pac196307040639*.

[199] H. Bozenhardt and E. Bozenhardt. (Jul. 28, 2016). "Bioprocess Facility Design — Layout Rules And Configurations," Bioprocess Online, [Online]. Available: *https://www.bioprocessonline.com/doc/bioprocess-facility-design-layout-rules-and-configurations-0001*.

[200] T. D. Pereira Chilima, F. Moncaubeig, and S. S. Farid, "Estimating capital investment and facility footprint in cell therapy facilities," *Biochemical Engineering Journal*, vol. 155, no. 107439, Mar. 2020. DOI: *10.1016/j.bej.2019.107439*.

[201] Cleanroom Technology. (Jun. 15, 2018). "Clean in place systems explained," [Online]. Available: *https://www.cleanroomtechnology.com/news/article_page/Clean_in_place_systems_explained/144045*.

[202] G. Page and R. Kral. (Sep. 2006). "Designing a Shorter Vertical Leg for Sanitary Steam Traps," [Online]. Available: *http://www.biopharminternational.com/designing-shorter-vertical-leg-sanitary-steam-traps*.

[203] J. Boyd, "Biomanufacturing Costs in Cities around the Globe," *Genetic Engineering & Biotechnology News*, pp. 58–60, Jun. 2020.

[204] T. D. Searchinger, "Creating a sustainable food future," World Resources Institute, 2013. [Online]. Available: *https://wrr-food.wri.org/*.

[205] C. Haringa, W. Tang, G. Wang, A. T. Deshmukh, W. A. van Winden, J. Chu, W. M. van Gulik, J. J. Heijnen, R. F. Mudde, and H. J. Noorman, "Computational fluid dynamics simulation of an industrial P. chrysogenum fermentation with a coupled 9-pool metabolic model: Towards rational scale-down and design optimization," *Chemical Engineering Science*, vol. 175, pp. 12–24, Jan. 2018. DOI: *10.1016/j.ces.2017.09.020*.

[206] C. Haringa, A. T. Deshmukh, R. F. Mudde, and H. J. Noorman, "Euler-Lagrange analysis towards representative down-scaling of a 22 m3 aerobic S. cerevisiae fermentation," *Chemical Engineering Science*, vol. 170, pp. 653–669, Oct. 2017. DOI: *10.1016/j.ces.2017.01.014*.

[207] E. S. Langer, "Biotech Facilities Average a Batch Failure Every 40.6 Weeks," *BioProcess International*, vol. 68, no. 8, pp. 28–29, 2008.

[208] E. S. Langer. (Sep. 30, 2016). "Average Batch Failure Rate Worsens," GEN - Genetic Engineering and Biotechnology News, [Online]. Available: *https://www.genengnews.com/magazine/279/average-batch-failure-rate-worsens/*.

[209] M. Staton. (Apr. 26, 2013). "Nutrient management recommendations for high-yield soybean production," Michigan State University Extension, [Online]. Available: *https://www.canr.msu.edu/news/nutrient_management_recommendations_for_high_yield_soybean_production*.

[210] L. Thorrez and H. Vandenburgh, "Challenges in the quest for 'clean meat'," *Nature Biotechnology*, vol. 37, no. 3, pp. 215–216, Mar. 2019. DOI: *10.1038/s41587-019-0043-0*.

[211] ABEC. (Nov. 2020). "Custom Single-Run Scalable Solutions," ABEC, [Online]. Available: *https://www.abec.com/single-use/*.

[212] D. Stanton. (Mar. 14, 2019). "Batch to the future: Amid single-use and 100 g/L, stainless steel will continue to shine," BioProcess International, [Online]. Available: *https://bioprocessintl.com/bioprocess-insider/upstream-downstream-processing/batch-to-the-future-amid-single-use-and-100-g-l-stainless-steel-will-continue-to-shine/*.

[213] W. Flanagan, A. Brown, M. Pietrzykowski, V. Pizzi, M. Monge, and A. Sinclair, "An Environmental Lifecycle Assessment of Single-Use and Conventional Process Technology: Comprehensive Environmental Impacts," *BioPharm International*, vol. 27, no. 3, Mar. 2014.

[214] E. Craven, "Gamma sterilization of medical devices," presented at the FDA Medical Device Advisory Meeting, Nov. 6, 2019. [Online]. Available: *https://www.fda.gov/media/132374/download*.

[215] International Irradiation Association, "The business and science of radiation processing in 2019," Strasbourg, Apr. 2019. [Online]. Available: *https://www.imrp-iia.com/wp-content/uploads/The-business-and-science-of-radiation-processing-in-2019.pdf*.

[216] P. Sinco, "Inside a gamma sterilizer," *Nuclear News*, p. 5, May 1999.

[217] V. Barba. (Sep. 12, 2019). "ABEC launches 6,000L single-use bioreactor to answer scalability needs," biopharma-reporter.com, [Online]. Available: *https://www.biopharma-reporter.com/Article/2019/09/12/ABEC-launches-6-000L-single-use-bioreactor*.

[218] N. Rubio, I. Datar, D. Stachura, D. Kaplan, and K. Krueger, "Cell-Based Fish: A Novel Approach to Seafood Production and an Opportunity for Cellular Agriculture," *Front. Sustain. Food Syst.*, vol. 3, 2019. DOI: *10.3389/fsufs.2019.00043*.

[219] G. Potter, A. S. Smith, N. T. Vo, J. Muster, W. Weston, A. Bertero, L. Maves, D. L. Mack, and A. Rostain, "A More Open Approach Is Needed to Develop Cell-Based Fish Technology: It Starts with Zebrafish," *One Earth*, vol. 3, no. 1, pp. 54–64, Jul. 2020. DOI: *10.1016/j.oneear.2020.06.005*.

[220] I. Goldberg, *Single Cell Protein*. Berlin, Heidelberg: Springer Berlin Heidelberg, 1985, vol. 1, ISBN: 978-3-642-46542-0. DOI: *10.1007/978-3-642-46540-6*.

[221] V. Meyer, E. Y. Basenko, J. P. Benz, G. H. Braus, M. X. Caddick, M. Csukai, R. P. de Vries, D. Endy, J. C. Frisvad, N. Gunde-Cimerman, T. Haarmann, Y. Hadar, K. Hansen, R. I. Johnson, N. P. Keller, N. Kraševec, U. H. Mortensen, R. Perez, A. F. J. Ram, E. Record, P. Ross, V. Shapaval, C. Steiniger, H. van den Brink, J. van Munster, O. Yarden, and H. A. B. Wösten, "Growing a circular economy with fungal biotechnology: A white paper," *Fungal Biology and Biotechnology*, vol. 7, no. 1, p. 5, Apr. 2, 2020. DOI: *10.1186/s40694-020-00095-z*.

[222] T. Linder, "Edible Microorganisms—An Overlooked Technology Option to Counteract Agricultural Expansion," *Front. Sustain. Food Syst.*, vol. 3, 2019. DOI: *10.3389/fsufs.2019.00032*.

[223] T. Kluyver, B. Ragan-Kelley, F. Pérez, M. Bussonnier, J. Frederic, J. Hamrick, J. Grout, S. Corlay, P. Ivanov, S. Abdalla, and C. Willing, "Jupyter Notebooks—a publishing format for reproducible computational workflows," in *Positioning and Power in Academic Publishing: Players, Agents and Agendas*, F. Loizides and B. Schmidt, Eds., 2016, p. 4, ISBN: 978-1-61499-649-1.

[224] M. Driscoll. (Apr. 30, 2014). "Reading Excel Spreadsheets with Python and xlrd," The Mouse Vs. The Python, [Online]. Available: *https://www.blog.pythonlibrary.org/2014/04/30/reading-excel-spreadsheets-with-python-and-xlrd/*.

[225] J. D. Hunter, "Matplotlib: A 2D Graphics Environment," *Computing in Science Engineering*, vol. 9, no. 3, pp. 90–95, May 2007. DOI: *10.1109/MCSE.2007.55*.

[226] A. Rohatgi, *WebPlotDigitizer*, version 4.2, San Francisco, California, USA, Apr. 2019. [Online]. Available: *https://automeris.io/WebPlotDigitizer*.

[227] F. Wiemer, *Pfasante/phd_thesis*, Sep. 17, 2020. [Online]. Available: *https://github.com/pfasante/phd_thesis*.

[228] E. H. Battley, "A reevaluation of the thermodynamics of growth of *Saccharomyces cerevisiae* on glucose, ethanol, and acetic acid," *Canadian Journal of Microbiology*, vol. 41, no. 4-5, pp. 388–398, Apr. 1995. DOI: *10.1139/m95-052*.

[229] L. Tijhuis, M. C. van Loosdrecht, and J. J. Heijnen, "A Thermodynamically Based Correlation for Maintenance Gibbs Energy Requirements in Aerobic and Anaerobic Chemotrophic Growth," *Biotechnology and Bioengineering*, vol. 42, pp. 509–519, 1993. DOI: *10.1002/bit.260420415*.

[230] J. J. Heijnen, "A thermodynamic approach to predict black-box model parameters for microbial growth," in *Biothermodynamics: The Role of Thermodynamics in Biochemical Engineering*, U. von Stockar, Ed., 1st ed., Lausanne: EFPL Press, 2013, ISBN: 978-1-4665-8217-0.

[231] R. Phillips, *Physical Biology of the Cell*, Second edition. London : New York, NY: Garland Science, 2013, 1057 pp., ISBN: 978-0-8153-4450-6.

[232] R. A. Alberty, *Thermodynamics of Biochemical Reactions*. Hoboken, N.J: Wiley-Interscience, 2003, 397 pp., ISBN: 978-0-471-22851-6.

[233] P. W. Atkins and J. De Paula, *Physical Chemistry*, 9th ed. New York: W.H. Freeman, 2010, 1139 pp., ISBN: 978-1-4292-1812-2.

[234] A. Flamholz, E. Noor, A. Bar-Even, and R. Milo, "eQuilibrator–the biochemical thermodynamics calculator," *Nucleic Acids Research*, vol. 40, no. D1, pp. D770–D775, Jan. 1, 2012. DOI: *10.1093/nar/gkr874*.

A

Baker's yeast analysis

Producing mass quantities of animal cells in large-scale, high-density culture is a novel problem. As an analog in industrial biotechnology, consider baker's yeast (*Saccharomyces cerevisiae*). Bakeries, breweries, and fuel ethanol plants use yeast delivered at varying moisture content: liquid, cream, compressed, and dry. Each of these is produced by similar fermentation operations, with differences in post-fermentation dewatering and drying [58]. A large market thus exists for yeast and price information is readily available, as presented in Table 1.2. With a wholesale price in the range of $2.20–$2.80/kg, and assuming a total margin of 33% (profit + taxes), the actual cost of baker's yeast production should be around $1.90/kg.

The conceptual process flow diagram in Figure A.1 follows from published process descriptions [50, 58]. Baker's yeast is grown aerobically on heat-sterilized molasses at 30 wt% sucrose and anhydrous ammonia.[151] The final production fermentors are modeled as 200 m^3 bubble column bioreactors (BCR), operating in a fed-batch mode. The growth temperature is 30 °C, controlled using chilled water in a jacket. Upon harvest, the yeast cells are

[151] Glucose from corn syrup can also be used but molasses is generally preferred as it tends to be less expensive and already contains many of the trace nutrients required for yeast growth.

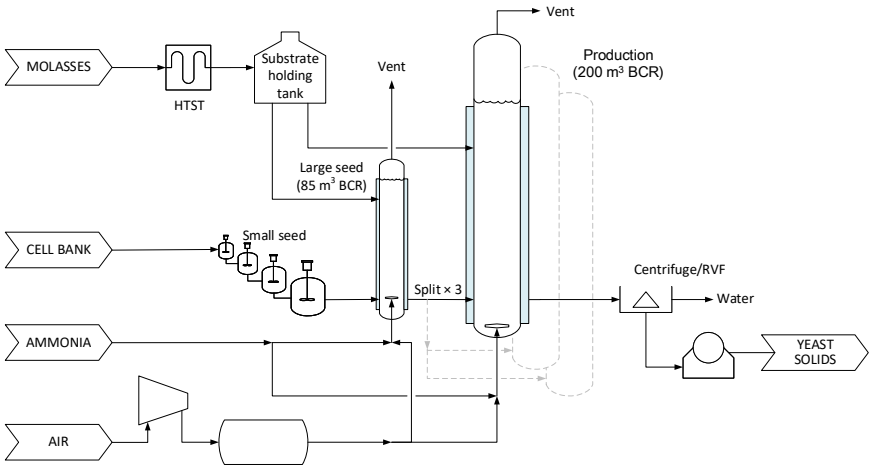

FIGURE A.1: Flow diagram for yeast production.

centrifuged to a cream yeast consistency of 20% solids. To make compressed yeast, the solids are further dewatered by rotary vacuum filter (RVF) to ~33%. The filter cake may subsequently be extruded and dried to make active dry yeast. A yeast factory is likely to sell a slate of all these products, so it will be assumed that the cost of production of the RVF product represents the average.

Yeast cell mass (DCM_m, microbial dry cell matter) has a CHON formula of $CH_{1.7}O_{0.46}N_{0.17}$ [228]. As discussed in Section 2.2, the enthalpy of formation ΔH_f for cell mass can be estimated as -96.5 kJ/mol using the correlation of Burnham [87]. The Gibbs energy of formation ΔG_f can further be estimated as -52.7 kJ/mol by applying the correlation of Battley [88]. Balancing the degree of reduction and nitrogen gives the anabolic reaction:[152]

$$0.18\ \text{Glc}\ (C_6H_{12}O_6) + 0.17\ NH_3 \rightarrow 1\ DCM_m + 0.07\ CO_2 + 0.47\ H_2O$$
$$\Delta H = -21.4\,\text{kJ/mol} \quad \Delta G = -23.6\,\text{kJ/mol} \quad \text{(A.1)}$$

[152]The sucrose in molasses is hydrolyzed to one molecule each of glucose and fructose before metabolism; both are subsequently consumed with roughly equal rates.

In aerobic fermentation, catabolic energy is usually provided by respiration:

$$1\ \text{Glc} + 6\ O_2 \rightarrow 6\ CO_2 + 6\ H_2O$$
$$\Delta H = -2,865\,\text{kJ/mol} \quad \Delta G = -2,922\,\text{kJ/mol} \quad \text{(A.2)}$$

The Gibbs energy dissipated during cell growth can be estimated from the carbon chain number C and degree of reduction γ of the carbon source [96]:[153]

$$\Delta G_{diss}[\text{ kJ/C-mol } DCM_m] =$$
$$200 + 18(6 - C)^{1.8} + \exp\left[\left[(3.8 - \gamma/C)^2\right]^{0.16} \times (3.6 + 0.4C)\right] \quad \text{(A.3)}$$

[153]For glucose ($C_6H_{12}O_6$), $\gamma = 24$ and $\Delta G_{diss} = 236$ kJ/mol.

A growth reaction is then obtained by combining Reactions A.1 for 1 mol DCM_m and A.2, factored by an extent that causes the combined reaction to have $\Delta G_r = -\Delta G_{diss}$ (in this case, 0.073 mol/mol DCM_m).

$$0.25\ \text{Glc} + 0.44\ O_2 + 0.17\ NH_3 \rightarrow 1\ DCM_m + 0.5\ CO_2 + 0.91\ H_2O$$
$$\Delta H = -229.8\,\text{kJ/mol} \quad \Delta G = -236.1\,\text{kJ/mol} \quad \text{(A.4)}$$

Maintenance is an additional Gibbs energy requirement associated with normal cell function. By another correlation [229], the maintenance energy (m_E, kJ/mol DCM_m-h) at 30 °C is 7.1 kJ/mol DCM_m-h, requiring respiration of 0.0024 mol glucose/mol DCM_m-h

$$m_E[\text{ kJ/mol-h}] = 4.5\ \exp\left[\frac{-6.94 \times 10^{-4}}{R}\left(\frac{1}{T} - \frac{1}{298}\right)\right] \quad \text{(A.5)}$$

The native growth rate of *S. cerevisiae* is μ=0.46/h (90 min doubling time) but in commercial yeast production the growth rate is typically limited to 0.2/h (3.5 h doubling time) to avoid excessive ethanol production [58].

Combining the growth reaction at μ=0.2/h and the maintenance reaction gives the overall process reaction [230]:

$$0.26\ \text{Glc} + 0.51\ O_2 + 0.17\ NH_3 \rightarrow 1\ DCM_m + 0.58\ CO_2 + 0.98\ H_2O$$
$$\Delta H = -265.1\ \text{kJ/mol} \quad \Delta G = -272.0\ \text{kJ/mol} \qquad \text{(A.6)}$$

This reaction predicts a yield of yeast from glucose of 0.50 g/g. Reed and Nagodawithana [58] report that the best yield under aerobic conditions is 0.54 g/g. The simple correlations above come quite close to this value without performing an experiment.

In highly aerobic fermentations, the electric power demands of the air compressor and chilled-water system are significant. These additional operating costs can be estimated by simulating a fed-batch production run as follows. At $t = 0$, the fermentor volume is set to 78 m^3 with 1,170 kg DCM_m inoculum (15 g/L; more on this later). The bioreactor conditions are 30 °C and 1.33 bar (5 psig) back pressure. The bottom pressure varies with the head exerted by the culture volume. The growth rate is initially set to μ=0.2/h. At regular time intervals, a new DCM_m amount is computed with a growth reaction:

$$DCM_{t+\Delta t} = DCM_t \exp(\mu \Delta t). \qquad \text{(A.7)}$$

and the corresponding stoichiometric requirements of substrate, ammonia, and oxygen (q-rates) in each interval are computed using Reaction A.6.

At the instantaneous reactor volume, the q-rate of oxygen can be expressed as a volumetric oxygen uptake rate (Equation 4.2). If the bioreactor is operating properly, the oxygen uptake rate is equal to the oxygen transfer rate (OUR=OTR) and the inlet gas sparge rate can be estimated with an O_2 mass transfer calculation, as given in Equation 2.15.

For yeast fermentation, DO at the top of the bioreactor is taken to be 1 mg/L, and the bottom DO is this value times the bottom/top pressure ratio. The inlet gas is assumed to be 21% O_2 and the outlet composition is computed with a mass balance on the gas phase, including some amount of evaporated (stripped) water, computed with Raoult's Law. The oxygen mass transfer coefficient k_La is estimated with the correlation of Heijnen and van't Riet [124], which is adequate for conceptual design:

$$k_La[\ s^{-1}] = 0.32 u_s^{0.2} \eta^{-0.84} \times 1.025^{T-20} \qquad \text{(A.8)}$$

where T is the fermentation temperature in °C and η is the broth viscosity in cp. Solving for the superficial velocity u_s (m/s) at the column average pressure gives the sparge rate required.

Bubble columns have a practical OTR limit of 150 mol O_2/m^3-h before excessive foaming or jet flooding occurs. The batch simulation therefore proceeds with μ=0.2/h until OUR=150, at which point it can be assumed that the fermentation becomes O_2-limited. This limitation is enforced by reducing μ (with Excel Solver or Goal Seek) such that the process reaction

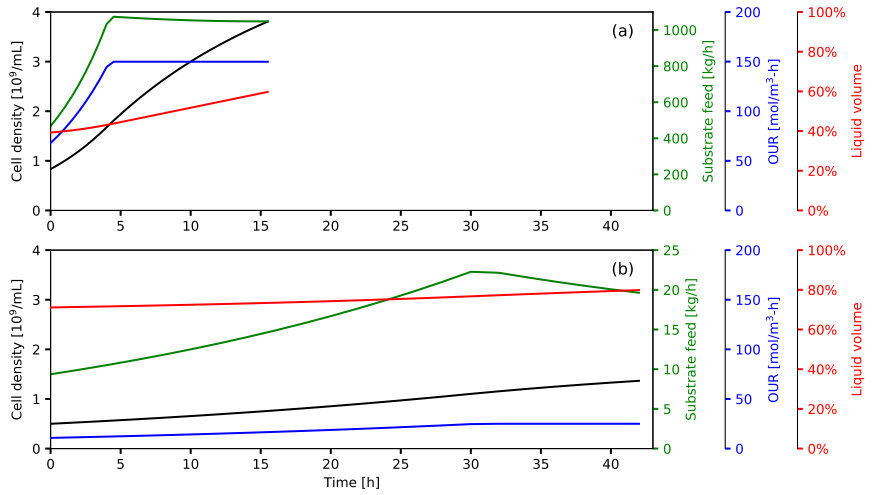

FIGURE A.2: Feed rate, cell density, and oxygen uptake rate predicted by fed-batch simulation for yeast. (a) Industry-standard fermentation. (b) Constrained by OUR and growth-rate limits.

meets this limiting OUR.[154] As shown in Figure A.2a, the fed batch has an early stage where the culture grows exponentially and a later stage where growth is oxygen-limited.

The endpoint of the fed batch is determined by a final viscosity (2 cp) and final working volume. The latter is kept relatively low (60%) to allow for gas holdup and foaming [114]. Viscosity η increases with the volume fraction of cells ϕ according to the Krieger-Dougherty model (Equation 2.1). If yeast cells are represented as spheres 5 μm in diameter [231], the limiting viscosity is reached at a volume fraction of approximately ϕ=0.28, or a cell density of 80 g/L (dry matter basis). Designing below this limit, a practical maximum cell density for baker's yeast can be taken as 70 g/L dry, or 4×10^9 cell/mL. The additional constraints of acceptable batch time (~16 h) and substrate concentration (30 wt%) dictate that there are limited sets of initial conditions that will hit this endpoint (78 m^3 at 15 g/L, as specified above). As shown in Figure A.2a, the simulation ends after ~16 h, producing 7,000 kg net DCM_m (8,200 kg total, including the inoculum) in a final volume of 120 m^3.

Taking the total turnaround time of the production fermentor as 24 h, a facility with 6 such fermentors operating 350 days per year could produce ~17 kTA of yeast. In lieu of a detailed scheduling exercise [67, 196], some shortcut assumptions are made. Given that viscosity and foaming are physical limits, it is assumed that the seed fermentors leading up to the production batch operate with similar endpoints, with the 70 g/L product from the seed fermentor diluted to 15 g/L in the next fermentor upon transfer. If it is further assumed that the seed batches have similar time efficiency to the production batches (i.e., 2.8 doublings in 24 h total turnaround time), then 6×200 m^3 production fermentors could be serviced by 6×28 m^3 final seed fermentors. Accounting for volumetric economies of scale, however, it is more cost-effective to split a larger seed batch (85 m^3) between three production

[154] See Note 123. Further note that the specific stoichiometric coefficients in Reaction A.6 depend on the growth rate, so these are recomputed at each time interval.

TABLE A.1: Abbreviated equipment list and total capital costs for yeast production.

	Qty	Cost each	Total cost
200 m^3 BCR	6	$818,000	$4,908,000
Seed train			$1,369,000
Pasteurizer	1	$221,000	$221,000
Prep tank	1	$593,000	$593,000
Air compressor	2	$1,375,000	$2,750,000
Centrifuge	2	$864,000	$1,728,000
RVF	2	$326,000	$652,000
Abbr. capital			$12,221,000
Missing capital	20%		$3,055,000
TPEC			$15,276,000
Lang factor = 4.5			
Total capital investment (TCI)			**$68,742,000**

fermentors [58, 198]. Figure A.4a shows a capital-optimized set of splits from F5 (the six production fermentors, ending with ~8,200 kg each) back to F1, a single 500 L seed fermentor that starts with 3 kg of yeast prepared in the lab. To the extent permitted by seed splitting, production batches could ideally be staggered by 24/6 = 4 hours, meaning that a production batch is finishing (and thus another is starting) every 4 hours, or twice in an 8-hour shift. The six fermentors are thus taken as a single train with shared upstream and downstream operations (media preparation, air compression, dewatering steps).

Table A.1 presents a list of the critical equipment for the yeast process. Using the techniques described in Humbird et al. [38] and Section 3.1, the cost of a 200 m^3 jacketed BCR in 316L stainless steel is estimated as $818k (bare equipment). Capital costs for appropriately sized air compressors, molasses feed sterilizer, centrifuges, rotary vacuum filter, and utilities equipment were estimated with Aspen Capital Cost Estimator [159], SuperPro Designer [56], or the correlations in Couper et al [161]. A 20% correction is added to account for missing minor equipment (e.g., pumps and tanks). An overall Lang factor of 4.5 (Table 3.1) is applied to the purchased equipment cost to arrive at a total capital investment (TCI) of $69M.

Variable operating costs include raw material costs, waste disposal, and utilities. For the baker's yeast process, the total consumptions of molasses and ammonia per batch are computed by integrating the feed curves in Figure A.2; additional feedstock required for the seed culture is ratioed to the net yeast made in the production fermentor. Water is also an important raw material. For baker's yeast culture, which uses minimally processed potable water, the cost is insignificant. Compressor power is estimated from the simulated aeration rate and an adiabatic horsepower calculation [161]. The chiller power demand is estimated with a rule of thumb of 1.24 hp/ton refrigeration [161]. Steam demand for SIP is likewise estimated from a rule of thumb [202], and utility demands for molasses sterilization are estimated in SuperPro. Finally, the total steam demand is converted to natural gas demand by assuming a 60% boiler efficiency. Raw material and utility demands and costs are summarized in Table A.2.

TABLE A.2: Variable operating costs for yeast production.

Raw materials	Per batch	Unit cost	$/kg yeast
Molasses	17,700 kg	$0.33	$0.72
Ammonia	1,040 kg	$0.30	$0.04
Well water	270 MT	$0.26	$0.01
Total raw materials cost			**$0.76**
Waste disposal	Per batch	Unit cost	$/kg yeast
WWT	150 m^3	$0.40	$0.007
Total disposal cost			**$0.007**
Utilities	Per batch	Unit cost	$/kg yeast
Compressor	13,400 kWh	$0.05	$0.08
Chiller	6,900 kWh	$0.05	$0.04
Dewatering	660 kWh	$0.05	$0.004
Steam	25 MT	$9.70	$0.03
Total utilities cost			**$0.15**
Total variable operating cost			**$0.92/kg**

Fixed operating costs include facility overhead and labor. As in Section 3, the former includes annual maintenance at 4% of TCI and insurance at 5% of TCI. As discussed in Section 3.3, labor costs were quantified in terms of operator attention per batch, based on a series of task/time assumptions. For every six batch starts, it is assumed that there are 4 passage steps in the lab, requiring 60 minutes of attention each, followed by transfers into increasingly large fermentors. The operator attention paid to seed and production fermentors is expressed as percentages of online time and offline (drain/clean/fill) time. For small seed fermentors ($<1m^3$), this is taken as 25% each to allow for some manual dis/assembly. For larger seed and production fermentors, this attention is taken as 10% each. An efficiency of 80% is imposed on these time estimates to account for breaks and administrative activities. For the continuous or nominally continuous parts of the process such as media prep, dewatering, air compression, and utilities, Reisman [196] presents a table of FTE/shift requirements for typical fermentation unit operations, of which there is one set per train (recall that the six fermentors are treated as a single train). One maintenance technician is also assumed per train, and one supervisor per 10 regular employees. Per position, 4.5 hires are assumed. The FTE estimates and total fixed operating costs are summarized in Table A.3.

As discussed in Section 3 (see Equation 3.2), if the capital cost estimated above is expressed as an annual rate ($/y), then capital and operating costs can be expressed as an aggregate cost of production in $/kg. For baker's yeast, i was taken as 10%, and the plant lifetime as 20 years. With a CCF of 12%, the TCI from Table A.1 can be expressed as $8.1M/y or $0.47/kg. The overall cost of production for baker's yeast is summarized in Table A.4 as $1.89/kg. After the comprehensive yet straightforward techno-economic analysis presented here, which leverages principles of thermodynamics, reactor design, process simulation, and plant economics, a known cost of production for baker's yeast

TABLE A.3: Fixed operating costs for yeast production.

Batch	Attention	h/batch	FTE/shift	$/y
Lab	60 min/step	0.8	0.2	$10,000
Small seed	25% time	2.5	0.6	$30,000
Large seed	10% time	1.5	0.4	$20,000
Production	10% time	3.0	0.8	$40,000
Total batch workers			2.0	$100,000
Continuous			FTE/shift	$/y
Media prep			0.5	$25,000
Dewater			0.8	$15,000
Utilities			1.0	$25,000
Maintenance			0.5	$50,000
Total continuous workers			2.8	$140,000
Supervisor			0.5	$33,600
Total labor per shift			5.3	$274,000
Total labor (all shifts)			24	$1,233,000
Labor burden (100%)				$1,233,000
Total labor cost				**$2,466,000**
Annual maintenance (4% of TCI)				$2,750,000
Annual insurance+tax (5% of TCI)				$3,437,000
Total fixed operating costs				**$8,653,000**

TABLE A.4: Total production cost for yeast cell mass (dry matter basis).

	$M/y	$/kg
Molasses	$12.4	$0.72
Ammonia	$0.65	$0.04
Process water	$0.15	$0.01
Electric power	$2.1	$0.12
Natural gas	$0.5	$0.03
Wastewater treatment	$0.1	$0.01
Total variable OPEX	*$15.9*	*$0.92*
Burdened labor cost	$2.5	$0.14
Annual maintenance	$2.7	$0.16
Annual insur. + tax	$3.4	$0.20
Total fixed OPEX	*$8.7*	*$0.50*
Annual capital charge	$8.1	$0.47
Total production cost	**$32.6**	**$1.89**

(estimated as $1.90/kg from its wholesale price) has been reproduced to within a few percent.

If the previous analysis was straightforward, then it is a result of perhaps 150 years of progress in the modeling and design of industrial fermentation processes for *S. cerevisiae* and other microbes [92]. It was offered here to demonstrate and establish confidence in the TEA methods that were used to examine animal cell culture in the preceding sections. Given the accuracy of this model for baker's yeast, it may be informative to see how it responds to some of the constraints that were discussed in Section 1.2 for large-scale animal cell culture. Referring to Figure 1.3, the example was optimized to the lower-right corner of this graph. Suppose that the yeast factory were de-intensified, i.e., shifted toward the upper-left, by imposing the following constraints:

- Production bioreactor size reduced to 20 m^3.
- Maximum growth rate reduced to μ=0.029/h.

- Maximum fermentor OUR reduced to 25 mol O_2/m^3-h; final working volume increased to 80% due to reduced gas holdup.

If the two designs are compared at a roughly equal total capital investment of ~$69M, the constrained process is limited to 27×20 m^3 bioreactors producing 1.7 kTA of yeast. Highlights of the analysis are briefly included here.

The overall process reaction was first updated for the lower growth rate. Compared to Reaction A.6, the CO_2 and water produced per mol DCM_m are significantly higher here; this is because the culture grows more slowly, using more substrate for maintenance in the time between doublings.

$$0.34\ \text{Glucose} + 0.94\ O_2 + 0.17\ NH_3 \rightarrow 1\ DCM_m + 1.01\ CO_2 + 1.42\ H_2O$$
$$\Delta H = -472\,\text{kJ/mol} \quad \Delta G = -483\,\text{kJ/mol} \quad \text{(A.9)}$$

A strip chart of OUR and cell density for a reasonably optimized fed-batch simulation with the above constraints is shown in Figure A.2b. An interesting feature of the constrained process is that the economics favor shorter batches with fewer doublings. As also discussed for the cell-culture fed batch in Section 2.3, μ_{max} is so low that any suppression of the growth rate due to the OTR constraint is a significant penalty. A longer batch that ends at higher cell density (at the expense of low average growth rate) therefore has a lower return than a shorter batch that runs 100% at μ_{max}.

The optimum time to end the batch is the point where the incremental cost to make another kg of cell mass is equal to the cumulative average cost, i.e., the point where continuing the batch will only drive the average cost up. As shown in Figure A.3a, the standard process can be continued for several hours after the growth rate begins to slow. In the constrained process (Figure A.3b), the utilization of capital and other fixed costs drops so rapidly that the batch must be stopped relatively soon after this point. As shown in Figure A.3c, it is also worth noting that the percentage of substrate consumed anabolically (to make new cell mass) in the constrained process drops below 50% very shortly after the growth rate begins to slow; i.e., in the last hours of the batch, more substrate is being used to keep existing cells alive than to make new ones. In the standard process, this anabolic fraction never falls below 60%.

The constrained process also favors a type of scale-out approach rather than scale-up. Figure A.4b shows that the optimum seed splits for the constrained yeast process are such that F2–F5 are essentially the same operations, split three times and run again. In principle, 2/3 of the final seed fermentor could be harvested, with the remainder grown again in the same fermentor (so-called "fill and draw" operation), though the production economics would be about the same at the same total production rate.

The production costs of the industry-standard process and the constrained process are summarized in Table A.5. At the much smaller facility size, fixed costs including labor are significantly higher, with the constrained facility making less than 10% as much product with more than double the employees.[155] Such increases in capital cost and labor are to be expected from

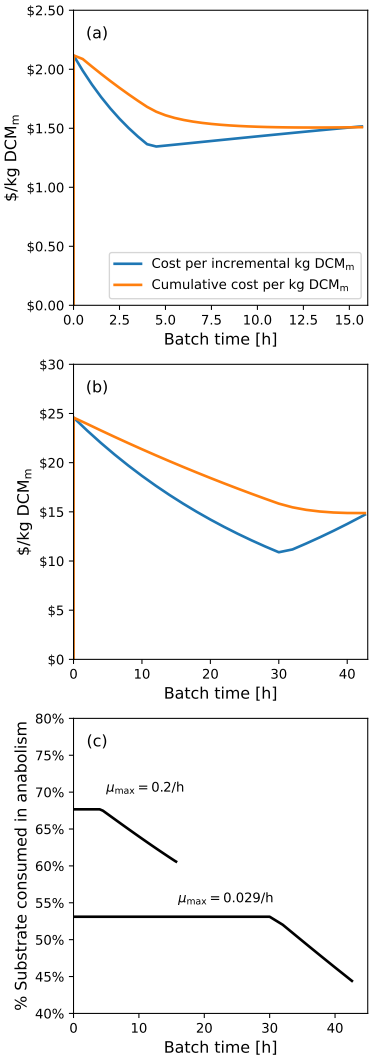

FIGURE A.3: (a), (b) Incremental and cumulative costs of cell mass (DCM_m) for the fed-batch F5 simulations in Figure A.2. (c) Percent of substrate consumed anabolically in the two simulations.

[155] Who are probably wondering why they were ever hired to run such an inefficient process.

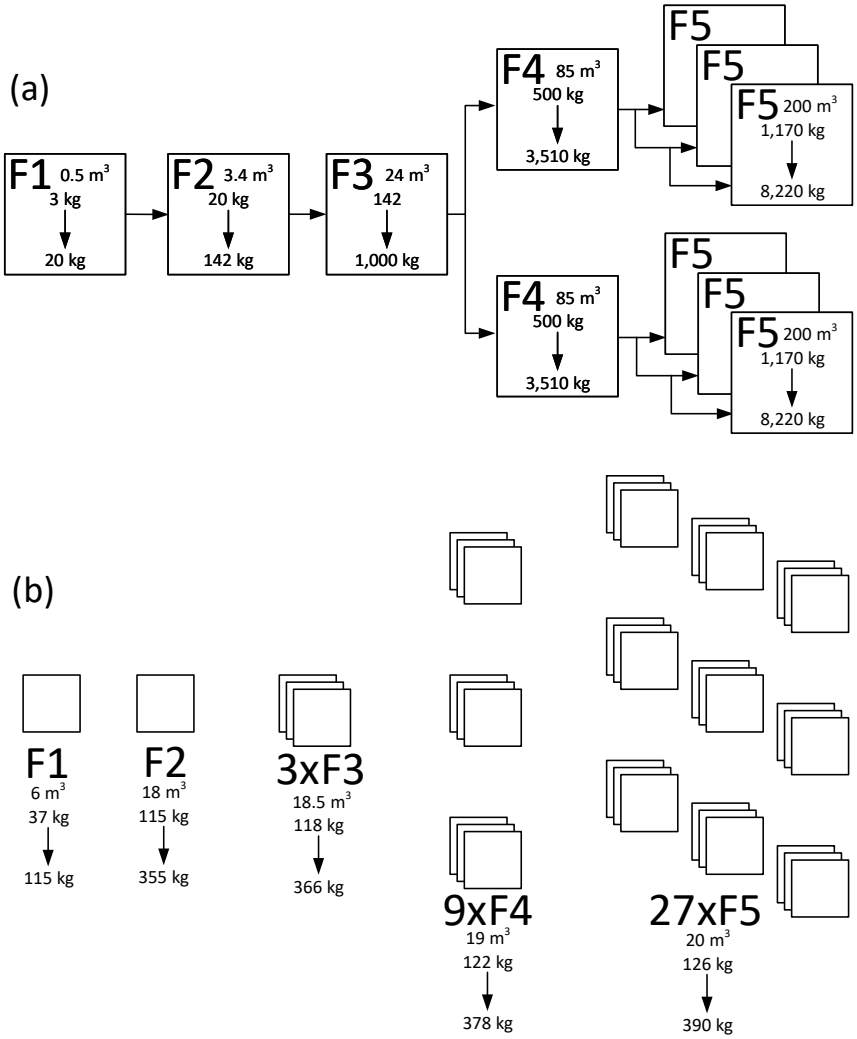

FIGURE A.4: Cell mass expansion splits for the fed-batch F5 simulations in Figure A.2a/b.

the constraints on growth rate and reactor volume: The estimate has largely been deprived of its characteristic economies of scale. This discussion should make clear the considerable challenges that will be faced in bulk animal cell culture due to its constraints on growth rate, bioreactor volume, and process intensity.

TABLE A.5: Analysis summary for standard and constrained yeast processes.

	Standard	Constrained (equal CAPEX)
Max. growth rate (h^{-1})	0.20	0.03
Max. OTR (mol O_2/m^3-h)	150	25
Production fermentors	6×200 m^3	27×20 m^3
Final seed fermentors	2×85 m^3	9×19 m^3
Cell density (g/L) dry	69	25
Yeast production (kTA)	17.3	1.7
Total CAPEX	$69M	$70M
Total FTE	24	56
Cost of production, $/kg dry matter		
Carbon (molasses)	$0.72	$0.89
Nitrogen (ammonia)	$0.04	$0.04
Water	$0.01	$0.02
Utilities	$0.16	$0.23
Labor	$0.14	$3.34
Overhead	$0.36	$3.63
Annual capital charge	$0.47	$4.74
Total COP, $/kg dry	$1.89	$12.90
Total COP, $/kg wet	$0.57	$3.87

B

Physical properties used in the analysis

Component	Abbrev.	MW[a]	Formula	ΔH_f kJ/mol	Ref.	ΔG_f kJ/mol	Ref.
O_2 (aq)		32.00	O_2	-11.70	[232]	16.40	[232]
O_2 (g)		32.00	O_2	0	[232]	0	[232]
NH_3 (g)		17.03	H_3N	-46.11	[233]	-16.45	[233]
NH_3 (aq)		17.03	H_3N	-80.29	[232]	-26.50	[232]
NH_4^+ (aq)		18.04	H_4N	-132.51	[232]	-79.31	[232]
CO_2 (g)		44.01	CO_2	-393.50	[232]	-394.36	[233]
CO_2 (aq)		44.01	CO_2	-413.80	[233]	-385.98	[233]
HCO_3^- (aq)		61.02	CHO_3	-691.99	[233]	-586.77	[233]
H_2O (l)		18.02	H_2O	-285.83	[232]	-237.19	[232]
H^+ (aq)		1.01	H	0	[233]	0	[233]
OH^- (aq)		17.01	HO	-229.99	[233]	-157.24	[233]
Glucose (s)	Glc	180.16	$C_6H_{12}O_6$	-1262.19	[232]	-915.90	[232]
Sucrose (s)		342.30	$C_{12}H_{22}O_{11}$	-2199.87	[232]	-1564.70	[232]
Lactate	Lac	90.08	$C_3H_6O_3$	-686.64	[232]	-516.72	[232]
Alanine	Ala	89.09	$C_3H_7O_2N$	-554.80	[232]	-371.00	[232]
Arginine	Arg	174.20	$C_6H_{14}O_2N_4$	-433.71	[87]	-229.20	[234]
Asparagine	Asn	132.12	$C_4H_8O_3N_2$	-766.09	[232]	-525.93	[232]
Aspartic acid	Asp	133.10	$C_4H_7O_4N$	-943.41	[232]	-695.88	[232]
Cysteine	Cys	89.09	$C_3H_7O_2NS$	-430.27	[87]	-338.82	[232]
Glutamine	Glu	146.15	$C_5H_{10}O_3N_2$	-805.00	[232]	-528.02	[232]
Glutamic acid	Glu	147.13	$C_5H_9O_4N$	-979.89	[232]	-697.47	[232]
Glycine	Gly	75.07	$C_2H_5O_2N$	-523.00	[232]	-379.91	[232]
Histidine	His	155.16	$C_6H_9O_2N_3$	-334.13	[87]	-179.80	[234]
Isoleucine	Iso	131.17	$C_6H_{13}O_2N$	-527.53	[87]	-343.90	[232]
Leucine	Leu	131.17	$C_6H_{13}O_2N$	-643.37	[232]	-352.25	[232]
Lysine	Lys	146.19	$C_6H_{14}O_2N_2$	-514.95	[87]	-303.80	[234]
Methionine	Met	117.15	$C_5H_{11}O_2NS$	-495.11	[87]	-502.92	[232]
Phenylalanine	Phe	165.19	$C_9H_{11}O_2N$	-400.46	[87]	-207.10	[232]
Proline	Pro	115.13	$C_5H_9O_2N$	-439.03	[87]	-285.60	[234]
Serine	Ser	105.09	$C_3H_7O_3N$	-603.06	[87]	-510.87	[232]
Threonine	Thr	119.12	$C_4H_9O_3N$	-635.48	[87]	-529.30	[234]
Tryptophan	Try	204.23	$C_{11}H_{12}O_2N_2$	-405.20	[232]	-114.70	[232]
Tyrosine	Tyr	181.19	$C_9H_{11}O_3N$	-573.26	[87]	-370.70	[232]
Valine	Val	117.15	$C_5H_{11}O_2N$	-611.99	[232]	-358.65	[232]

[a] Sulfur, where present, is omitted from the MW for consistency with the protein stoichiometry in Section 2.2.